IOP Publishing Journal of Physics D: Applied Physics

J. Phys. D: Appl. Phys. **50** (2017) 443002 (51pp) https://doi.org/10.1088/1361-6463/aa8675

Topical Review

Insights into the use of polyethylene oxide in energy storage/conversion devices: a critical review

Anil Arya and A L Sharma

Centre for Physical Sciences, Central University of Punjab, Bathinda-151001, Punjab, India

E-mail: alsharmaiitkgp@gmail.com

Received 24 May 2017, revised 22 July 2017
Accepted for publication 16 August 2017
Published 6 October 2017

Abstract

In this review, the latest updates in poly (ethylene oxide) based electrolytes are summarized. The ultimate goal of researchers globally is towards the development of free-standing solid polymeric separators for energy storage devices. This single free-standing solid polymeric separator may replace the liquid and separator (organic/inorganic) used in existing efficient/smart energy technology. As an example, polyethylene oxide (PEO) consists of an electron donor-rich group which provides coordinating sites to the cation for migration. Owing to this exclusive structure, PEO exhibits some remarkable properties, such as a low glass transition temperature, excellent flexibility, and the ability to make complexation with various metal salts which are unattainable by another polymer host. Hence, the PEO is an emerging candidate that has been most examined or is currently under consideration for application in energy storage devices. This review article first provides a detailed study of the PEO properties, characteristics of the constituents of the polymer electrolyte, and suitable approaches for the modification of polymer electrolytes. Then, the synthesization and characterizations techniques are outlined. The structures, characteristics, and performance during charge-discharge of four types of electrolyte/separators (liquid, plasticized, and dispersed and intercalated electrolyte) are highlighted. The suitable ion transport mechanism proposed by researchers in different renowned groups have been discussed for the better understanding of the ion dynamics in such systems.

Keywords: polyethylene oxide, constituents of polymer electrolytes, structural and microstructural properties, electrochemical properties

(Some figures may appear in colour only in the online journal)

List of abbreviations and acronyms

BMITFSI	1-butyl-3-methylimidazolium bis(trifluoromethanesulfonyl)imide
$BMIMPF_6$	1-ethyl-3-methylimidazolium hexafluorophosphate
BMPyTFSI	1-butyl-4-methylpyridinium bis(trifluoromethanesulfonyl)imide
CPE	Composite polymer electrolyte
DMMT	Dodecylamine modified montmorillonite
DOP	Dioctyl phthalate
EC	Ethylene carbonate
EDLCs	Electrical double layer capacitors
EMIMTFSI	1-ethyl-3-methylimidazolium bis(trifluoromethylsulfonyl)imide
EMIM-TY	(1-ethyl-3-methylimidazolium tosylate
EMITf	1-ethyl-3-methylimidazolium trifluoromethanesulfonate

ESD	Energy storage device
ESW	Electrochemical stability window
GPE	Gel polymer electrolyte
LAGP	$Li_{1.5}Al_{0.5}Ge_{1.5}(PO_4)_3$
LATP	$Li_{1.3}Al_{0.z}Ti_{1.7}(PO_4)_3$
LGPS	$Li_{10}GeP_2S_{12}$
$LiAsF_6$	Lithium hexafluoroarsenate
LIB	Lithium ion battery
LiBOB	Lithium bis-(oxalato)borate
$LiCoO_2$	Lithium cobalate oxide
$LiNO_3$	Lithium nitrate
LiTNFSI	Lithium (trifluoromethanesulfonyl) (N-nonafluorobutanesulfonyl)Imide
MMT	Montmorillonite
$MUSiO_2$	Monodispersed ultrafine SiO_2
MWCNT	Multiwalled carbon nanotube
NaMMT	Sodium montmorillonite
NaPCPI	Sodium pentacyanopropenide
NaTCP	Sodium 2, 3, 4, 5-tetracyanopirolate
NaTFSI	Sodium bis(trifluoromethanesulfonate) Imide
NaTIM	Sodium 2,4,5-tricyanoimidazolate (Natim).
OMLS	Organically modified layered silicate
PC	propylene carbonate
PE	Polymer electrolyte
PEG	Polyethylene glycol
PEGMEM	Poly(ethyleneglycol) methyl ether methacrylate
PEO	Polyethylene oxide
PG	Poly(ethylene glycol dimethyl) ether
PNC	Polymer nanocomposites
PVP	Poly (vinyl pyrrolidone)
$PYR_{13}FSI$	N-methyl-N-propylpyrrolidinium bis(fluorosulfonyl)imide
SPE	Solid polymer electrolyte
TEGDME	1,3 dioxolane (DIOX)/tetraethyl eneglycol dimethylether
VTF	Vogel–Tammann–Fulcher
$Zn(CF_3SO_3)_2$	Zinc trifluoromethanesulfonate
ZrO_2	Zirconia oxide

1. Introduction

Energy is the lifeblood of modern society. Global warming, finite supplies of fossil fuels and city pollution conspire to make the use of renewable energy, together with electric transportation, a global imperative [1]. The increased and extreme dependency of humans in recent years on fossil fuels of finite supply, and uneven global distribution, had led to two problematic consequences: (1) the vulnerability of nation states to imports of fossil fuels, and; (2) CO_2 emissions that are acidifying our oceans and creating global warming [2].

So, the control of the environment/climate has drawn the attention of the scientific community towards development and the replacement of fossil fuels by an alternative and efficient energy source, such as solar, tidal, and wind energies. In our modern society, extensive global attention has been focused toward fulfilling the demand of alternative and miniaturized renewable energy storage and conversion devices (ESCDs) offering high performance and durability, to balance supply with demand. Energy storage is essential in order to restore it as electricity, and the perfect approach is to convert chemical energy into electrical energy. The most convenient energy storage devices are batteries, which have the portability of stored chemical energy with the ability to deliver it as electrical energy at a high conversion efficiency, without the gaseous exhaust of fossil fuels [1, 3].

Lithium ion batteries (LIBs) are expected to witness remarkable growth as an energy source for the modern way of life because of their application in the consumer market: in cell phones, digital cameras, laptops, smartphones, uninterrupted power supply (UPS), etc; and also due to their storage of 2–3 times as much energy per unit of weight weight and volume as compared to earlier batteries. The first breakthrough in LIBs, by John Goodenough, and commercialization by the Sony Corporation in 1991, has drawn much research attention over the past two decades, due to their much higher energy density than alkali metals. Goodenough said in a statement. '*Cost, safety, energy density, rates of charge and discharge and cycle life are critical for battery-driven cars to be more widely adopted*'. A battery converts chemical energy into electrical energy. Its structure is composed of a positive electrode as a cathode ($LiCoO_2$), a negative electrode as an anode (graphite), and electrolyte, as shown in figure 1. Simultaneous movement of ions and electrons occurs in the battery system; ions flow through the electrolyte while electrons are generated at the anode and flow towards the cathode via an external circuit. The amount of charge of a battery depends on the storage capacity of ions between the electrodes, while the capacity is determined by the rate of lithium ion migration (to and fro) through the electrolyte. So, the electrolyte is a critical component of an LIB, as it provides a path for the transport of ions as well as acts as a physical barrier to prevent the internal short-circuiting of the battery. Table 1 summarizes the requirements for selection of an electrolyte-cum-separator for an efficient lithium ion battery system [4].

At, present, the LIB is the ideal choice for the automotive sector by manufacturers including Tesla Inc. and Volkswagen AG, due to their ease of transportation, environmental friendliness, and lower cost [5]. Allied Market Research published a report entitled '*World Lithium-Ion Battery Market: Opportunities and Forecasts, 2015–2022*'. Its main point was that the global LIB market is expected to generate revenue of $46.21 billion by 2022, with a compound annual growth rate (CAGR) of 10.8% during the forecast period (2016–22). At a 37 % revenue share, the LIB is the battery of choice for portable devices and electric vehicles. There are no other systems up to now that threaten today's market for LIBs (figure 2) [6].

Recently, in 2017, John Goodenough, inventor of the LIB, has developed the first all solid-state battery cells using sodium- or lithium-coated glass electrolyte, and has claimed that these new battery cells have three times more energy density (1200 charge–discharge cycles) than existing rechargeable batteries. He has concluded that they store and transmit energy at lower temperatures (−20 °C to 60 °C) than traditional lithium-ion packs and can be made using globally abundant supplies of sodium. One advantage

of this battery is the prevention of dendrite growth due to the glass-based electrolyte, which enhances the safety of the battery. Also, manufacturers including Tesla and Volkswagen have set their sights on lithium-ion to usher in a new generation of plug-in vehicles [7]. The ultimate goal of both academics and industry researchers is to develop an advanced polymer electrolyte (PE) system with high ionic conductivity, long shelf life, and high energy density, which is leak proof, safe, and has a wide operational window, easy process ability, flexible geometry, and light weight. PEs act as a bridge between conventional solvent-based liquid systems and solvent-free electrolytes [8]. They are an outstanding candidate due to their key application in ESCDs such as solid-state batteries, satellites, electric vehicles, supercapacitors, and the consumer portable electronic and telecommunications markets. They will power the implantable biomedical devices, hybrid electric vehicles and military/national security communication and surveillance equipment of tomorrow [9–11]. Development of the various types of electrolytes with different salt systems from the viewpoint of safety is depicted in figure 3, and table 2 provides a glimpse of the merits and demerits of the LIB.

In this review article, the recent progress in polyethylene oxide (PEO) based PEs for application in energy storage devices is elaborated fully. The discussion will be focused towards the material selection criteria along with characteristics of the constituents of PEs, synthesis methods and ionic liquid/plasticizer incorporated polymer electrolyte (GPE) and dispersed and intercalated type solid polymer electrolytes (SPE). Some of the latest developments in the field of gel, liquid, dispersed/intercalated polymer electrolytes with improved and significant results are elaborated. Finally, the roles of nanofiller, nanoclay, plasticizer and ionic liquid in the enhancement of electrochemical properties with suitable proposed transport mechanisms are included.

1.1. Definitions

The following terms are used for the study of the performance of an energy storage device.

A *battery* is an electrochemical device that converts chemical energy into electrical energy. It comprises of two electrodes (anode and cathode) with a separator sandwiched between them.

The *cathode* is a positive electrode and a reduction of chemical reaction occurs in it, along with the acceptance of electrons from an external circuit.

A *separator* provides a physical barrier to prevent the internal short-circuiting of the battery; it can be a solid or liquid or gel electrolyte. It allows the transport of ions by providing a medium for flow.

The *anode* is the negative electrode, where oxidative chemical reactions occur, along with the release of electrons in an external circuit.

Open circuit voltage is the thermodynamic voltage in the device when no external current is flowing within the system.

Closed circuit voltage is the voltage of the device when an external current flows in the system.

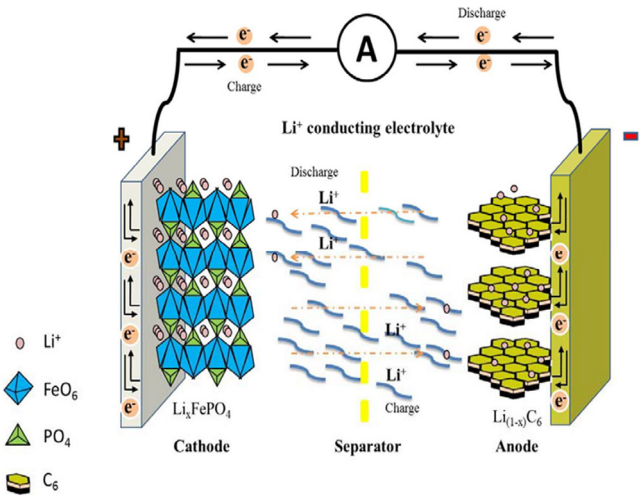

Figure 1. Schematic illustration of a typical lithium-ion battery. Reproduced from [4] with permission of The Royal Society of Chemistry.

Charge is the mechanism of loading of energy when the system reverses back.

Discharge is the mechanism of unloading of stored energy to the system via an external load.

Specific energy is the maximum energy of a cell that can be used per mass of the active material.

Energy density is the maximum energy of a cell that can be stored per unit volume.

Coulombic efficiency is the ratio of discharging time and charging time.

C-rate is the measure of charging and discharging current of an electrochemical cell.

Glass transition temperature is the temperature at which an amorphous polymer changes from a glassy to a rubbery phase and leads to an enhancement in polymer flexibility.

2. Performance and classification of PEs

PEs have received a remarkable amount of research investment over the last decades, due to extreme demand of practical material application in devices, and they are an alternative approach to the replacement of organic liquid-based electrolytes. LIBs are suitable as ESCDs due to growing demand in daily life. But there are some safety concers, such as poor thermal stability, flammable reaction products, and leakage of electrolyte and internal short circuits [12].

Although the polymers are insulators, a report by Wright and colleagues in 1973 on poly ethylene oxide (PEO) and alkali metal salts (NaI) systems confirmed non-negligble conductivity in the polymers, and that led to increased focus on the development of PEs. Their technological importance was realized by Armand in the early 1980s due to their flexibility and deformability and they were introduced as SPEs [13]. To date, the high molecular weight poly (ethylene oxide) (PEO)-based polymeric electrolytes are one of the most promising candidates for PE preparation, due to their semi-crystalline nature and the presence of the ether group, which supports faster ionic transport due to beneficial polymer flexibility.

Table 1. General requirements for separators used in lithium ion batteries. Reproduced from [4] with permission of The Royal Society of Chemisty.

Parameter	Requirement
Chemical and electrochemical stabilities	Stable for an extended period of time
Wettability	Wet out quickly and completely
Mechanical property	$>1000\,\mathrm{kg\ cm^{-1}}$ (98.06 MPa)
Thickness	20–25 μm
Pore size	<1 μm
Porosity	40–60%
Permeability (Gurley)	$<0.025\,\mathrm{s}\ \mu\mathrm{m}^{-1}$
Dimensional stability	No curl up and lay flat
Thermal stability	<5% shrinkage after 60 min at 90 °C
Shutdown	Effectively shut down the battery at elevated temperatures

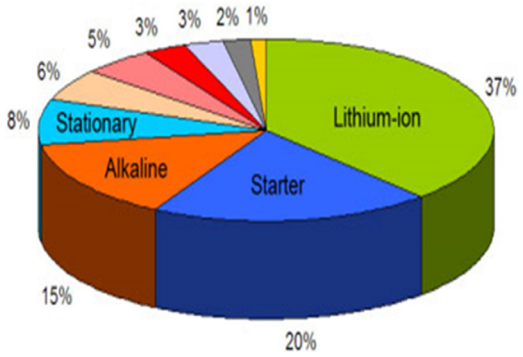

Figure 2. Revenue contributions by different battery chemistries. Reproduced with permission from [6].

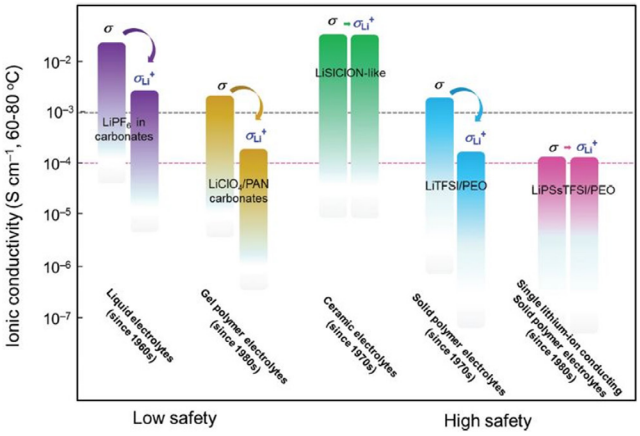

Figure 3. Roadmap for the development of Li-ion conducting electrolytes for rechargeable lithium and Li-ion batteries, including liquid electrolytes, gel polymer electrolytes, ceramic electrolytes, solid polymer electrolytes and single lithium-ion conducting solid polymer electrolytes. The requirements of total ionic conductivity (σ) and individual Li^+ conductivity (σ_{Li+}) for battery operation are shown as gray and pink dashed lines, respectively. Reproduced from [1] with permission of The Royal Society of Chemistry.

Therefore, a PEO-based SPE is the most preferred polymer host in the research system due to its flexible backbone and ability to solvate lithium ions, with the coordination number dependent upon the salt concentration and identity of the anion.

The main advantage of a PEO is its high solvation power. Hence it can form a complex easily with many alkali salts and provides a direct path for cation migration due to the presence of $(–CH_2–CH_2–Ö–)_n$ in the polymer backbone. But the low conductivity value (10^{-7}–10^{-6} S cm^{-1}) and poor mechanical properties of PEOs at ambient temperatures limit their use in devices. In order to overcome this drawback, the most common approach is the altering of the morphology, using the nanofiller or plasticizer or ionic liquid and salt with large anions in the polymer matrix. Polymer blending is one of the best adopted techniques to improve the properties of the host polymer and is the physical mixing together of two individual polymers. This gives superior properties to those of an individual polymer and can be easily controlled by varying the composition of the polymer used [14, 15]. The electrical and mechanical properties can be further improved by the addition of nanofiller and plasticizer. Another approach is the use of organic solvents, but the resulting electrolytes film suffers from the high volatility and thus flammability of the solvent as well from its reaction with lithium metal electrodes; this restricts its use in efficient energy storage devices. The ability to control and enhance the mechanical strength independently, ionic conductivity, voltage stability, and the thermal properties of an electrolyte are highly desirable in the development of electrochemical devices. Generally, in a polymer blend there are two phases present, with the first providing a conduction path to the ion and the later one providing mechanical stability to the electrolyte. In this review, first of all, the PEs are divided into their different parts, followed by a discussion of the principal requirements for the polymer host, salt, solvent, nanofiller, ionic liquid and nanoclay. Then the preparation technique and characterization techniques for PEs are described in a systematic manner. The reported results up to the present time, on PEO-based systems with different modification approaches for improving their properties, are introduced. In the last section, the proposed transport mechanisms of different systems of electrolytes are outlined.

2.1. Intrinsic properties of PEO

So far, PEO is the best polymer for the preparation of PEs for fast ion transport, due to its structure. Another main advantage of a PEO is its high solvation power, such that it can form a complex easily with many alkali salts and provides a direct path

Table 2. Merits, demerits and applications of the lithium ion battery (LIB).

Merits	Demerits	Applications
High energy density, and zero memory effect	Requires protection circuit to maintain current and voltage within limits	Solar and wind energy storage
Low internal resistance and self-discharge	Suffer from ageing effect	Electric vehicles and electronics
Good coulombic efficiency and high OCV	Degrades at high temperature and when stored at high voltage	Defense applications
Low maintaince cost and long life span	Not fully mature	Communication and space applications
Low effective capacity loss at high discharge rate	Transportation regulations required when shipping in larger quantities	Space applications
Fast charging and slow discharging	Battery must be sealed properly	Energy storage systems

for cation migration due to the presence of $(–CH_2–CH_2–Ö–)_n$ in the polymer backbone.

2.1.1. Basic structure. PEO is obtained by the ring-opening polymerization of ethylene oxide ($–CH_2–CH_2–Ö–$; mol. wt. 44 g mol^{-1}) (figure 4(a)). Pristine PEO shows a helical structure and a thread of 1.93 nm per unit quadratic cell (figure 4(b)). PEO is a linear polymer containing the polar ether group ($–C=Ö–$) with a lone pair of electrons and has a strong tendency to coordinate with alkali metal salts to form PEs. The ether group of PEO, having oxygen atoms at their centers, are suitable for PEs due to effective interaction with the conductive species, and provide good solvation properties [16–18].

2.1.2. Chemical properties. The high dielectric constant of PEO (~ 4–5) evidences its suitability to dissolve various salts. Another superior property of PEO is its high chain flexibility; it supports the faster transport of cations, which is the core requirement for a fast ionic conductor.

2.1.3. Morphological properties. It is a semi-crystalline material with about 70–85% crystallinity and an amorphous elastomeric phase at room temperature. PEO is a semi-crystalline polymer having a crystalline phase as well as amorphous phase. High ionic conductivity occurs in the amorphous regions above the glass transition temperature (T_g) and segmental motion of polymer chains promotes the ionic conductivity. The crystalline phase of PEO prevents ion migration as it is supported by the amorphous phase. Since an amorphous arrangement of molecules lacks long-range order, it reduces the chain reorganization tendency which supports fast ion transport. So, the main strategy at present is to suppress the crystallinity of PEO and enhance the amorphous phase so that it can be employed as a separator and ionic conductor in energy storage devices [19].

2.1.4. Physical properties. Poly (ethylene oxide) is an interesting polymer host due to its low glass transition temperature (−60 °C), high melting point (65 °C), excellent flexibility and low toxicity. The low glass transition temperature supports faster ion transport, as above the glass transition temperature the polymer phase changes from rigid to a viscous phase, which in turn enhances the polymer flexibility. The thermal stability of PEO can be improved by dispersing nanofiller or plasticizer, which will decrease the T_g and increase the degradation temperature of the polymer [20]. This decrease in T_g leads to fast ionic transport or high ionic conductivity, and the degradation temperature increase enhances the thermal stability window.

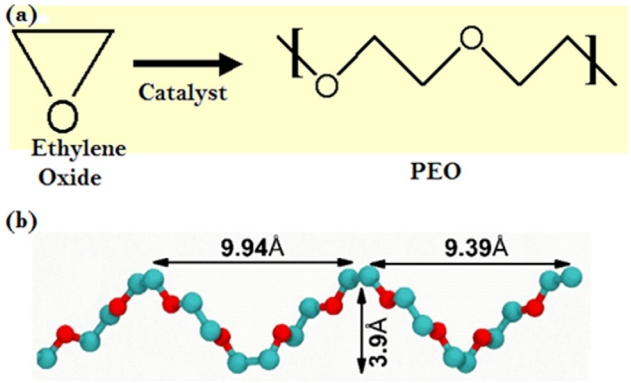

Figure 4. (a) Synthesis of polyethylene oxide. Reproduced with permission from [17]. (b) Helical portion of the PEO chain (hydrogens are omitted for clarity). Reproduced from [18] with permission of The Royal Society of Chemistry.

2.1.4.1. Approaches for modification of PEO. Although PEO has several advantageous, such as its electrochemical, chemical, and physical properties, its poor ionic conductivity makes it inadequate for applications. To overcome this drawback, various approaches are proposed based on the addition of materials with varying properties (figure 5). Among many PNCs, two attempts dominate for improving the properties of PE. The first approach is the incorporation of nanofiller in the polymer salt matrix, which prevents polymer chain reorganization, and free volume is produced. This increases the ionic conductivity of PEs. Also, the mutual interaction between nanofiller supports more dissociation of salt, and conductivity increases due to an increase in free charge carriers. The second approach is the incorporation of a low viscosity and low molecular weight plasticizer.

2.2. Extrinsic properties of PEO electrolyte system

A simple battery system consists of three components: two electrodes (cathode and anode) and an electrolyte/separator, which plays a dual role. So, during the operation of a battery, the PE plays an important role as it provides a path for the swimming of ions between the electrodes. For a successful

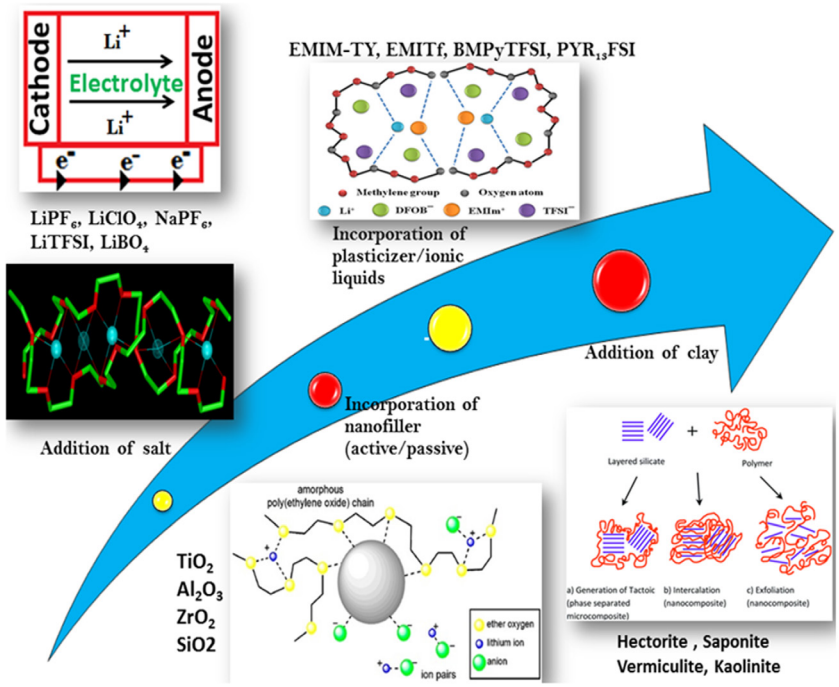

Figure 5. Approaches for enhancement of properties of polymer electrolytes.

battery system it becomes important to select suitable materials used for the preparation of PEs, such as a polymer host, salt, solvent, nanofiller, nanoclay, and an ionic liquid. Different materials have different properties which affect the overall function of the electrolyte in a battery system, and are discussed below.

2.2.1. Properties of polymer host. In a LIB system the electrolyte is sandwiched between electrodes and allows migration of Li ions during battery operation. The electrolyte is a major factor that affects the electrochemical properties. The polymer host must have certain properties so that it can fulfill our criteria of a suitable PE.

2.2.2. Properties of solvent. A good solvent is energetic, for the better dissolution of salt and polymer via dipole-dipole interactions (polymer–solvent, salt–solvent). So the solvent must possess basic characteristics such as a high dielectric constant for better dissolution of salt, low viscosity for faster ion motion, and a high electrochemical stability window (ESW). It must be inert toward cell components, and a principal characteristic is that it must provide an ionic conductive solid electrolyte interface layer on the electrodes. The high dielectric constant of solvent is an important parameter as it prevents the formation of the ion pairs, since ion pairs do not play any role in ionic conductivity. The solvent must fully swell and stretch the polymer chains within this, so that a more favorable interaction can occur between the cation and electron donor group of the host polymer [21].

2.2.3. Properties of salt. In fulfilling the criterion of faster ion transport and high ionic conductivity, salt plays an important role. Besides solvent and polymer, the dissociation rate of salt directly affects the ionic conductivity. So the salt must possess suitable properties, such as a low lattice energy for more dissociation of salt, and a lower cation size for faster movement in the polymer matrix. One important requirement is the stability of the anion towards electrodes and a non-toxic nature. Also, the high ionic conductivity and voltage stability window of the salt directly affects the overall conductivity of the electrolyte. As the mobility of ions plays an important role in determining conductivity, so salts with a smaller cation size and larger anion size are beneficial for obtaining optimal performance in an electrolyte.

2.2.4. Properties of ionic liquid. The incorporation of ILs is a recent promising approach adopted to enhance the mechanical and electrochemical properties. The ILs are molten salts with large anions at room temperature, and bulky anions also support the dissociation of salt in a polymer matrix, which affects the electrochemical properties. On the basis of their composition, there are three types of ILs: aprotic, protic and zwitter. They are used for: lithium batteries and supercapacitors; fuel cells; and IL-based membranes, respectively [22, 23]. Another interesting advantage of an IL is that the change in the structure of both cation and anion in a very extensive and fashionable way allows the tailoring of the IL's properties in accordance with the foreseen applications [24]. The addition of ILs in the polymer salt system also enhances the interfacial contact of electrodes with electrolyte and enhances the properties of the system.

2.2.5. Properties of plasticizer. Another effective approach to enhance the ionic conductivity of a PE-based system is the incorporation of a plasticizer such as EC, DEC, or PEG. Plasticizers are low molecular weight substances, and when added

in a polymer matrix they increase its flexibility. The addition of plasticizer increases the free volume required for transport by penetrating between polymer chains. Since plasticizers are small in size they can easily penetrate in between polymer chains. This modifies the polymer chain arrangement by disrupting the cohesive force between polymer chains, which increases the segmental motion of polymer chains and more free volume is created. As for fast ion transport, the polymer matrix must possess a high amorphous content. To achieve the above, the incorporation of plasticizer is the best approach, which significantly enhances the amorphous phase as well as giving a better dissociation of salt into free cations and anions. The overall increase in the flexibility is an indication of a decreased glass transition temperature T_g and it evidences the increase in conductivity. So, the plasticizer must possess certain properties for the better performance of electrolyte in the application [25].

2.2.6. Properties of nanofiller. The addition of nanofiller in PEs not only enhances the conductivity but also improves mechanical properties such as the physical strength of PEs. The filler acts as a solid plasticizer that enhances the transport properties and reduces crystallinity and glass transition temperature due to an increase in the dielectric constant. Fillers with the Lewis acid surface group interact with both polymer and ion and reduce the ion coupling. The polymer provides a path for the conduction of ions and filler affects the polymer stiffness in supporting the ionic transport.

2.2.7. Properties of nanoclay. Among the large numbers of layered solids, clay minerals, especially the smectite group, are the most widely used for the reinforcement of polymer matrices and thus for the fabrication of polymer nanocomposites, because of their unique structure and reactivity together with their high strength and stiffness and the high aspect ratio of each platelet. The clay layered silicate composites prevent anion entry in polymer chain while supporting cation intercalation and increasing the conductivity. The low ionic conductivity is generally due to concentration polarization because of simultaneous mobility of ions (cations and anions). The above problem can be resolved by a nanoclay having a high cation exchange capacity which permits only cations in the polymer matrix. This suppresses the concentration polarization and the formation of ion pairs, which provides a suitable path for cation migration through intercalated channels of the clay [26].

Table 3 summarizes the characteristics of all constituents of the PE together, for a better guide.

2.3. Types of PEs

PEs are the best candidates so far over the liquid electrolyte based systems in the commercialized market. A lot of research is focused towards the improvement of various properties of PEs. There are three different types of PEs, based on their composition: (i) IL-based PEs; (ii) gel or plasticized PEs, and; (iii) SPE, which is further classified into dispersed and intercalated type SPEs on the basis of the formation of the polymer matrix. All the types are discussed in detail below.

2.3.1. Ionic liquid based polymer electrolytes ILs are room temperature molten salts which are composed of bulky asymmetric organic cations and organic or inorganic anions. ILs plays the role of plasticizers (which increase the amorphicity and flexibility of the SPEs) and also provide free charge carriers for conduction in SPEs. Unlike inorganic salts that require a solvent for dissociation into cation and anion, ILs do not require any solvent for dissociation and are entirely composed of dissociated organic cations and inorganic or organic anions. Incorporation of ILs is the latest approach as a replacement for plasticizers, for the improvement of the conductivity of PEs due to their unique and beneficial properties such as: low vapor pressure, excellent chemical and thermal stability, non-flammability, and large ionic conductivities. ILs consist of weak Lewis acidic cations and weak Lewis basic anions, causing the interaction between the ions and the polymers to be weak relative to ion-coordinating conventional electrolytes [27].

2.3.2. Gel polymer electrolytes Since the first report by Feuillade and Perche in 1975, gel PE (GPE) become an attractive system for LIB applications [28]. GPE is an intermediate state between solid and liquid with a semisolid structure where the liquid electrolyte is incorporated into a solid polymer matrix. Unlike the SPE, the host polymer itself does not contribute to the conductivity or dissolving of the ions. A composite gel/solid polymer electrolyte has the same features, but the nano-sized ceramic fillers are dispersed in the polymer matrix. GPE has the ability to suppress the formation of dendrite on the surface of lithium metal and to improve safety. Gel electrolytes have high ionic conductivities and enhanced interfacial contacts between electrode and electrolyte due to encapsulation of liquid electrolyte in the polymer matrix. GPE provides us with improved shape flexibility and safety. The addition of plasticizers in the polymer matrix results in an overall enhancement of the ionic conductivity due to penetration between polymer chains, which increases polymer flexibility. GPE provides us with the simultaneous presence of the cohesive properties of the polymer matrix and the diffusive properties of liquid electrolytes [29]. GPE also provides improved thermal and electrochemical properties.

2.3.3. Solid polymer electrolyte (SPE). SPE act as the separator as well as an electrolyte. SPE is a solvent-free system with a polymer matrix, with a cation of smaller radii as a mobile species and a bulky anion attached to a high molecular weight polymer chain. The optimized system of an SPE is formed by dissolving a low lattice energy salt, host polymer with electron donating group in a solvent with a high dielectric constant for the better dissolution of salt. The first report by Wright in 1973 on poly (ethylene oxide) + alkali metal salt complexes (PEO) boosted the research into solid state ionic conductors. Further, the application of polymer electrolyte in LIBs by Armand in 1978 inspired researchers worldwide. The polymer host provides the coordinating sites for cation migration in the electrolyte system. The interaction of salt with polymer dissociates it in cation and anion, and when an electric field is applied, the cation moves via the segmental motion of polymer chains.

Table 3. Fundamental characteristics of various constituents of the polymer electrolyte matrix.

Polymer host	Plasticizer
• Provide fast segmental motion of polymer chain • Low glass transition temperature • High molecular weight • Low viscosity • High degradation temperature • High dielectric constant • Must have electron donor groups	• Low melting point • High boiling point • High dielectric constant • Low viscosity • Easily available • Economic • Inert to both electrodes • Good safety and nontoxic nature
Solvent	**Nanofiller**
• Abundant in nature • Non aqueous in nature • Low melting point • Low viscosity • Large flash point • High dielectric constant • Good solubility for polymer and salt	• High polarity • Low melting and high boiling point • Safe and nontoxic • Environmental friendly and cost effective • Inert to all cell components • Act as Lewis acid for interaction with polymer • High dielectric constant for better dissociation of salt
Salt	**Nanoclay**
• Low lattice energy for more availability of free ions • High ionic conductivity • High mobility • Broad voltage stability window • Low ion pair formation at high content • Large anion size • Small cation size for fast migration between the electrodes • High thermal and chemical stability • Large ion transference number • Inert towards cell components	• Layered/unique structure with high aspect ratio (~1000) • Complex rheological behavior • Amorphous behavior with acid base properties • Greater ability for intercalation and swelling • Increased solubility of salts • High swelling index (water and polar solvents) • High cation exchange capacity (CEC) (~80 meq/100 g) • High external/internal surface area (~31.82 m^2 g^{-1}) • Appropriate interlayer charge (~0.55) • Adjustable hydrophilic/hydrophobic balance
Ionic liquid	
• Good thermal stability • Wide electrochemical stability • Low melting point • Low viscosity for fast transport • Negligible volatility • Non-flammability • Negligible vapor pressure • High ionic conductivity • High polarity • High dielectric constant	

The amorphous phase is a basic requirement for ion transport, while crystallinity hinders the migration path of action. The ion conduction in SPE is mainly via two mechanisms: (i) hopping, (ii) via polymer chain segmental motion.

2.5.3.1. Dispersed type SPE. These types of electrolytes are also called dispersed solid electrolytes, and are high conducting multiphase solid systems. They have a two phase mixture in which the first phase contains an ion conducting solid such as AgI, CuI, etc, and the second phase contains an inorganic insulating nanofiller such as Al_2O_3, SiO_2, TiO_2, $BaTiO_3$ and zeolite powders. Without changing the structural and chemical nature of compounds, a significant improvement in mechanical strength, hardness and stiffness of the polymer matrix has been achieved with the addition of nanofiller [18]. The ceramic fillers, due to their large surface area, prevent local chain reorganization, with the results of locking in at ambient temperature, and a high degree of disorder characteristic of the amorphous phase, which favors faster transport. Another important parameter is the particle size of the nanofiller, as it directly affects the ionic conductivity.

2.5.3.2. Intercalated/exfoliated type SPE. Pioneering work was carried out by Toyota Central Research Laboratories on Nylon 6-Montmorillonite (MMT) nanocomposites in 1950. They obtained encouraging enhancements in mechanical properties along with heat distortion temperature and a decrease in permeability, with only a small weight percentage content of MMT, by an *in situ* polymerization method. Intercalated nanocomposites are formed when the polymer chains are inserted into the layered silicate structure with fixed interlayer spacings. Conversely, exfoliated nanocomposites are formed when the individual silicate layers are individually dispersed in the polymer matrix [30, 31].

3. Polymer electrolyte material technologies

3.1. Polymer electrolytes preparation technique

3.1.1. Solution casting technique. The solution cast (SC) technique is one of the easiest traditional methods for the preparation of polymer electrolytes. In this method, the polymer is dissolved in a compatible solvent (with a low boiling point and a high dielectric constant, e.g. acetonitrile, dimethyl form amide, etc) at room temperature, followed by the adding of the required amount of non-aqueous salt in the polymer matrix. The quantity of salt is obtained w.r.t the amount of polymer host. After complete dissolution of polymer and salt a homogenous mixture is obtained. Then the nanofiller/plasticizer is dispersed in the mixture and further stirring is performed until a homogenous solution is obtained. Then the resulting solution is casted on well-cleaned petri dishes (glass or polypropylene) in a controlled atmosphere and dried at room temperature for a few days. Further, the film can be dried in a vacuum oven at a certain temperature for the complete removal of the solvent. Finally, a free-standing mechanically

stable polymer film with flexibility is obtained, and is kept in a vacuum desiccator to avoid moisture absorption, for further characterization [32].

3.1.2. Hot-press technique. The hot-press technique for the preparation of polymer electrolyte is one of most interesting emerging techniques owing to the advantage of needing no solvent. Generally, in this technique an appropriate amount of polymer and salt are mixed physically and the homogenous powder obtained is heated up to the melting point temperature of the polymer host, with continuous mixing. The soft slurry obtained is pressed by placing it between two stainless steel electrodes in order to obtain good quality polymer films. The same procedure is followed for the dispersion of nanofiller in the polymer salt system. First, an optimized composition of polymer-salt is chosen for preparation of a composite polymer electrolyte [33, 34].

3.2. Characterization techniques

Characterization is an essential part of the study of the requirements of a polymer electrolyte before a complete application in an energy storage device. However, it is customary to employ various techniques for the characterization of polymer nanocomposite materials, such as high mechanical strength, shape variation, and high electrochemical properties. So, it becomes important to study the surface properties, electrical properties, structural properties and interfacial properties. Characterization results are helpful in correlating the ionic conductivity, crystallinity and transport properties of polymer electrolytes in changes of morphology and structural properties. Techniques often recommended for characterizing the PNC films are discussed briefly in the sub-sections below.

3.2.1. Morphological/microstructural study. X-ray diffraction (XRD) is used to determine the atomic arrangement within a material. XRD can also be used to calculate the interplaner spacing and crystalline size which helps in understanding the various physical properties of materials. In the case of polymer electrolytes, XRD is used for calculating crystallinity and the amount of amorphous phase content. Also, the presence of sharp peaks indicates the crystalline nature of a sample, while broad regions show amorphous content. The exterior and interior morphological studies of polymer electrolytes are studied by field emission scanning electron microscope (FESEM), while the presence of various types of molecular intercations in the polymer system are identified by Fourier transform infrared spcetroscopy (FTIR). FTIR enabled us to obtain molecular structure without destroying the sample, and the position of interaction of the cation with the polymer in the case of the polymer blend. FTIR is also used for studying local molecular structures and functional group analysis and the interaction between polymer chains and the formation of a complex.

FESEM provides the smoothness and homogenity of the surface of the sample. FESEM is also used for investigating surface morphology, texture, topography (done in high vacuum 10^{-5}–10^{-7} Torr with a 100 eV–40 keV electron beam). As the FESEM sample is required to be of a conductive nature, so on insulating samples an ultra-thin gold coating is added prior to mesuarement. Another advantage of the coating is that surface resolution is improved. EDX can also be used along with FESEM to investigate the elemental composition of dopant in the polymer matrix. Elemental mapping is also of great interest, in order to know the uniform dipsersion of nanoparticles added in the polymer host.

The crystalline size, crystallinity and amorphous phase region can be obtained from XRD. The crystallinity is obtained using equation (1);

$$X_c\,(\%) = \frac{A_c}{A_c + A_a} \times 100\%. \tag{1}$$

Here, A_c = area of crystalline peaks and A_a = area of amorphous peaks.

3.2.2. Electrical analysis. The ionic conductvity of the polymer electrolyte is measured by impedance plot (Z'' versus Z') by placing a polymer electrolyte film between two stainless steel (SS) blocking electrodes in the configuration SS|PE|SS. Prior to the measurement, the thickness of the film and the area of the electrodes must be measured. Admittance analysis and dielectrc analysis is done by obtaining the dielectric constant, dielectric loss by using the real (Z') and imaginary part (Z'') of impedance (figure 17). The ionic conductvity is calculated using equation (2);

$$\sigma = \frac{1}{R_b}\frac{t}{A}\ \mathrm{S\,cm^{-1}}. \tag{2}$$

Here, 't' is the thickness of the sample, A is the area of the electrodes, and R_b is the bulk resistance obtained by the intercept of the spike or semicircle on the real axis.

Further transforming the Nyquist plot data into the dielectric data, the real and imaginary parts of the complex conductivity can be obtained using the given equations (3*a*) and (3*b*):

$$\sigma' = \omega\varepsilon_o\varepsilon'' \tag{3a}$$

$$\sigma'' = \omega\varepsilon_o\varepsilon'. \tag{3b}$$

Here, σ' is a real part of ac conductivity and σ'' is an imaginary part of ac conductivity, ω is $2\pi f$, ε' is a real part of dielectric constant and ε'' is imaginary part of dielectric constant.

3.2.3. Transference number analysis. As discussed earlier, ionic conductivity is an important parameter for the better performance of electrolytes. Another crucial parameter is the ion transference number, which for an ideal electrolyte is unity. In the case of polymer electrolytes, transport is usually by the movement of ions, and ionic conductivity dominates while electronic conductivity is negligible. So, the transference number enables us to calculate the contributions of both electrons and ions. For an ideal electrolyte $t_{ion} = 1$. The Wagner AC impedance technique is used to obtain the ion transference number, by placing a polymer film between stainless steel electrodes (SS||PE||SS). A DC polarization technique is used to calculate the cation transference number by measuring the current and steady state resistance before and after

polarization (Li||PE||Li). The low cation transference number affects the energy density/power density of battery and supercaapcitor due to less to and fro jump of the ion. The following equations (4) and (5) are used for calculating the ion and cation transference number.

$$t_{\text{ion}} = \left(1 - \frac{I_e}{I_t}\right). \tag{4}$$

Here, I_t, is the total initial current due to the contributions of ions and electrons and I_e is the residual current due to electrons contribution only.

For the cation transference number

$$t_{\text{cation}} = \left(\frac{I_s(V - I_o R_o)}{I_o(V - I_s R_s)}\right). \tag{5}$$

Here, V is the applied DC voltage for sample polarization, I_o and I_s are the currents before and after polarization, and R_o and R_s are the initial and steady-state resistance of the passivation layers.

3.2.4. Stability analysis. Thermal, mechanical and voltage stability of a polymer electrolyte is an essential requirement during cell fabrication for application in energy storage devices. ESW is obtained by linear sweep voltammetry (LSV) from the variation of current and voltage and it should be equal to the electrode stability window. In this technique, a fixed potential is applied and the breakdown voltage at the abrupt change of current is the ESW. Since mechanical stability is desirable for a safe device, the mechanical properties of the polymer electrolyte are characterized by obtaining Young's modulus by stress-strain curve, and storage modulus and loss modulus by dynamical mechanical analysis (DMA). A higher Young's modulus indicates improved mechanical strength of electrolyte. So, the stress–strain curve is used for calculating Young's modulus and the DMA for obtaining the storage modulus and loss modulus.

3.2.5. Thermal analysis. Differential scanning calorimetry (DSC) is a thermal analytical technique used to quantitatively interrogate the thermal phase transitions in an inert atmosphere, and may be either of two types, endothermic or exothermic; endothermic are melting, glass transitions, or decompositions, while an exothermic transition includes crystallization of the material in the polymeric materials. DSC measures the temperatures and heat flow associated with transitions in materials as a function of time and temperature in a controlled atmosphere Ar or N_2. In the case of polymer electrolytes, the glass transition temperature, melting point and crystallinity enable us to obtain information regarding the transport of ions in the polymer matrix. The glass transition temperature (T_g) is when the polymer phase changes in a step from glassy to a rubbery or viscous phase, and polymer flexibility increases. The glass transition temperature is a crucial parameter since it is linked to polymer flexibility and directly correlated with enhancement in the ionic conductivity.

From the experimental measurements, further parameters can be obtained that will be beneficial for the study of polymer materials and correlation with the XRD and impedance results.

The crystallinity of the synthesized polymer can be obtained using equation (6) and is an important parameter, since it is linked to the XRD which provides key insights for enhancement of the electrochemical properties.

$$X_c\,(\%) = \frac{\Delta H_m^{\text{sample}}}{\Delta H_m^o} \times 100\%. \tag{6}$$

Here, $\Delta H_m^{\text{sample}}$ is the experimental melting enthalpy and ΔH_m^o is the melting enthalpy for a 100% crystalline host polymer.

Another important technique for investigating the thermal stability and thermal degradation of polymer electrolytes is thermal gravimetric analysis (TGA). It provides us with the decomposition range of polymer salt and the whole polymer matrix. It can be operated in the dynamical and isothermal modes. The former deals with the simple heating of the sample placed inside an alumina crucible up to ~ 500 °C at a fixed rate. The latter one, as the name suggests is at a constant temperature. This sample is kept for a period of time at a constant temperature in order to study the thermal stability of the materials. One important parameter during measurement in both techniques is the scan rate value. Although it is not specified, a lower scan rate value is always preferred for the proper analysis of a sample.

3.2.6. Electrochemical analysis. The electrochemical performance of a battery and supercapacitor enables us to measure the energy density, power density, specific capacity and cyclic stability. Galvano-static charge/discharge and cyclic voltammetry (CV) provide us with the above information regarding the battery and supercapacitor. CV is carried out to measure the specific power ($P_{\text{sp.}}$) and specific energy ($E_{\text{sp.}}$) at different scan rates in a user-defined voltage range. The galvano-static charge/discharge (CD) is beneficial for obtaining the discharge capacitance and cyclic stability qualities of the battery. Specific capacitance in the case of supercapacitor can also be obtained by measuring the discharge time interval (Δt) and current applied (i), as given below by equations (7)–(9);

$$C_d = \frac{2i \times \Delta t}{m \cdot \Delta V} \tag{7}$$

where i = discharge current, Δt = discharge time interval, m = mass of active material, and ESR is the inward resistance of the cell.

$$\text{Energy}_{\text{spec.}} = \frac{C_d V^2}{8} \tag{8}$$

$$\text{Power}_{\text{spec.}} = \frac{V^2}{8\,\text{m} \times \text{ESR}}. \tag{9}$$

4. Reported results (current updates)

Remarkable progress for a safe and alternative energy source with high energy density and capacity for the commercial industry can be achieved by the lithium ion battery. But there are safety issues with an LIB using a liquid or gel polymer electrolyte which can be addressed by using an SPE. Therefore, many methods have been reported in the optimizing of the electrochemical properties and mechanical/

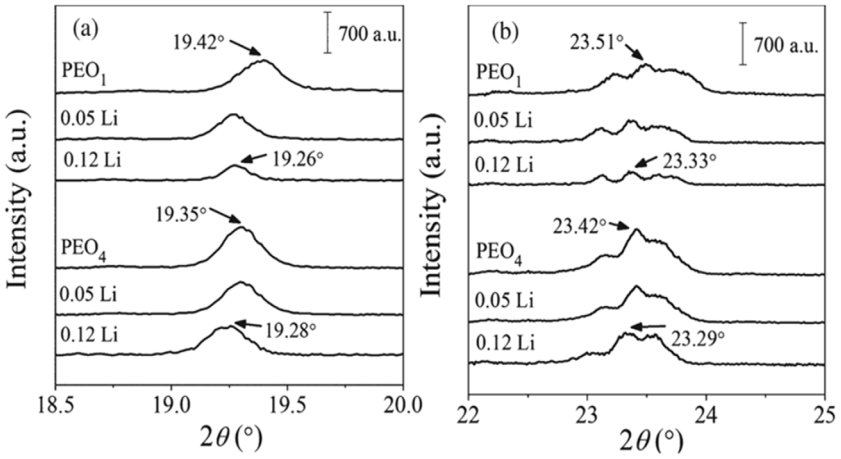

Figure 6. XRD diffractograms at: (a) 2 theta = 19° and (b) 2 theta = 24° for PEO_1 and PEO_4 at salt concentrations $Y_S = 0$, 0.05 and 0.12. [35] John Wiley & Sons. © 2017 Society of Chemical Industry.

morphological properties of polymer electrolytes which can satisfy the needs of all solid-state lithium polymer electrolyte batteries. A review of the significant research findings on polymer electrolytes is reported below.

4.1. Polymer in salt system

Over the last four decades, a lot of salts were used to prepare the polymer salt system and the addition of salt in the polymer hots is one simple approach to enhance the conductivity, transference number and stability window. The role of the salt is to reduce the crystallinity and enhance the polymer chain segmental motion which supports fast ionic transport. One important parameter is the glass transition temperature, which is directly related to ionic conductivity.

The influence of viscosity-molar masses of PEO and the fraction of salt on the ionic conductivity, thermal properties, crystalline structure and intermolecular interaction was investigated [35]. DSC analysis concluded that the solvation of salt in the polymer is independent of the molar mass of PEO, and almost negligible differences are observed in T_g as well as ΔC_p for different molar masses of PEO. All SPEs show an amorphous phase content at lower salt content that is almost independent of the molar mass of PEO. The XRD pattern of pure PEO exhibits two distinct peaks at 19° ((1 2 0) plane) and at 24° ((0 3 2) and (1 1 2) planes) and confirms the monoclinic crystalline structure. The pure polymer system and polymer salt system undergo phase separation, as evidenced by XRD (figure 6). The FTIR spectrum shows no shifting in the two shoulders at 1144 and 1061 cm^{-1} and is an indication of almost no influence of the polymer molar mass. SPEs prepared with morphologies close to equilibrium show no significant difference of σ_{DC} for PEOs with different molar masses at W_S = const. Further, the mobility and diffusion coefficient of the charge carriers in a PEO host polymer are also independent of the molar mass of PEO for the morphologies close to equilibrium, while for non-equilibrium morphologies an increased value of the diffusion coefficient is observed for a PEO with $M = 4 \times 10^6$ g mol^{-1}.

Boschin *et al* [36] synthesized SPEs NaFSI$(PEO)_n$ and NaTFSI$(PEO)_n$ with different ether oxygen to sodium (O:Na) molar ratios (n). The glass transition temperature (T_g) obtained in the first scan from DSC analysis for NaTFSI$(PEO)_9$ was at 237 K and during the second scan the T_g increased to 242 K, which may be attributed to increased Na^+ concentration in the amorphous region. For NaFSI$(PEO)_{20}$ and the NaFSI$(PEO)_6$ based SPE, no change in T_g was observed. DSC analysis concluded that for a low salt concentration ($n = 20$ and $n = 9$) there was little or no impact on the dynamics as observed by T_g.

The highest ionic conductivity, at 293 K, was 4.5×10^{-6} S cm^{-1} for NaTFSI$(PEO)_9$, while at 343 K both NaTFSI $(PEO)_n$ and NaFSI$(PEO)_n$, with $n = 20$ and $n = 9$, showed similar conductivities and followed a non-linear, Vogel–Tammann–Fulcher (VTF) behavior on cooling, which evidences the presence of an amorphous phase. The conductivities for NaTFSI $(PEO)_{20}$ and NaTFSI$(PEO)_6$ overlap in the range 283–312 K, and at 343 K the conductivity of NaTFSI$(PEO)_{20}$ (3×10^{-4} S cm^{-1}) is slightly higher than for NaTFSI$(PEO)_6$ (1.3×10^{-4} S cm^{-1}). The observed difference in conductivity may be due to two reasons; one is the difference in T_g (about 20 K) and the second is the number of ion pairs. Raman spectra (figure 7) shows bands at 844 cm^{-1} (CH_2 rocking) and 860 cm^{-1} (C–O stretching), typical of neat PEO for both NaX$(PEO)_9$ and NaX$(PEO)_6$. For NaTFSI$(PEO)_9$ and NaTFSI$(PEO)_6$ the 740 cm^{-1} band is assigned to 'free' TFSI, containing two TFSI conformers, C_1 (cis) and C_2 (trans). The T_e band observed at 744 cm^{-1} is assigned to Na^+-TFSI contact ion pairs. The deconvoluted spectra evidence of a larger amount of ion pairs (44 ± 16% NaTFSI$(PEO)_6$, as compared to both NaTFSI $(PEO)_9$ and NaTFSI$(PEO)_{20}$, is in correlation with the ionic conductivity data. It was concluded that the NaFSI $(PEO)_{20}$ and NaFSI$(PEO)_9$ show almost

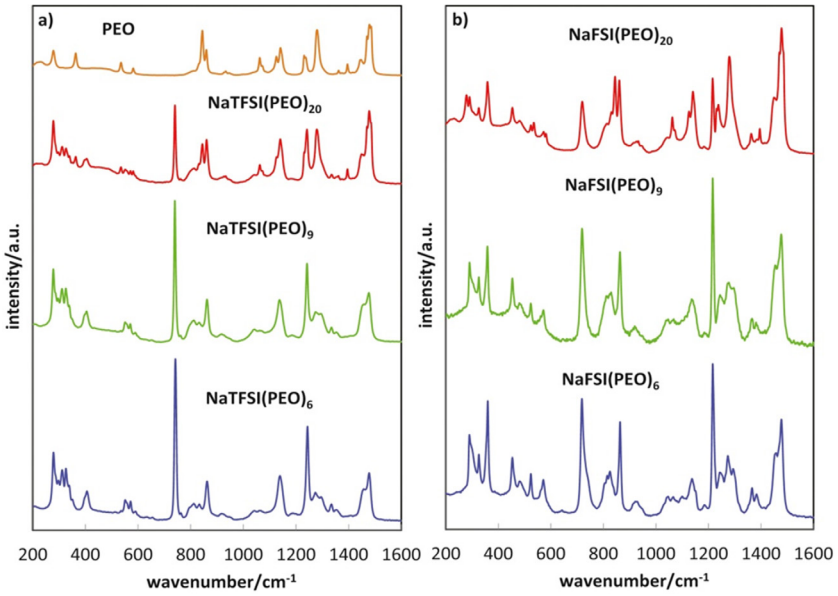

Figure 7. Raman spectra of: (a) neat PEO and NaTFSI(PEO)$_n$, and (b) NaFSI(PEO)$_n$, all in the range 200–1600 cm^{-1}. Reprinted from [36], Copyright 2015, with permission from Elsevier.

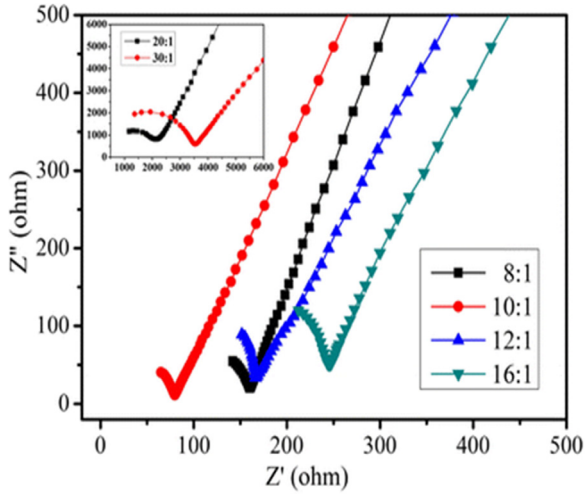

Figure 8. Nyquist impedance plots for the PEO–LiDFOB solid polymer electrolyte with different EO:Li molar ratios at 23 °C. [37] 2015 © Springer-Verlag Berlin Heidelberg 2015. With permission of Springer.

similar relative amounts of contact ion pairs, while for higher concentration, $n = 6$, the FSI-based SPE indicates the absence of ion aggregation.

Polu *et al* [37] prepared SPEs using a high molecular weight poly(ethylene oxide) (PEO) complexed with lithium difluoro(oxalato)borate (LiDFOB) via solution casting technique. XRD analysis suggests a decrease of crystallinity on the addition of salt in the PEO due to the destructive effect of the lithium salt on the ordered arrangement of the polymer chains. This modification in the structure of the host polymer indicates an enhancement of the amorphous content. DSC analysis evidences a decrease of crystallinity and glass transition temperature, which indicates an increase in polymer flexibility. Further, thermal stability was increased to 240 °C and was better than for pure PEO. The highest ionic conductivity was 3.18×10^{-5} S cm^{-1} for Ö/Li = 10 and may be due to an increase in the number of charge carriers (figure 8). The decrease in ionic conductivity at high salt content is due to ion association or charge multiplet formation. As it is well known that ionic conductivity dominates in the amorphous phase, so the impedance data is in good agreement with both XRD and DSC.

Recently, the preparation of a novel flexible and free-standing SPE based on PEO and poly (vinyl pyrrolidone) (PVP) complexed with lithium nitrate ($LiNO_3$) was reported by Jinisha *et al* [32], using a solution casting method. The absence of peaks corresponding to salt in the XRD pattern indicates a complete dissociation of salt. The Li^+ and NO_3^- ions of the salt also interact with the polymer backbone of the PEO which improves the order and alignment of the PEO structure and is evidenced by the small increase of peak intensity for the characteristic peaks of PEO beyond a 15 wt.% salt content. The FTIR spectrum confirms the interaction of Li^+ with the carbonyl group in PVP and results in the disruption of crystallization of the complex. Also, the absence of vibration bonds for the salt in all SPEs confirms the complete dissolution of salt in the polymer blend. The addition of PVP in the PEO changes the surface with micro-cracks of pure PEO to a porous surface. The further addition of salt smoothened the surface morphology, indicating a decrease of crystallinity of the PEO, and is in good agreement with the FTIR and XRD analyses. TGA analysis confirms the improved stability of SPE above 400 °C as compared to the PEO at 340 °C. DSC analysis shows a decrease of crystallinity up to 15 wt.% $LiNO_3$ (34.04%); at higher levels than this, the increase of crystallinity is due to ion aggregation. The interaction of salt with polymer disturbs the order of polymer chains, which in turn affects the relative crystallinity and results in a flexible SPE. The highest ionic conductivity is 1.13×10^{-3} S cm^{-1} for 15 wt.% $LiNO_3$. Further addition of salts restricts the ionic and polymeric segmental mobility due to the formation of ion pairs and ion clusters. The Li^+ transference number obtained

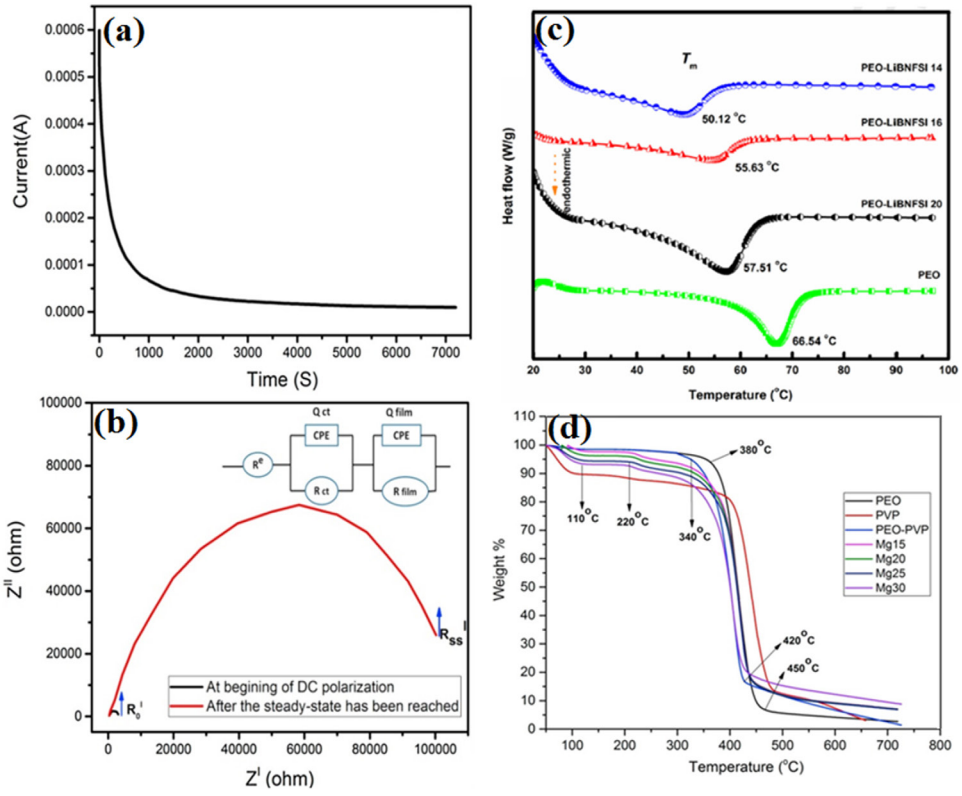

Figure 9. (a) Polarization curve of the cell, (b) impedance plots of the cell before polarization and after the steady state has been reached. Inset of (b) represents the equivalent circuit for deconvolution of electrochemical impedance plot (Reprinted from [32], Copyright (2017),with permission from Elsevier), (c) DSC thermogram of pure PEO, PEO-LiBNFSI 20, PEO-LiBNFSI 16 and PEOLiBNFSI 14 (Reprinted from [38], Copyright (2017), with permission from Elsevier) and (d) TGA curves of PEO, PVP, PEO-PVP blend and SPE membranes (Reprinted from [39], Copyright (2017), with permission from Elsevier).

by the Evand and Vincent method was 0.332, which is in good agreement with the theoretical value (figures 9(a) and (b)). The ESW was of the order of 5 V, which makes them a suitable candidate for a high-voltage Li ion battery.

Another report, by Karuppasamy *et al* [38], deals with the preparation of SPE by adding a bulky anion-based novel lithium bisnonafluoro-1-butanesulfonimidate salt in the PEO polymer matrix by the solution cast method. ATR-FTIR analysis confirmed the complexation of LiBNFSI with the PEO host. The addition of salt in the polymer matrix shifts the peak toward a lower wavenumber side, which indicates interaction between the cation and the ether group of the polymer. The deconvoluted spectra of C–S of stretching of LiBNFSI is evidence of the increase of free ion concentration with increases in salt concentration. The XRD pattern confirms the complete dissolution of salt in the polymer matrix and a decrease of peak intensity indicates a decrease of crystallinity. The increased amorphous phase supports fast ion conduction. DSC analysis also supported the XRD data and may be due to the weakening of the interaction between polymer chains and salt, which in turn reduces the amount of energy consumed in breaking the bond. The decrease of the melting point towards a lower temperature shows an increase of amorphous content (figure 9(c)). The mechanical strength was higher for Ö/Li = 20 (2 MPa) and decreases with the increase of salt, due to an increase of polymer flexibility. The highest conductivity was 2.2×10^{-4} S cm^{-1} (at 333 K) for Ö/Li = 14, due to the faster migration of ions. The cation transference number obtained was 0.31, which is suitable for an electrolyte in application devices. The ESW was 5.4 V, as observed from LSV.

Anilkumar *et al* [39] investigated a solid polymer blend electrolyte based on poly (ethylene oxide) (PEO)–Poly (vinyl pyrrolidone) (PVP) as polymer and Mg $(NO_3)_2$ as salt. A free-standing and flexible film was obtained, with a decreased intensity of crystalline peaks as evidenced by XRD. The salt was completely dissociated in the polymer matrix and an enhanced amorphous region was observed due to PVP. FESEM analysis of the PEO showed cracks in the film which were modified upon blending with PVP and resulted in a flexible film. Further addition of salts in the polymer matrix resulted in a microstructure with pores (1.5 μm) which are required for fast ionic transport. The microstructure topography was changed and was in correlation with XRD data. Thermo gravimetric analysis showed film stability up to 380 °C for all SPEs (figure 9(d)). The maximum ionic conductivity was observed for Mg 30 at around 5.8×10^{-4} S cm^{-1} at RT, which was four orders higher than for pure polymer blend [40]. The activation energy was at a minimum for Mg 30 at around 0.31 eV. The ionic transference number was 0.997 and the cation transference number was 0.33. The ESW was approximately 4 V, obtained from CV, and the open circuit voltage for the Mg ion cell was 1.46 V.

The ionic conductivity, structure, and segmental motions of two types of high-crystallinity PEO/$NaPF_6$ electrolytes with ethylene oxide Ö/Na = 8, 6 were investigated by Luo

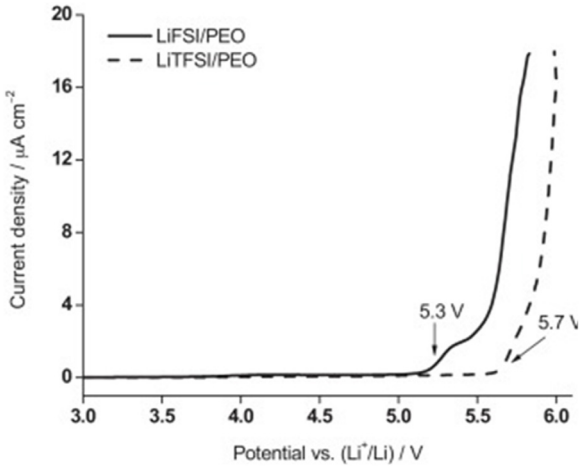

Figure 10. Linear sweep voltammograms of polymer electrolyte of LiX/PEO (X = FSI and TFSI) with a molar ratio EO/Li$^+$ = 20 at 80 °C; scan rate: 0.5 mV s^{-1}. Reprinted from [42], Copyright 2014, with permission from Elsevier.

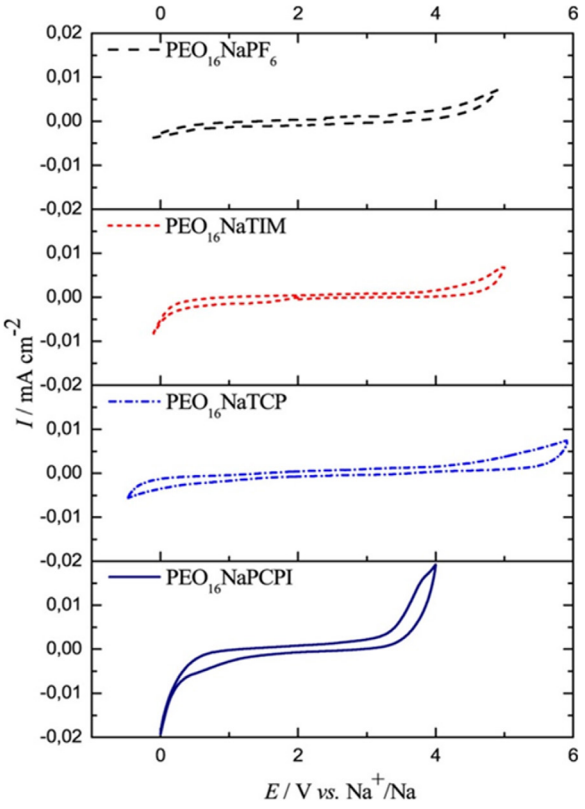

Figure 11. Cyclic voltammetry of electrolytes of PEO-based, solid-polymer electrolytes with salts of $NaPF_6$, NaTIM, NaTCP and NaPCPI at 50 °C. Reproduced from [43]. CC BY 4.0.

et al [41]. DSC analysis concludeed that a high melt-point crystalline phase formed during the isotherm at 343 K while the low melt-point crystalline phase formed at 295 K on cooling and melted at 325 K upon heating. XRD analysis indicated a complete complex formation as no corresponding peak for PEO and salt was observed. Further, a ^{1}H static NMR spectrum was used to calculate the crystallinity at room temperature. The ionic conductivity of PEO_8:$NaPF_6$ was 7.7 × 10^{-7} S cm^{-1} which was five times more than that of PEO_6:$NaPF_6$ (1.4 × 10^{-7} S cm^{-1}). Also, NMR analysis showed a high segmental mobility in PEO_8:$NaPF_6$ due to the low activation energy of 0.31 eV, which was 3–4 times lower than those found in PEO_6:$NaPF_6$. The cooperative motion of several ethylene oxide monomers occured due to strong coordination between the polymer segments and the Na^+ ions, while the large-angle segmental motion in the PEO–salt complex along the coil axis enhanced the ion motion or conductivity.

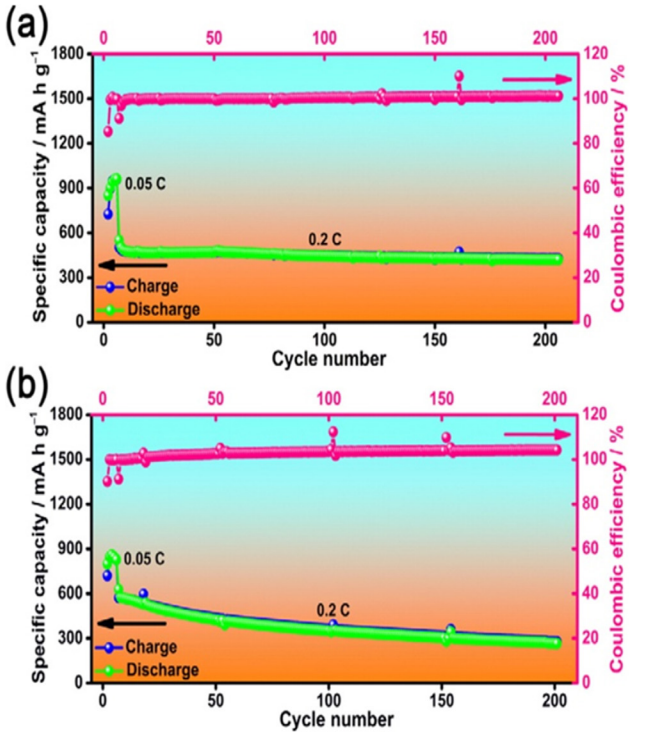

Figure 12. Cycling performances of the Li − S cells at 0.2 C (after 5 cycles for activation at 0.05 C) at 60 °C. (a) LiTNFSI/PEO (EO/Li$^+$ = 20) blended polymer electrolyte; (b) LiTFSI/PEO (EO/Li$^+$ = 20) blended polymer electrolyte. Reprinted with permission from [44], Copyright 2016 American Chemical Society.

Zhnag *et al* [42] prepared an SPE with lithium bis(fluorosulfonyl)imide (LiFSI) as salt and a high molecular weight poly(ethylene oxide) as host polymer. DSC analysis showed that the LiFSI-based polymer electrolyte had a lower T_g (−45 °C) than that of the corresponding LiTFSI-based polymer (−36 °C). The lower value of the glass transition temperature suggested a stronger plasticizing effect of LiFSI as compared to the LiTFSI. The polymer electrolyte of LiFSI/PEO exhibited ionic conductivity as high as 1.3 × 10^{-3} S cm^{-1} at 80 °C. The cation transference number obtained was 0.14 for LiFSI/PEO and 0.18 for LiTFSI/PEO at 80 °C. The ESW obtained for LiFSI/PEO was about 5.3 V versus Li$^+$/Li, and LiTFSI/PEO showed an improved stability window of about 5.7 V versus Li$^+$/Li (figure 10). The electrochemical analysis of the cell using LiFSI/PEO electrolyte at 80 °C showed a specific charge capacity of 159 mAh g^{-1} and a discharge capacity of 146 mAh g^{-1} at the first cycle at C/5 rate with coulombic efficiency of 99% after the first cycle.

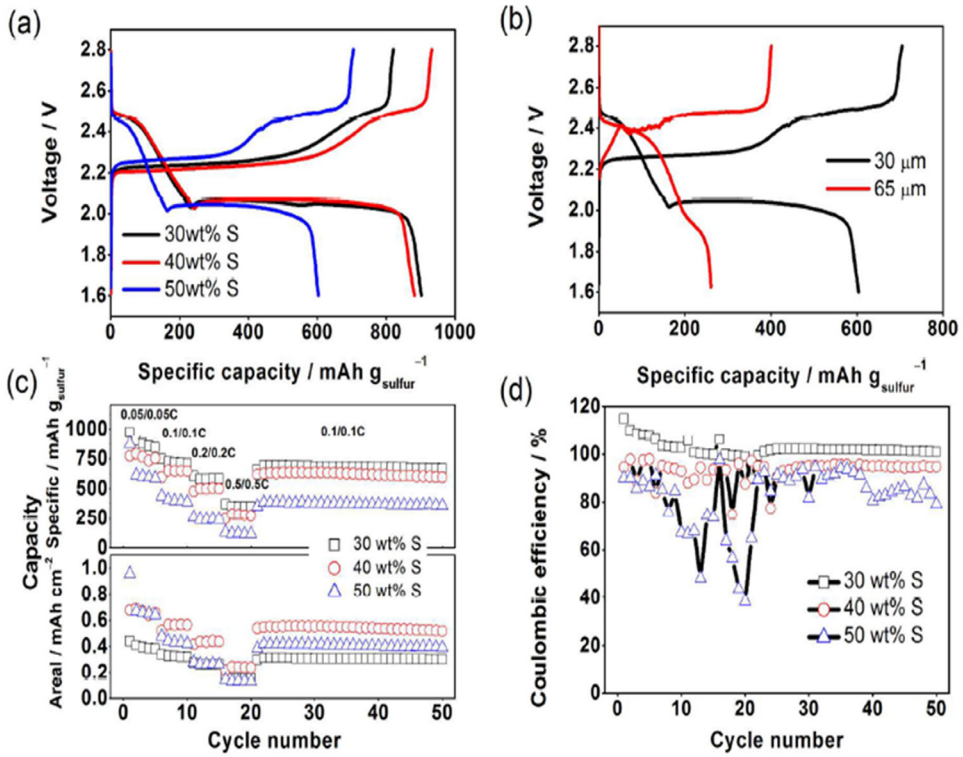

Figure 13. Discharge/charge profiles of the Li–S cells using the LiFSI/PEO electrolyte in the first cycle at a discharge/charge rate of 0.05/0.05 C at 70 °C, (a) S cathodes with the thicknesses around 30 μm but different S contents, (b) S cathodes with the same S content of 50 wt% but different electrode thicknesses. Discharge capacity and real capacity (c), and Coulombic efficiency (d) versus cycle number for the LiFSI-based Li–S cells at 70 °C. Reprinted with permission from [45]. Copyright 2017 American Chemical Society.

Michalska *et al* [43] prepared a new family of fluorine-free solid-polymer electrolytes, using poly (ethylene oxide) (PEO) as polymer and sodium salts with diffuse negative charges: sodium pentacyanopropenide (NaPCPI), sodium 2, 3, 4, 5-tetracyanopirolate (NaTCP) and sodium 2,4,5-tricyanoimidazolate (NaTIM). The electrochemical stability of electrolytes was lowest for NaPCPI (3 V versus Na^+/Na); 5 V versus Na^+/Na was obtained for electrolytes with NaTCP and NaTIM salt showed a stability window of 4.5 V (figure 11). The ionic conductivity was measured for PEO doped with $NaPF_6$, NaTCP and NaTIM, and at O:Na molar ratios of 16:1 showed optimal σ values, and for the NaPCPI membrane at 20:1. $PEO_{16}NaPF_6$ exhibited σ of the order of 0.1 mS cm^{-1} above 60 °C. The novel $PCPI^-$ and Huckel-type anions showed ionic conductivities of the order of 0.1 mS cm^{-1} above 50 °C, which is higher than for the $PEO_{16}NaPF_6$ based system. At 70 °C, PEO_{16}NaTCP showed ionic conductivity values (so-called liquid-like) greater than 1 mS cm^{-1}. It was concluded that the ionic conductivity of the electrolyte depends on the cation–anion interactions, and that the ion pair having lower cation–anion interaction energies dissociates more salt, which increases the number of free charge carriers. Also, the bulkier anion acts as a plasticizing agent and reduces the crystallinity of the polymer matrix, which results in increased polymer flexibility and mobility of the charge carriers. The increase in ionic conductivity may be attributed to a negative charge diffused over the entire anion via conjugated π bonds and electron-withdrawing cyano substituents. The calculated dissociation energies of the most stable ion pairs decreases as the salts change from $NaPF_6$ > NaPCPI > NaTIM > NaTCP, and the corresponding ion pair dissociation energies are 485, 443, 420 and 407 kJ mol^{-1}, respectively. TGA analysis shows the thermal stabilities for a polymer electrolyte with NaPCPI, NaTCP and NaTIM salts as being up to 600 °C, 540 °C and 570 °C, respectively. DSC analysis evidences the correlation of the change in T_g with respect to salt concentration. Also, the aromatic nature of Huckel-type anions provides flexibility to the PEO matrix, which supports faster ion transport, as evidenced by an enhancement in ionic conductivity.

Ma *et al* [44] reported the preparation of an SPE based on perfluorinated sulfonimide salt-based SPEs, composed of lithium (trifluoromethanesulfonyl) (n-nonafluorobutanesulfonyl)imide (Li[(CF_3SO_2)(n-$C_4F_9SO_2$)-N], LiTNFSI) and poly (ethylene oxide) (PEO) using an SC technique. The obtained ionic conductivity value was 3.69×10^{-4} S cm^{-1} at 90 °C and an anodic electrochemical stability at 4.0 V versus Li^+/Li, and sufficient thermal stability (>350 °C). As shown in figure 12(a), the Li − S cell with LiTNFSI/PEO ($EO/Li^+ = 20$) blended polymer electrolyte affords the average discharge specific capacity of ~ 450 mAh g^{-1} at 0.2 C for more than 200 cycles, which is higher than that of ~ 310 mAh g^{-1} at 0.5 C at 60 °C. Fortunately, the cycling stability is superior, with a negligible capacity loss for hundreds of cycles. However, this trend in consecutive capacity loss (i.e. poor cycling stability) during cycling (200 cycles) at 0.2 C at 60 °C is observed in the LiTFSI-based electrolyte (figure 12(b)). This indicates that the LiTNFSI-based SPEs would be potential alternatives for application in high-energy solid-state Li batteries.

Table 4. Ionic conductivity, cation/ion transference number, thermal stability, voltage stability window and cyclic stability of polymer salt complex.

Materials used	Electrical conductivity (S cm^{-1})	Transference number (ion/cation)	Electrochemical stability window	Thermal stability	Cyclic stability	Ref.
PEO-LiDFOB	3.18×10^{-5}	—	—	240 °C	—	[37]
PEO-PVP + $LiNO_3$	1.13×10^{-3} S cm^{-1}	0.332	5 V	400	—	[32]
PEO-LiBNFSI	2.2×10^{-4} S cm^{-1}	0.31	5.4	—	—	[38]
PEO-PVP + $Mg(NO_3)_2$	5.8×10^{-4}	0.99/0.33	4	380	—	[39]
PEO-LiFSI	1.3×10^{-3} S cm^{-1} at 80 °C	0.14	5.3	—	Specific charge capacity of 159 mAh g^{-1} and discharge capacity of 146 mAh g^{-1} at the first cycle, coulombic 99% after the first cycle.	[42]
PEO-LiTFSI	1×10^{-3} S cm^{-1} at 80 °C	0.18	5.7	—	—	[42]
PEO-NaPCPI	0.1 mS cm^{-1} above 60 °C	—	3	600	—	[43]
PEO-NaTIM	—	—	4.5	570	—	[43]
PEO-NaTCP	1 mS cm^{-1} at 70 °C	—	5	540	—	[43]
PEO-LiTNFSI	3.69×10^{-4} S cm^{-1} at 90 °C	—	4 V	>350 °C	average discharge specific capacity of ~450 mAh g^{-1} at 0.2 C for more than 200 cycles	[44]
PEO-LiFSI	1.0×10^{-4} S cm^{-1} at 70 °C	—	—	—	Specific discharge capacity 100 − 400 mAh $g^{-1}_{sulphur}$ at 0.5 C after 50 cycles.	[45]

Judez *et al* [45] reported the preparation of a polymer electrolyte based on lithium bis(fluorosulfonyl)imide ($Li[N(SO_2F)_2]$,LiFSI) salt and poly(ethylene oxide) (PEO) as polymer host. The ionic conductivity obtained was 1.0×10^{-4} S cm^{-1} at 70 °C. Also, the good electrochemical stabilities of the Al current collector were seen with both SPEs, as evidenced by the experiments of cyclic voltamogram and electrochemical impedance spectroscopy of the Al electrode.

The cycling performance of Li–S polymer cells is studied and presented in figure 30. For the first cycle, almost the same discharge capacity (900 mAh $g^{-1}_{sulphur}$ 30 wt.% S versus 800 mAh $g^{-1}_{sulphur}$ for 40 wt.%) was observed with 30 wt.% and 40 wt% S. For 50 wt. % sulphur loading the discharge capacity was 600 mAh $g^{-1}_{sulphur}$, which may be due to the electronically insulating nature of S (figure 13(a)). A further increase of thickness to 65 μm reduces the discharge capacity to 250 mAh $g^{-1}_{sulphur}$. This decrease may be due to a longer and more tortuous ion pathway leading to salt depletion because of a low cation transference number. Also, the lack of back diffusion of polysulfide causes insulating layers and prevents utilization of the deeper-residing Sulphur, and the insulating nature of sulphur also plays an active role with an increase of thickness. The specific discharge capacity of all the cells is maintained at 100 − 400 mAh $g^{-1}_{sulphur}$ at 0.5 C and no capacity fading was observed after 50 cycles, irrespective of thickness or sulphur content (figure 13(c)).

Ibrahim *et al* [46] studied the effect of $LiPF_6$ on the PEO as polymer host. The highest conductivity is obtained at 4.1×10^{-5} S cm^{-1} for 20 wt.% of $LiPF_6$, and beyond that the decrease in conductivity is due to a decrease in the number of free charge carriers, which reduces the segmental motion of the polymer chain. Both the melting temperature and crystallinity show decreases, which is evidence of the enhancement of the amorphous phase.

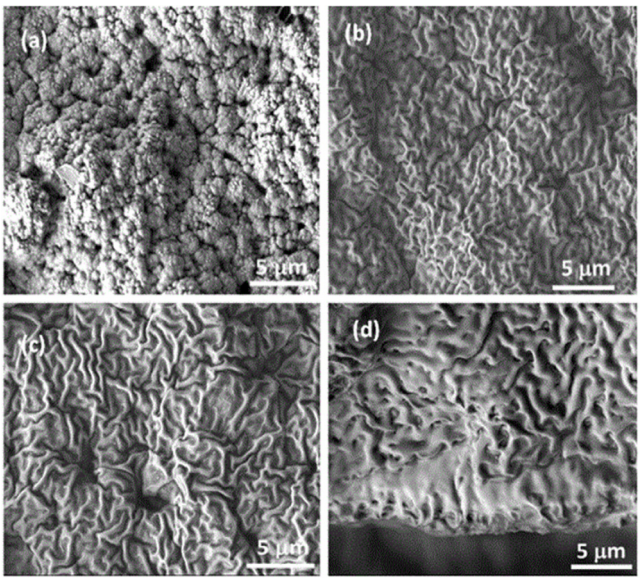

Figure 14. FE-SEM micrographs of PEO/(PVDF-HFP)-LITFSI-X wt.% PMIMTFSI solid polymer electrolytes: (a) X = 0, (b) X = 20, (c) X = 50, and (d) X = 50 (cross-section). Reprinted with permission from [49]. Copyright 2016, AIP Publishing LLC.

Thiam *et al* [47] prepared solvent-free and oligomer-free 3D polymer electrolytes. The DSC analysis shows decreases in T_m and ΔH_m. It may be due to the constraint produced by the cross-linking, which reduces the tendency of the chain

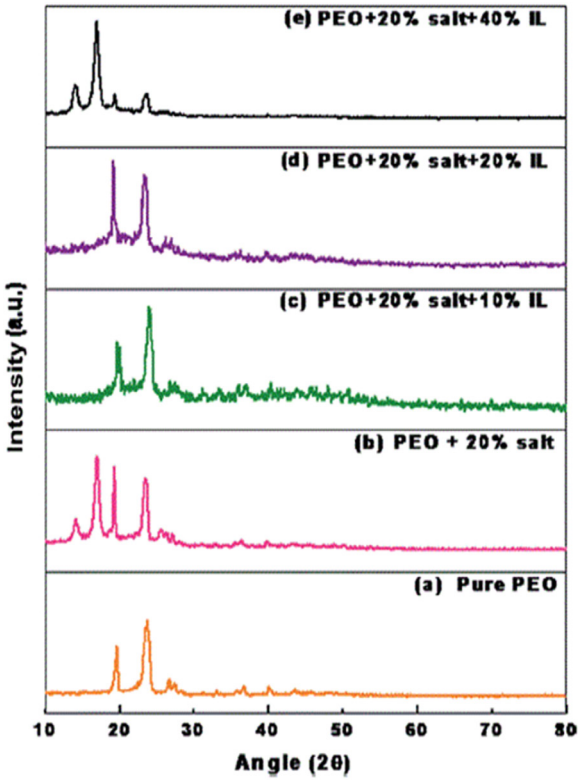

Figure 15. XRD pattern for (a) pure PEO and polymer electrolyte PEO + 20 wt% LiTFSI + X% IL (b) X = 0, (c) X = 10, (d) X = 20, (e) X = 40 at room temperature. Reproduced from [51] with permission of The Royal Society of Chemistry.

reorganization. Hydrogenation does not affect the glass transition temperature. The highest ionic conductivity was 1.7×10^{-4} S cm^{-1} and is the highest of the *r* network electrolytes. It was concluded that the network electrolyte is better than the other modified polymer electrolytes. Table 4 summarizes some important results of ionic conductivity, cation and ion transference numbers, thermal stability, voltage stability window and cyclic stability of the polymer salt complex.

4.2. Ionic liquid based polymer electrolytes

Ionic liquids are low-temperature molten salts and are characterized by weak interactions, due to the combination of a large cation and a charge-delocalized anion. The addition of salt to the pure polymer having an insulating nature is evidence of the increase of ionic conductivity, up to two or three orders in magnitude. So, the addition of an IL suppresses the crystallinity and promotes the release of a greater number of charge carriers. Another suitable approach is the incorporation of an IL (EMITf, EMIM-TY, BMPyTFSI $PYR_{13}FSI$ EMIMTFSI, BMITFSI) having a bulky cation and large anion in the polymer host. Also, the incorporation of an IL causes an overall increase in the ionic conductivity of an electrolyte system [22, 48].

Das *et al* [49] prepared a polyethylene oxide/poly (vinylidene fluoride-hexafluoropropylene)-lithium bis(trifluoromethane)sulfonamide as salt and a 1-propyl-3-methyleimidazoliuum bis(trifluromethylesulfonyl)- imide

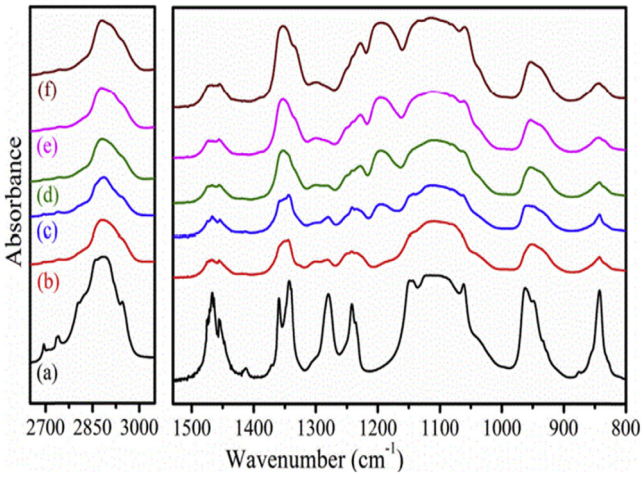

Figure 16. FT-IR spectra of (a) pure PEO and PEO20-LiDFOB-IL electrolyte membranes with different IL contents (b) 0%, (c) 10%, (d) 20%, (e) 30% and (f) 40%. Reprinted from [52], Copyright 2017, with permission from Elsevier.

(PMIMTFSI) ionic liquid. DSC analysis concluded that the decrease in glass transition temperature with the increase of IL content indicated an increase in polymer chain segmental motion and led to fast ion transport. The thermal stability of all samples was almost 350 °C and was almost independent of the content of the IL. Figures 14(a)–(d) show the FESEM images for varying IL contents; a sponge-like homogeneous structure with micropores is observed in the films and is attributed to the porous structure of the PVDF-HFP polymer. The addition of IL in the polymer salt system smoothens the surface, as evidenced by the decrease in crystallinity.

Chaurasia *et al* [50] investigated the modification in crystallization kinetics behavior of PEO + $LiClO_4$ with IL 1-ethyl-3-methylimidazolium hexafluorophosphate ($BMIMPF_6$) via an SC technique. A polarizing optical microscope (POM) showed spherulites (of the order of microns and millimeters) in the form of spherical aggregates of lamellae which evidenced the polymer crystallinity in the absence of pronounced stress or flow. The spherulites grew radially, which is a measure of the mechanism of crystallization in the polymer. It was observed that the growth is very fast for a 10 wt.% salt concentration, and the diameter increased from ~ 100 μm (within 10 s) to 310 μm (at 120 s). The addition of ILs in the polymer salt system reduced the spherulites size and increased the number of nucleating sites. The spherulites growth rate (G_s), obtained from the spherulite size versus time plot for the polymer salt system, was 1.77 μm s^{-1}, and decreased to 0.67 μm s^{-1} for the polymer salt with the ionic liquid. The decline in the G_s value indicated the incorporation of the IL in the polymer salt system, which hindered the spherulites' growth rate of the polymer PEO.

Gupta *et al* [51] prepared a polymer electrolyte using polymer poly (ethylene oxide) (PEO), lithium salt bis(trifluoromethylsulfonyl) imide (LiTFSI) and ionic liquid (IL) trihexyltetradeylphosphonium bis(trifluoromethylsulfonyl)imide via an SC technique. XRD analysis evidenced the simultaneous presence of a halo region and crystalline peaks, which indicated the semi-crystalline

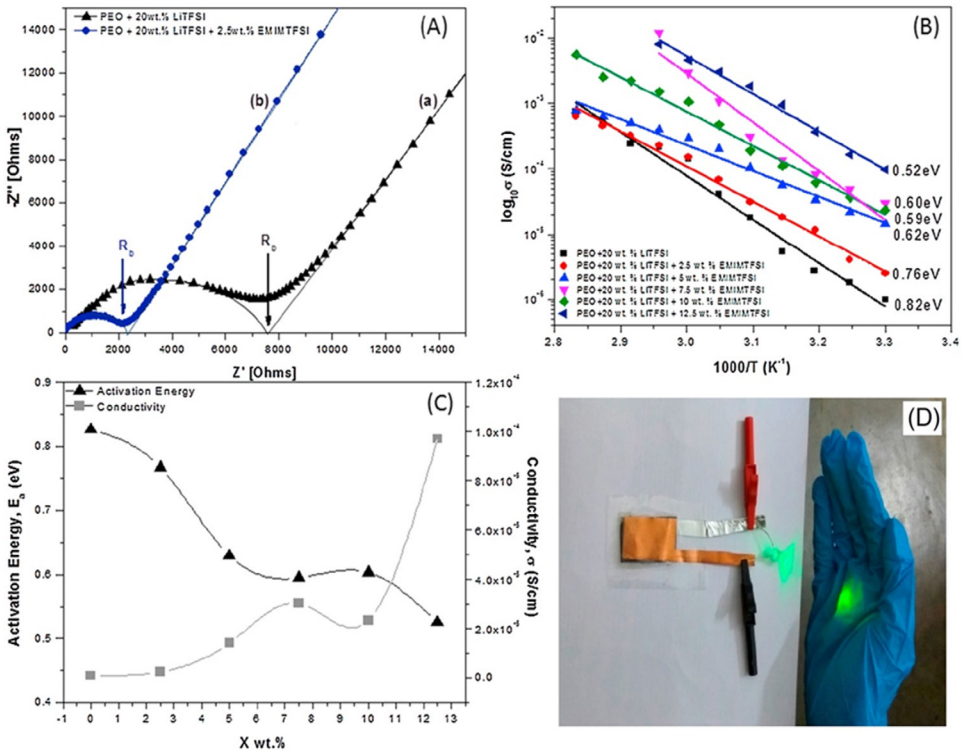

Figure 17. (A) Typical Nyquist plots of (a) PEO + 20 wt.% LiTFSI (b) PEO + 20 wt.% LiTFSI + 2.5 wt.% EMIMTFSI; (B) temperature dependent conductivity; (C) activation energy and room temperature conductivity of the GPE membranes PEO + 20 wt.% LiTFSI + *x*wt.% EMIMTFSI ($x = 0$, 2.5, 5, 7.5, 10 and 12.5) and (d) a prepared LPB cell (Li/PEO + 20 wt.% LiTFSI + 12.5 wt.% EMIMTFSI/$LiMn_2O_4$) in working condition. Reprinted from [53], Copyright 2017, with permission from Elsevier.

nature of the PEO and that the addition of IL enhanced the amorphous phase (figure 15). SEM analysis showed the ion association at high IL content due to recrystallization. All samples were thermally stable up to 350 °C. The cation transference number obtained was 0.37 and the ion transference number was 0.99. The highest conductivity was 4.2×10^{-5} S cm^{-1} for 20% IL, and ESW was 3.34 V.

Polu *et al* [52] investigated the effect of ionic liquid 1-ethyl-3-methyllimidazolium bis(trifluoromethylsulfonyl) imide (EMImTFSI) on poly(ethylene oxide) (PEO) + lithium difluoro(oxalato)borate (LiDFOB) based polymer salt matrix. XRD analysis indicated a decrease of crystallinity due to coordination interactions between Li^+ and $EMIm^+$ cations with ether oxygen atoms of PEO, leading to the fast segmental motion of polymer chains. The XRD analysis was supported by DSC, which showed a decrease of the melting peak area and supported the idea of fast ion transport with the incorporation of an IL. FTIR analysis confirmed the interaction between the ether group of the PEO with the cation of salt and the IL. The shift of the C–O–C stretching peak of PEO towards the lower wavenumber side evidenced the cation interaction with the ether group of the polymer host (figure 16). The addition of the IL increased ionic conductivity and was 1.85×10^{-4} S cm^{-1} at room temperature, attributed to an increase in the number of charge carriers with IL incorporation. Further, the increase of temperature increased the conductivity due to an increase of free volume owing to polymer expansion. A decrease of activation energy was seen from 0.68 to 0.447 with 40% IL content in the polymer salt matrix. Electrochemical analysis showed an initial specific capacity of 155 mAh g^{-1} at the low current rate for the 40% IL system up to 50 cycles, and after that the capacity was 134.2 mAh g^{-1}.

Balo *et al* [53] reported the preparation of a gel polymer electrolyte (GPE) based on polymer polyethylene oxide (PEO)-lithium bis(trifluoromethylsulfonyl) imide (LiTFSI) with ionic liquid (IL) 1-ethyl-3-methylimidazolium bis(trifluoromethylsulfonyl)imide (EMIMTFSI). A DSC study showed a decrease in T_g with an increasing amount of IL, which evidenced the enhancement of polymer flexibility and free volume, which supported the fast transport of ions in the polymer electrolytes. Also, the variation of crystallinity from 80% → 24.4% → 4.3% for pure PEO, PEO + 20 wt.% LiTFSI, and PEO+20 wt.% LiTFSI + 10 wt.% EMIMTFSI respectively, evidenced the intrachain and interchain hopping of ions due to the plasticization effect of ILs in the GPE. A TGA graph showed two decomposition temperatures T_{d1}(related to uncomplexed polymer) and T_{d2} (related to complexed polymer), and the stability of pristine PEO (334 °C) decreased to 309 °C on the addition of salt, due to low lattice energy and more dissolution of salt. All GPEs showed thermal stability up to 310 °C, with the highest being 363 °C for PEO + 20 wt.% LiTFSI + 5 wt.% EMIMTFSI. The conductivity increases with increases of both temperature and ionic liquid content may be attributed to increased polymer chain flexibility, due to the former and reduction of crystallinity by the latter. The room temperature conductivity of the sample, of 2.50×10^{-6} S cm^{-1} (PEO + 20 wt.% LiTFSI), increased to 1.43×10^{-5} S cm^{-1} (PEO + 20 wt.% LiTFSI + 2.5 wt.%

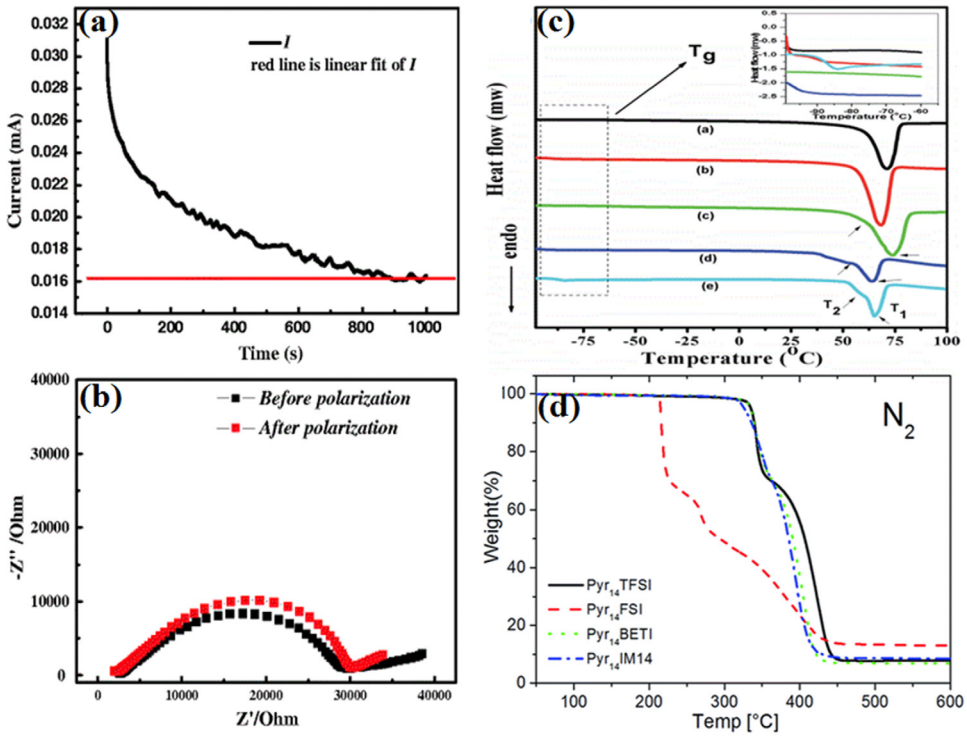

Figure 18. (a) Chronoamperometry of the cell with $P(EO)_{20}LiTFSI + PP1.3TFSI$ at 20 °C $\Delta V = 0.010\ V_{dc}$ pulse, (b) impedance response of the same cell before and after the DC polarization ([56] 2012 © Springer-Verlag 2012. With permission from Springer), (c) DSC thermograms of (a) pristine PEO (b) PEO + 20 wt.% BMIMMS (c) PEO + 10 wt.% NaMS (d) (PEO + 10 wt.% NaMS) + 20 wt.% BMIMMS and (e) (PEO + 10 wt.% NaMS) + 60 wt% BMIM-MS (Reproduced from [57] with permission of The Royal Society of Chemistry) and (d) TGA of polymer electrolytes in inert atmosphere. Scan rate 5 °C min^{-1}. Reproduced from [58]. CC BY 3.0.

IL) with a highest value of 2.08×10^{-4} S cm^{-1} at 12.5 wt.% ILs (figures 17(a)–(c)). The increase may be due to a lowering of activation energy with IL addition, and temperature variation showed Arrhenius type behavior. The total contribution in all GPEs was due to ions, as a high transport number ($t_{ion} > 0.99$) was observed, and a cation transference number ($t_+ = 0.39$). The ESW was around 4.6 V and is suitable for a battery application. The charge and discharge of PEO + 20 wt.% LiTFSI + 12.5 wt.% EMIMTFSI was performed in the range 2.0–4.0 V with a C/10 current rate. The discharge capacity at the first cycle was around 56 mAh g^{-1} due to the formation of a solid electrolyte interface, and 110 mAh g^{-1} in the fifth cycle and 120 mAh g^{-1} in the tenth cycle. The discharge efficiency (η) was more than 98% after 100 cycles, and cyclic performance was the same in both flat and bent conditions.

Cheng *et al* [54] reported the preparation of a $P(EO)_{20}$ LiTFSI based electrolyte with 1-butyl-4-methylpyridinium bis(trifluoromethanesulfonyl)imide (BMPyTFSI) ionic liquid using a solution casting method. The SEM analysis showed a loose and porous morphology for $P(EO)_{20}LiTFSI$ electrolyte, and the addition of ILs in the polymer salt matrix changed the morphology, resulting in a compact and smooth morphology. DSC analysis showed that the addition of BMPyTFSI in the polymer salt matrix weakened the interaction among the polymer chains and prevented polymer recrystallization. The ionic conductivity reported for the polymer salt complex at 40 °C was 1.6×10^{-6} S cm^{-1}, which increased to 6.9×10^{-4} S cm^{-1} with the addition of ILs. The low temperature increase in ionic conductivity is due to the high self-dissociating and ion-transporting abilities of the ionic liquid, while the high temperature increase is associated with polymer segmental motion and salt dissociation. The temperature dependence variation of the ionic conductivity followed the Vogel–Tamman–Fulcher (VTF) equation in the temperature range of 20–80 °C, and activation energy significantly decreased from 21.3 kJ mol^{-1} for the polymer salt matrix to 14.1 kJ mol^{-1} after the addition of the IL. The ESW for the polymer salt system was 4.8 V and increased to 5.3 V after the addition of ILs. This enhancement may be attributed to the formation of a stable passive layer.

Chaurasia *et al* [55] prepared PEO:IL (1-ethyl-3-methylimidazolium tosylate, EMIM-TY) based polymer electrolyte films by a solvent-free hot-pressing technique. The XRD pattern showed absolute peaks of the PEO in the range $2\theta = 15°$–$30°$, riding over a small 'halo' and indicating a partially amorphous phase. The addition of an ionic liquid in the polymer showed a shift and splitting in the PEO films and may be due to a change in PEO-structure geometry due to interaction and complexation with the IL. A new peak growth was seen at $2\theta \sim 16°$ on the addition of ionic liquid, and started growing in the (PEO + EMIM-TY) membranes at the expense of the intensity of prominent peaks of pristine PEO at 18.95° and 23.35°. This additional peak was evidence of PEO + EMIM-TY complex formation. The crystallinity calculated from XRD showed a decrease from 32% to 27% with the addition of up to 0.3 mol of $EMIMBF_4$ ILs, and from 83% to 64% with

20 wt.% ionic liquid EMIM-TY. DSC thermograms of pristine PEO showed an endothermic melting peak at 66.36 °C and the addition of ionic liquid (EMIMTY) resulted in the appearance of two endothermic peaks. The main peak T_{m1} was assigned to the melting temperature of crystalline (uncomplexed) pure PEO, whereas the second endothermic peak T_{m2} was assigned to the crystalline complexed material. The crystallinity of the polymer electrolyte membranes decreased with an increasing amount of ionic liquid (EMIM-TY) up to ~ 20 wt.% and after that it started to increase.

FTIR analysis indicated possible complexation between the ether group of the PEO and the end groups of the imidazolium cation ($EMIM^+$) of IL (EMIM-TY). The changes in the C–O–C vibrations of the PEO and C–H stretching vibrations of the IL cation aromatic ring clearly indicated that the polymer PEO complexes with the ionic liquid through the ether group of the PEO becoming loosely attached to the imidazolium ring of the IL cation ($EMIM^+$). The ionic conductivity of the polymer PEO was very poor (~ 5.8×10^{-8} S cm^{-1}) and increased considerably with an increasing amount of ionic liquid in the PEO membrane. At 40 wt.%, the ionic conductivity of the polymer electrolyte PEO + EMIM-TY membrane was ~ 2.87×10^{-5} S cm^{-1} at 30 °C. The increase in conductivity was due to an increased number of charge carriers provided by the higher concentration of the ionic liquid.

Yongxin *et al* [56] reported the preparation of new type of polymer electrolyte based on N-methyl-N-propylpiperidinium bis (trifluoromethanesulfonyl) imide (PP1.3TFSI), PEO, and lithium bis (trifluoromethanesulfonyl) imide (LiTFSI) as salt. Thermal analysis was done by TGA and all films were thermally stable up to 200 °C. FTIR analysis showed a decrease of crystallinity after incorporation of the IL in the polymer salt matrix. The addition of IL improved the ESW of the polymer salt system from 4.5 V to 4.7 V (versus Li/Li^+). The highest ionic conductivity obtained was ~ 2.06×10^{-4} S cm^{-1}, and was much greater than the polymer salt system, which had a conductivity value of only 3.95×10^{-6} S cm^{-1} at room temperature. The increase of temperature to 60 °C increased the ionic conductivity to 8.68×10^{-4} S cm^{-1}, and for the sample without IL it was 3.26×10^{-5} S cm^{-1}. The cation transference number of Li/P(EO)$_{20}$LiTFSI + 1.27PP1.3TFSI/Li cell (10 mV signal) was 0.339 and is suitable for battery applications, as shown in figures 18(a) and (b). Further, the electrochemical analysis was done and capacity was 120 mAh g^{-1} with stability up to 20 cycles with coulomb efficiency greater than 99%.

Singh *et al* [57] prepared a polymer electrolyte using a PEO as a host polymer, sodium methylsulfate (NaMS) as salt and 1-butyl-3-methylimidazolium methyalsulfate (BMIM-MS) as an IL. An SEM micrograph showed a change of the pure PEO surface from rough to smooth upon the addition of the IL, which indicated faster ionic transport and the absence of a crystal domain. The increase in FWHM and the absence of crystalline peaks corresponding to the PEO indicated an enhancement in the amorphous content of the polymer system, as evidenced by XRD. The DSC graph showed a decrease of melting enthalpy with the addition of the IL, which indicated a decrease of crystallinity. The decrease in the glass transition temperature suggested fast ion transport (figure 18(c)).

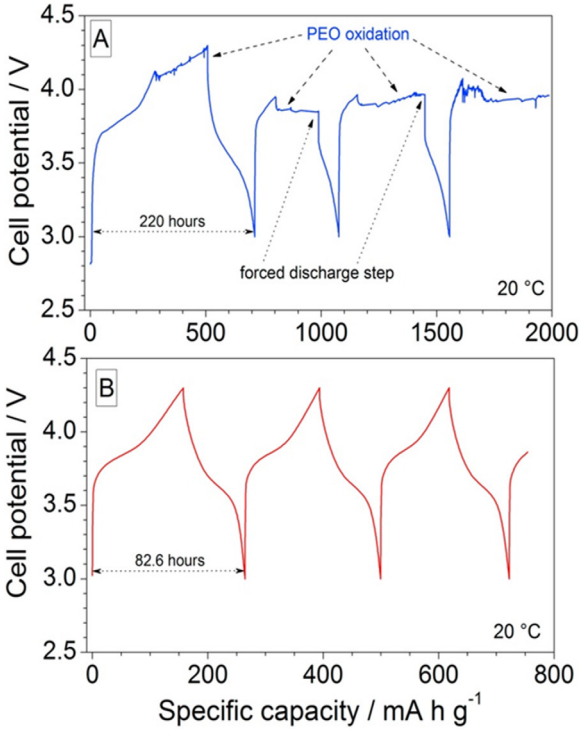

Figure 19. Voltage versus capacity profiles, obtained at 0.02 C and 20 °C, of Li/NMC half-cells with the PEO-E polymer electrolyte. Panel (A): cell tested as manufactured. Panel (B): cell kept in rest condition for more than one week before cycling tests. Reprinted from [59], Copyright 2017, with permission from Elsevier.

The thermal stability of all systems was above 300 °C, as measured by TGA. The highest ionic conductivity value was 1.05×10^{-4} S cm^{-1} for 60 wt.% of IL loading at room temperature. The cation transference number obtained was 0.46, and it was a good ionic conductor, with an ion transference number of 0.99. The ESW was 4–5 V and showed the applicability of the electrolyte for application in energy storage devices.

Vries *et al* [58] reported on ternary polymer electrolytes incorporating ionic liquids (cation: Pyr_{14} and Pyr_{1201}; anion: $(FSO_2)_2N^-$, $(C_2F_5SO_2)_2N^-$, $(C_4F_9SO_2)(CF_3SO_2)N^-$) in a poly(ethylene oxide) (PEO), lithium bis(trifluoromethanesulfonyl)imide (LiTFSI) based polymer salt system. A TGA analysis showed that all samples were thermally stable up to 200 °C and FSI^- containing samples had a lower thermal stability (figure 18(d)). The ionic conductivity obtained was 10^{-4} S cm^{-1} at room temperature and 10^{-3} S cm^{-1} at 60 °C.

Simoneeti *et al* [59] investigated a quaternary, polyethylene oxide (PEO)-LiTFSI based electrolytes with N-methyl-N-propylpyrrolidinium bis(fluorosulfonyl)imide ($PYR_{13}FSI$) as an ionic liquid. DSC analysis evidenced the formation of a heterogeneous phase and the reorganization of the internal structure of the polymer electrolyte was evidenced by a shift of the melting peak. An optical microscopy image for freshly prepared PEO electrolyte sample evidenced only modest IL phase separation, while upon two weeks of aging the presence of a large amount of segregated ionic liquid was confirmed. DSC analysis concluded that salt concentration increases the plasticizing effect and confirms the coexistence

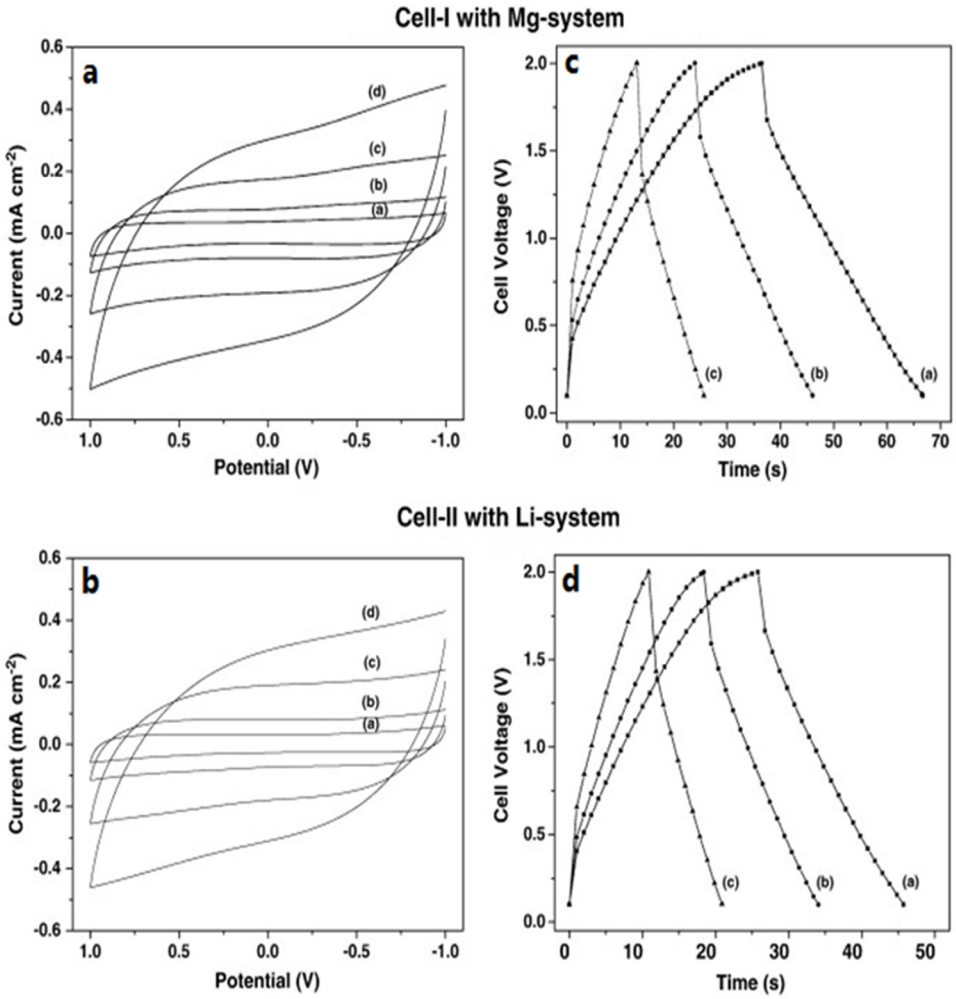

Figure 20. Cyclic voltammograms of (a) cell-I, (b) cell-II at different scan rates: (a) 10, (b) 20, (c) 50 and (d) 100 mV s^{-1} and charge–discharge characteristics of (a) cell-I, (b) cell-II at different current densities of (a) 150, (b) 200, and (c) 300 μA cm^{-2}. Reprinted from [64], Copyright 2011, with permission from Elsevier.

of heterogeneous phases. The analysis of impedance measurements showed conductivity values of 3.4×10^{-4} S cm^{-1} (−20 °C), 2.43×10^{-3} S cm^{-1} (20 °C), and 9.1×10^{-3} S cm^{-1} (60 °C), attributed to the formation of a 3D network of highly conductive IL pathways with increasing IL content. Also, no effect of prolonged storage periods was observed on the conductivity and impedance response, suggesting the presence of good ageing resistance. The thermal stability of all SPEs was up to 200 °C and was independent of ionic liquid concentration. The ESW was 4.5 V (versus the Li/Li^+ redox couple) and is attributed to release of the thin ionic liquid film during the phase separation process onto the external electrolyte surface, which prevented the contact of the PEO host with carbon. The role of ILs was further studied by manufacturing Li/NMC polymer cells, and up to 4.15 V a good profile was obtained and at high voltage a rough profile was obtained (figure 19(a)). For a second panel no evidence of oxidation or degradation was noticed in the range 3–4.0 V with a capacity value of 107 mAh g^{-1} (figure 19(b)), and may have been due to IL released by the PEO electrolyte bulk present in both the polymer separator and in the composite cathode. Another report by Simonnnet *et al* [60] reported the PEO-LiTFSI-PYR_{13}FSI-EC quaternary polymer electrolytes by the hot press method. The ionic conductivity obtained was 1.5×10^{-4} and 1.6×10^{-3} S cm^{-1} at −20 and 20 °C.

Choi *et al* [61] investigated the effect of room temperature IL 1-butyl-3-methylimidazolium bis(trifluoromethanesulfonyl) imide (BMITFSI) (between 20 and 80 parts by weight (pbw)) on the poly(ethylene oxide)-(lithium bis(trifluoromethanesulfonyl) imide) [PEO-LiTFSI] based polymer salt matrix using ball milling and a hot-pressing technique. They showed that the incorporation of ILs in the SPE significantly reduced the electrolyte resistance, and the effect was more noticeable at lower temperatures. The addition of ILs increased the ionic conductivity of the polymer salt complex from 4.0×10^{-6} S cm^{-1} (25 °C) to 3.9×10^{-3} S cm^{-1} (20 °C). The highest conductivity was found to be 3.2×10^{-4} S cm^{-1} (25 °C) and 3.2×10^{-3} S cm^{-1} (80 °C) for the PEO-LiTFSI-BMITFSI (80 °C) system. The increase of conductivity was attributed to the reduction of coordinating interaction of Li^+ ions with the O atoms of PEO segments and the anion of RTIL which led to a larger number of charge carriers supporting the fast ionic transport. CV data showed the enhancement of cathodic stability of RTIL below the plating potential

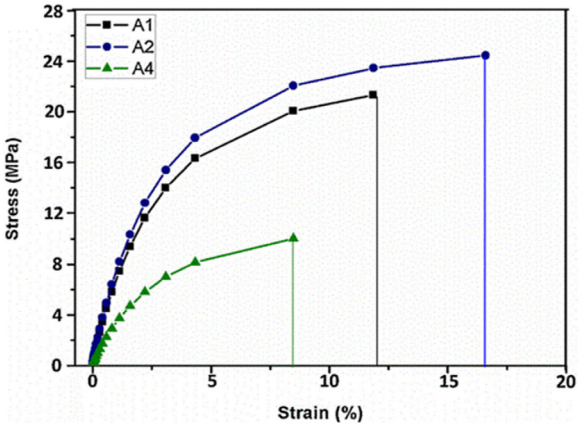

Figure 21. Stress–strain behavior of electrolyte samples A1 (polymer-salt), A2 (0 wt.% IL) and A4 (10 wt.% IL). Reprinted from [65], Copyright 2016, with permission from Elsevier.

of lithium on the addition in the polymer salt complex, and may have been due to the formation of a stable passivation layer on the lithium electrode which conducted Li^+ ion effectively but prevented further reaction with RTIL. The charge/discharge showed an initial discharge capacity of 90 mAh g^{-1} and increased to 140 mAh g^{-1} after five cycles.

The preparation of PEO–LiTFSI based polymer electrolytes by incorporating different N-alkyl-N-methylpyrrolidinium bis(trifluoromethanesulfonyl)imide, PYR1ATFSI ionic liquids was reported by Kim *et al* [62]. The ionic conductivity was $> 10^{-4}$ S cm^{-1} for all systems and the battery test of cell $Li/P(EO)_{10}LiTFSI + 0.96$ $PYR_{1A}TFSI/LiFePO_4$ showed capacities of 125 mAh g^{-1} and 100 mAh g^{-1} at 30 °C and 25 °C, respectively. Joost *et al* [63] reported the polymer electrolyte based on $PEO_{20}LiTFSI$ $[Pyr_{14}TFSI]_6$. The ionic conductivities obtained were 5.0×10^{-4} at 20 °C and 2.5×10^{-3} at 60 °C.

Pandey *et al* [64] reported the performance characteristics of electrical double layer capacitors (EDLCs) based on poly (ethylene oxide) (PEO)/ magnesium and lithium trifluoromethanesulfonate (triflate + ionic liquid 1-ethyl-3-methylimidazolium trifluoromethanesulfonate (EMITf) on multiwalled carbon nanotube (MWCNT) electrodes. The PEO complexes with Mg and Li salts and added ionic liquid EMITf were used to fabricate the EDLC cells with optimized compositions, namely: (a) $PEO_{25}{\cdot}Mg(Tf)_2$ + 40 wt.% EMITf, and (b) $PEO_{25}{\cdot}LiTf$ + 40 wt.%. EMITf had an ionic conductivity of ~ 10^{-4} S cm^{-1} at ambient temperatures. The PEO-$Mg(Tf)_2$ and PEO-$Mg(Tf)_2$-EMITf electrolytes offered less ionic conductivity compared to Li^+ ion conducting polymer electrolytes. The ESW was obtained by CV at the two scan rates of 1 and 5 mV s^{-1} and was of the order of 4 V for the Li^+ ion conducting polymer electrolyte. The stability window for the Mg^{2+} ion conducting polymer electrolyte was up to 4.8 V. The capacitance values calculated for both cells were ~ 0.03 F g^{-1} (for the Mg-system) and ~ 0.01 F g^{-1} (for the Li-system). The comparative analysis of the cells concluded that divalent Mg^{2+} ions also played an active role in the formation of a double layer and helped in the neutralization of more negative charges gathered at the electrode.

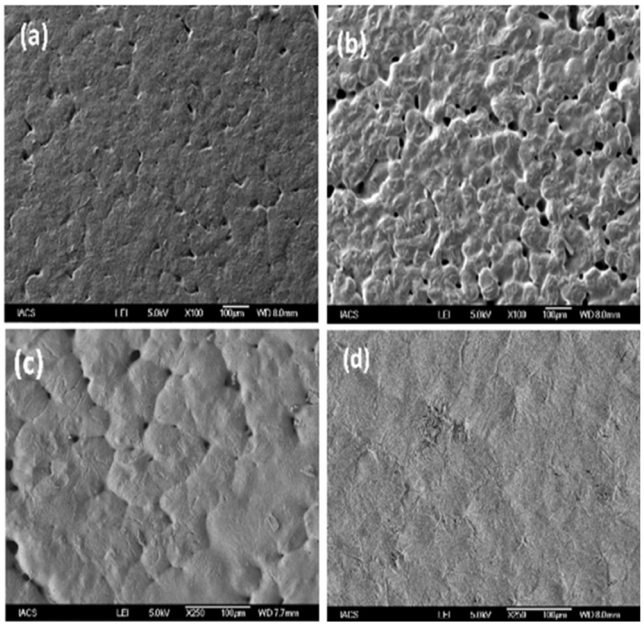

Figure 22. FE-SEM images of (a) PEO-$LiClO_4$ (b) PEO-$LiClO_4$-30 wt.% EC (c) PEO-$LiClO_4$-30 wt.% DMC (d) PEO-$LiClO_4$-30 wt.% PEG polymer electrolytes. Reprinted from [66], Copyright 2015, with permission from Elsevier.

Figures 20(a) and (b) show the cyclic voltamogram of both EDLC cells recorded in the potential range of −1.0 to 1.0 V at different scan rates. The mirror image symmetry observed in both cells evidences the capacitive behavior of the cells, with a double layer formation at the interfaces. But at a higher value of scan rate the slight deviation is due to the finite value of the equivalent series resistance (ESR) in polymer electrolyte based EDLCs. The capacitance value for Li^+ ion Cell-I is 3.1 F g^{-1}, and for Mg^{+2} cell-II it is 2.4 F g^{-1} at a scan rate of 10 mV s^{-1}, confirming the superiority of Mg-based electrolyte over Li ion-based. The performance of the cycle was tested for 50 cycles and confirmed the proper formation of the interfaces during the initial cycling process. The galvanostatic charge–discharge was performed from 0 to 2.0 V at room temperature (~ 25 °C), as shown in figures 20(c) and (d). The obtained capacitance value is in good agreement with CV studies. The high Columbic efficiency (η) of ~ 90% obtained from the charge–discharge experiment evidences the proper interfacial contacts between MWCNT electrode and both electrolytes.

The effect of EMImTFSI on the electrical, electrochemical and interfacial properties of $(PEO)_8LiTFSI$-10% NC based polymer electrolyte was reported by Karuppasamy *et al* [65]. XRD analysis suggested the complete dissolution of salt in the polymer matrix. Further addition of ionic liquid decreased the crystallinity of polymer and also disrupted the polymer chain reorganization tendency which supports fast ionic transport or conductivity. The addition of IL also enhanced the polymer flexibility and segmental motion, as evidenced by DSC analysis. To support the XRD and DSC data, FTIR was carried out, which provided strong evidence of a decrease of crystallinity in terms of shifting and decrease of intensity of peaks. Stress–strain behavior showed elongation and strains at break

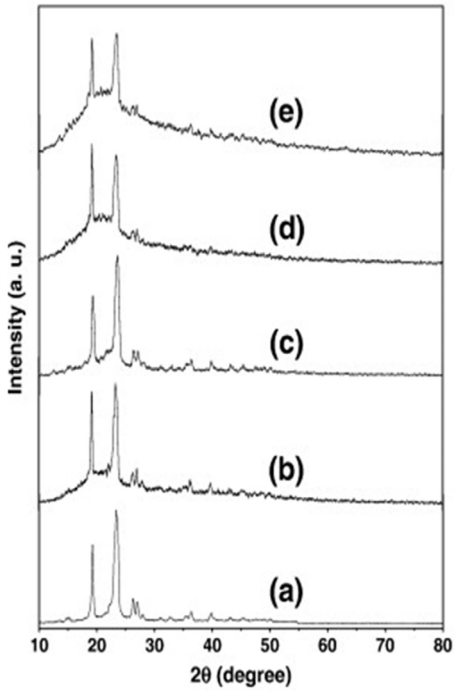

Figure 23. XRD pattern of (a) pure PEO, (b) $(PEO)_{25}$.LiTf complex and $(PEO)_{25}$.LiTf + *x*wt.% EMITf system for (c) $x = 5$, (d) $x = 20$, and (e) $x = 40$. Reprinted from [67], Copyright 2011, with permission from Elsevier.

of 24 MPa and 8% for electrolyte with 0% IL. After the addition of IL, the elongation and strain at break were 10 MPa and 12%. This reduction in mechanical strength may be due to the higher plasticization and increased polymer chain flexibility (figure 21). The highest ionic conductivity obtained was of the order of 10^{-2} S cm^{-1} at 343 K for 10 wt.% IL content, and ESW was 3.97 V.

4.3. Gel polymer electrolyte

The addition of salt to the pure polymer having an insulating nature increased ionic conductivity by up to two or three orders. So, the addition of a low molecular weight plasticizer/ionic liquid suppresses the crystallinity and promotes the release of a greater number of charge carriers. There are various plasticizers, such as EC, PC, DEC, PEGDME, PEG, SN and ionic liquid, which are reported to enhance conductivity and battery performance. The main role of plasticizer is to increase the free volume which provides an easy path to the cation for migration within the electrolyte system. The enhanced amorphous phase content is also related to enhanced ionic conductivity and may be due to more dissociation of salts to release more free charge carriers, which are required for a highly efficient system.

The effect of poly ethylene glycol, propylene carbonate, ethylene carbonate and dimethyl carbonate on a PEO-$LiClO_4$ based polymer electrolyte was reported by Das *et al* [66]. The simultaneous presence of crystalline and amorphous regions of the polymer was confirmed by SEM images. The smooth surface morphology after addition of salt was an indication of enhanced amorphous content via the interaction between ether oxygen of PEO and Li^+ ions. Also the PEG plasticizer led to smoother surfaces in comparison to other plasticizers (figure 22). Also the temperature dependent ionic conductivity for all plasticized polymer electrolytes followed the well known VTF relation, which was evidence of the confirming coupled motion of Li^+ ions and segment of the polymer chain.

Kumar *et al* [67] reported the preparation of lithium ion conducting polymer electrolytes based on polyethylene oxide (PEO)–lithium trifluoromethanesulfonate ($LiCF_3SO_3$ or LiTf) with an ionic liquid 1-ethyl 3-methyl imidazolium trifluoromethanesulfonate (EMITf). The optical micrographs of pure PEO film show the spherulitic texture of the PEO along with dark boundaries indicating the amorphous content in the polymer. Further addition of salt resulted in a larger proportion of dark boundaries or regions which evidenced the increase of amorphous content, while for the large content of ionic liquid, a mud-like dense liquid wrapped around the spherulites was observed. A broad hump observed between 15° and 30° suggested a partially amorphous nature of the polymer and the addition of salt increased the intensity (figure 23). Further addition of ILs increased the intensity of the hump and showed a decrease in the degree of crystallinity of the polymer electrolyte. The presence of crystalline peaks even after the addition of high content of ILs was evidence of the persistence of the crystalline nature of the plasticized PEO-complex and is in correlation with the optical micrograph. FTIR spectra indicated a change in the band corresponding to the polymer host which indicated the presence of interactions of ionic liquid component ions with the host polymer PEO. The presence of two bands at 749 and 757 cm^{-1} were due to pure PEO (CH_2 rocking mode), and PEO_{25}-LiTf complex ($\delta_{s\text{-}CF3}$ mode of vibration of free triflate ions) predicted that some proportion of pure PEO was left un-complexed in the PS complex and the further addition of ILs in the PS complex resulted in the disappearance of the un-complexed PEO peak, which confirmed the interaction of ILs cation with the ether group of the PEO.

Raman analysis evidenced the interaction of the PEO with the ionic liquid EMITf. Then the addition of salt in the pure polymer reduced the peak at 1062 cm^{-1} and another peak appeared at 1033 cm^{-1} corresponding to the SO_3 stretching mode of free triflate anions. The additional peaks observed in Raman (1033 cm^{-1}) and FTIR (1016 cm^{-1}) on the addition of EMITf were due to the vis-à-vis reduction of intensity of the PEO peak at 1062 cm^{-1} and confirmed the interaction of the PEO with the ionic liquid EMITf.

The thermal stability of pure PEO was ~340 °C and increased to ~375 °C upon the addition of salt. Further addition of ILs in polymer salt complexes reduced thermal stability to ~350 °C due to the volatility of ILs. DSC analysis showed a decrease of the melting peak corresponding to pure PEO from ~69 °C to ~62 °C upon the addition of salt. Further addition of ILs decreased the endothermic peak and indicated disruption of the polymer chain. The crystallinity of pure PEO film decreased from ~ 89% to 71% upon the addition of salt, while at high ILs content crystallinity was 22%. The addition of salt in the pure polymer host increased the T_g and indicated a reduction in the flexibility of PEO chains, due to crosslinking

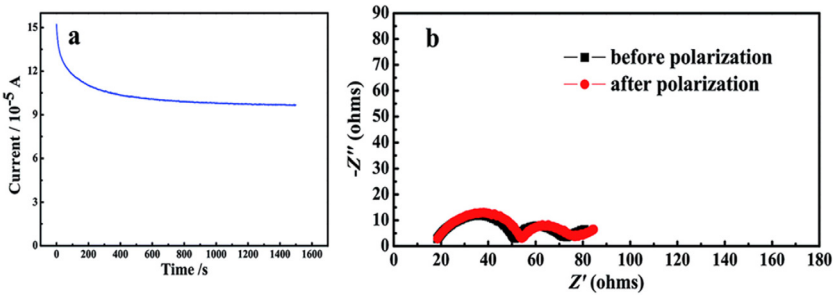

Figure 24. (a) Chronoamperometry profiles for the GPE at 25 °C in block cells using Li metal as both electrodes with step potential of 10 mV. (b) Nyquist profiles of the cell electrochemical impedance spectroscopy response before and after polarization. Reproduced from [68]. CC BY 3.0.

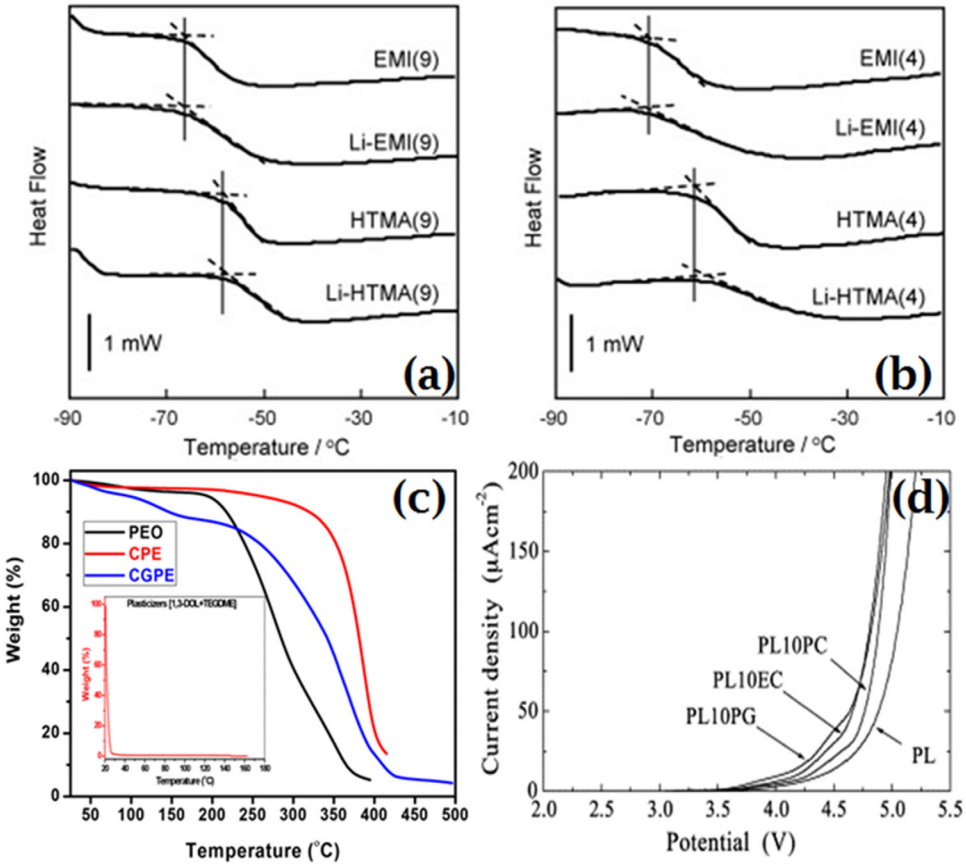

Figure 25. DSC profiles of ionic liquid/PEO-PMA gel electrolytes on heating. Heating rate: 10 °C min^{-1} (a) PEO-PMA matrix with $n = 9$, (b) PEO-PMA matrix with $n = 4$ (Reprinted from [70], Copyright 2008, with permission from Elsevier), (c) thermogravimetric analysis of PEO, CPE (0% plasticizer), and CGPE (20% plasticizer) ([71] John Wiley & Sons. © 2016 Wiley Periodicals, Inc.) and (d) onset potentials for oxidative degradation of the Li/SPE/SS cells at 80 °C. Reprinted from [73], Copyright 2002, with permission from Elsevier.

of the polymer through the salt. Further, the addition of ILs decreased T_g, suggesting an increase in polymer flexibility.

The addition of salt increased the ionic conductivity, and the highest conductivity was ~ 3×10^{-4} S cm^{-1} for 40 wt.% ILs content. The σ versus $1/T$ variation showed a sudden jump at ~ 60–65 °C for all the polymer electrolyte films, which was attributed to jumping from semi-crystalline to amorphous (i.e. solid to liquid) phase transition at T_m of the PEO. The decrease of height of this jump with increasing IL content is associated with enhancement of amorphous content and shows Arrhenius-type behavior. The lowest value of activation energy obtained was for 5 wt.% IL content, and a further increase of IL content almost saturated the activation energy value.

The total ionic transference number obtained was found to be > 0.99, and evidenced the dominance of ionic conduction in the polymer electrolyte. The effect of temperature and ionic liquid ion mobility was studied by using ^{7}Li NMR. The ^{7}Li NMR absorption spectra of the polymer salt system showed a narrow line width with an increase of temperature to 100 °C. A decrease in the line width with a gradual increase in temperature evidenced the increase in Li mobility with increasing temperature. A narrow line width for the IL-doped polymer

salt matrix revealed an increase in ion mobility as well as the role of IL as a plasticizer; hence the increase in polymer flexibility and a decrease of viscosity. The ESW was studied by CV and was in the range of −1.4 to 1.6 V (i.e. ~3.0 V) for the polymer salt complex. Further, the addition of ILs increased the voltage window from −2.6 to 2.3 V (i.e. ~ 4.9 V).

Li *et al* [68] reported the preparation of GPE using PEO as host polymer and $LiPF_6$ as liquid electrolyte solution via an *in situ* polymerization method. SEM images of GPE evidenced that a uniform structure is an indication of favorable transport for Li^+. The electrochemical window of GPE was measured by LSV and was 4.9 V. The ionic conductivity obtained was 3.3×10^{-3} S cm^{-1} and was independent of temperature. The high cation transference number of 0.76 indicates its suitability for the application (figure 24). The electrochemical profile shows that the reversible capacity of the $LiFePO_4$ at 0.5 C for GPE is 133 mAh g^{-1}. The discharge capacity is 103 mAh g^{-1} after 500 cycles with the capacity retention of 81%.

Zhu *et al* [69] reported the preparation of two types of gel polymer electrolyte by incorporating 1-ethyl-3-methylimidazolium bistrifluoromethanesulfonylimide (EMI-TFSI) and N-methyl-N-propylpiperidinium bistrifluoromethanesulfonylimide (PP_{13}-TFSI) in PEO as polymer host by an SC technique. DSC analysis concluded that both ILs weakened the mutual interaction between polymer chains and disrupted the polymer crystallization. The ionic conductivity achieved was 10^{-5} S cm^{-1} at room temperature and the maximum for PEO_{20}LiTFSI + 1.0 EMI-TFSI was of the order of 2.67×10^{-4} S cm^{-1} at 40 °C. After the incorporation of ILs, the decomposition voltage reached was up to 5.2 V. The discharge profiles for the cell $LiFePO_4/PEO_{20}$LiTFSI + 1.0EMI-TFSI/Li showed a specific capacity of 132 mAh g^{-1} at a 0.05 C rate, with a voltage of about 3.4 V versus Li/Li^+. After an increase in C-rate up to 0.2, the capacity obtained was 117 mAh g^{-1}.

Egashira *et al* [70] reported the preparation of gel polymer electrolyte using two kinds of ionic liquid having different cations (EMITFSI and HTMATFSI), and poly(ethylene oxide) branched poly(methyl methacrylate) (PEO-PMA) using ion-exchange reaction. The DSC graph of the gel electrolyte is shown in figures 25(a) and (b). The peak corresponding to the glass transition temperature showed a noticeable shift depending on both polymer matrices, the ionic liquid component and the existence of LiTFSI. The highest ionic conductivity obtained was 2.3×10^{-4} S cm^{-1} and the lowest activation energy was 30 kJ mol^{-1}, for the Li-EMI(9). It was concluded that the quaternary ammonium-based ionic liquid is better than the imidazolium-based ionic liquid for enhancing ion mobility, hence the ionic conductivity.

Natarajan *et al* [71] reported the composite gel polymer electrolyte using magnesium aluminate ($MgAl_2O_4$) and LiTFSI as salt with a combination of 1,3-dioxolane (DOL) and tetraethylene glycol dimethyl ether (TEGDME) as a plasticizer by a simple solution casting technique. The smoother surface seen by FESEM showed better ionic conductivity in the case of the composite gel polymer electrolyte. The thermogravimetric curves showed improved thermal stability as compared to the pure PEO (figure 25(c)). The addition of plasticizer had almost no effect on the glass transition temperature and may be due to the formation of an amorphous phase by the addition of salt in the polymer matrix. The highest ionic conductivity was obtained for 20 wt.% of plasticizer and was of the order of 3.4×10^{-4} S cm^{-1} at 30 °C.

Jayasekara *et al* [72] synthesized an interpenetrating network structure where rods of polymer electrolyte were placed in the nanoscale channels of anodic aluminum oxide (AAO) membranes, using PEO as polymer and lithium triflate ($LiSO_3CF_3$) as salt. The highest ionic conductivity obtained was 5×10^{-4} S cm^{-1} and is four orders higher than the pure polymer electrolyte. The decrease of the melting point observed from the DSC analysis suggests the decrease of crystallinity. The crystalline thickness plays an important role in ion conduction, and was 4 nm for the polymer electrolyte with AAO membrane as compared to 20 nm for the pure PEO, and was an indication of enhanced amorphous content.

Kim *et al* [73] investigated the effect of EC, PC, and PG on PEO-$LiN(CF_3SO_2)_2$ (LiTFSI) based polymer matrix. The cation transference number with PG was 0.516 which was greater than that of the plasticizer-free electrolyte (0.487), while for EC and PC it was 0.381 and 0.262, respectively. The ionic conductivity and diffusion coefficient was also higher for electrolyte doped with PC, which may be due to the interaction of PC with the host polymer and salt [74]. The interaction of PC with the PEO disrupts the coordination interaction between the cation and the PEO, which enhances the ion mobility. Later one reduces the ion pairing effect and more free charge carriers are released. The ESW for all samples was ~ 4 V at 80 °C (figure 25(d)).

Ma *et al* [75] synthesized TiO_2-grafted NHPE comprising of ion-conducting poly(ethyleneglycol) methyl ether methacrylate (PEGMEM) and non-polar stearyl methacrylate (SMA) using an *in situ* polymerization/crystallization method. The successful synthesis of a TiO_2-grafted PEGMEM/SMA nanohybrid was confirmed by ^{1}H-NMR spectroscopy and FTIR spectroscopy. It was noted that 5 wt.% TiO_2-grafted NHPE offered the highest ionic conductivity of 0.74×10^{-4} S cm^{-1} at 25 °C, of the PEGMEM/SMA polymer electrolyte, and the conductivity increased to 1.10×10^{-4} S cm^{-1} at 30 °C. Also, the decrease in activation energy from 5.51 → 4.86 kJ mol^{-1} confirmed that lithium ions have more mobility in TiO_2-grafted NHPE. The charge–discharge study shows that the cell delivers an initial discharge capacity of 153.5 mAh g^{-1} at 1 C with a capacity retention of 96% after 300 cycles (figure 26).

The addition of plasticizer in $(PEO)_9$-LiTf + 10 wt.% TiO_2 polymer matrix showed that the meting point (T_m) decreased from 60 °C to 50 °C and the glass transition temperature (T_g) from −46 °C to −50 °C on the addition of 50 wt.% plasticizer [76]. EC was chosen as the plasticizer due to its low viscosity compared to other plasticizers. This reduction in T_g weakened the complexation between Li^+ ions and the polymer chain, enhancing cation migration. Conductivity was also enhanced to 1.6×10^{-4} S cm^{-1} on the incorporation of 50 wt.% EC plasticizer. The addition of plasticizer enhances the amorphous phase, as evidenced by a decrease in T_g.

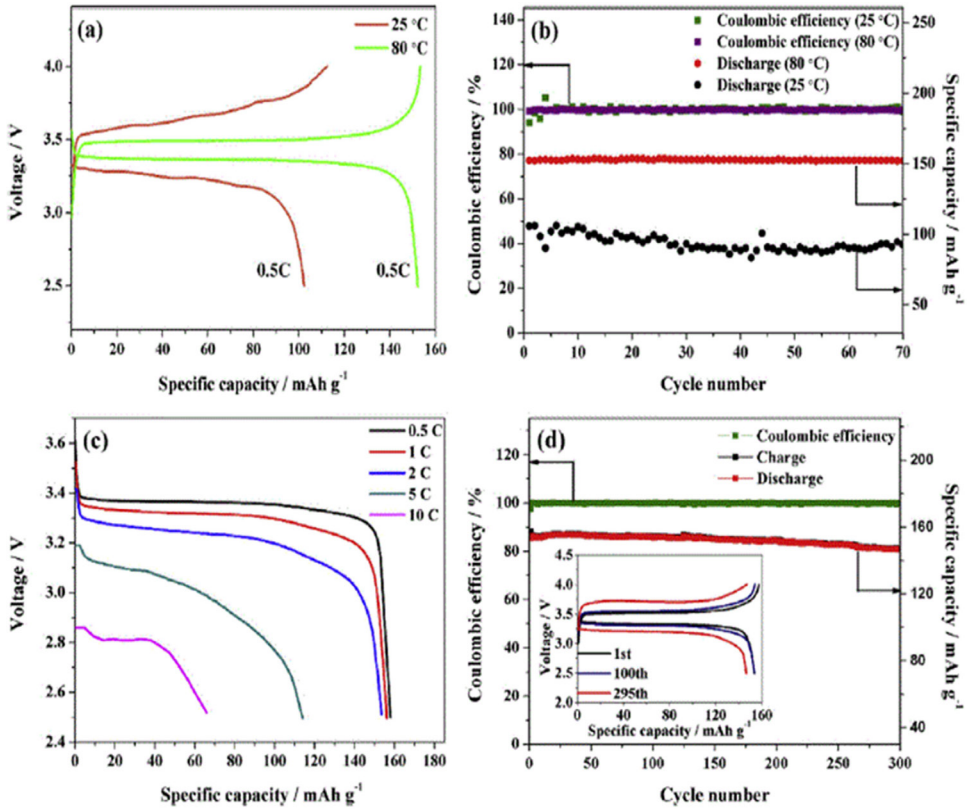

Figure 26. (a) Initial charge–discharge profiles and (b) cycling performance of $LiFePO_4$/Li cells using TiO_2-grafted NHPE at 25 °C and 80 °C at 0.5 C. (c) Discharge curves for $LiFePO_4$/TiO_2-grafted NHPE/Li cell at various C-rates and 80 °C. (d) Cycling stability of $LiFePO_4$/TiO_2-grafted NHPE/Li battery at 1 C and 80 °C. Inset: charge/discharge curves at different cycles. Reprinted from [75], Copyright 2016, with permission from Elsevier.

Bandara *et al* [77] synthesized composite polymer electrolyte using the PEO, alumina nano-fillers and tetrapropylammonium iodide as salt. The highest conductivity was obtained for the 5 wt.% alumina nanofiller and was 2.4×10^{-4} S cm^{-1}, 3.3×10^{-4} S cm^{-1} and 4.2×10^{-4} S cm^{-1} at 0 °C, 12 °C and 24 °C, respectively. The enhancement in conductivity may be due to the formation of conducting paths by the nanofiller surface. Also the activation energy was smaller for the 5 wt.% alumina and was 0.20 eV. This reduction in activation energy promoted fast ion transport or a high ionic conductivity.

Chen *et al* [78] investigated the effect of succinonitrile (SN) plasticizer on PEO-LiTFSI-1% LGPS based polymer electrolyte prepared by an SC technique. A DSC analysis indicated that SN played an active role in increasing the flexibility of polymer chains and a more amorphous phase was formed. Also, the addition of SN reduces the interaction of cations with the ether group of the polymer, which supported the faster migration of ions. Initially, up to 10% SN, crystallinity decreased but at higher concentrations the increase in crystallinity was due to the dominance of the insulating nature of SN, which blocked conducting pathways. The maximum ionic conductivity was 1.58×10^{-3} S cm^{-1} at 80 °C and 9.10×10^{-5} S cm^{-1} at 25 °C for 10% SN. The increase in conductivity was due to an increase of the fraction of an amorphous phase, and was supported by DSC data. The decrease of conductivity at the higher content of SN was due to non-ionic plastic crystal nature, which led to the insulating nature of SN and blocked the free ions. The SPE was thermally stable up to 255 °C and electrochemically up to 5.5 V. The cycling and rate performance of the solid-state lithium battery Li/PEO_{18}-LiTFSI-1% LGPS-10% SN/$LiFePO_4$ is presented in figures 27(a)–(d) and the specific capacities were 158.1, 144.0, 133.3 and 86.2 mAh g^{-1} at 0.1, 0.2, 0.5 and 1 C. The discharge specific capacity was still maintained at 152.1 mAh g^{-1} after 60 cycles, and was 94.7% of the maximum specific capacity with 99.5% coulombic efficiency. At high rate (0.5 C) the reversible capacity increased due to the activation process. The discharge capacity after 100 cycles was 120 mAh g^{-1}, which was an excellent performance for the prepared SPE.

Pitawala *et al* [79] reported on the combined effect of nanofiller (Al_2O_3) and plasticizer (EC) on $(PEO)_9$-LiTf ($O/Li^+ = 9$) based SPE. The maximum conductivity was 2.1×10^{-5} S cm^{-1} obtained for 15 wt.% nanofiller. The conductivity enhancement was higher for nanofiller based polymer electrolyte than plasticized polymer electrolyte. The loss of mechanical property due to the addition of plasticizer was regained by the addition of nanofiller. Lewis acid base type interactions provided a favorable additional site for cation migration, while plasticizer enhanced the amorphous phase, as was evident from DSC data. The addition of DOP plasticizer provided the highest ionic conductivity value, of 7.60×10^{-4} S cm^{-1} for PEO-15 wt.% ($LiCF_3SO_3$) + 20 wt.% DOP, as reported by Klongkan [76]. The addition of DOP plasticizer in a PEO-15 wt.% ($LiCF_3SO_3$) SPE showed a drop in strength, elongation, and Young's modulus due to the greater mobility of the polymer chains provided by polymer–plasticizer

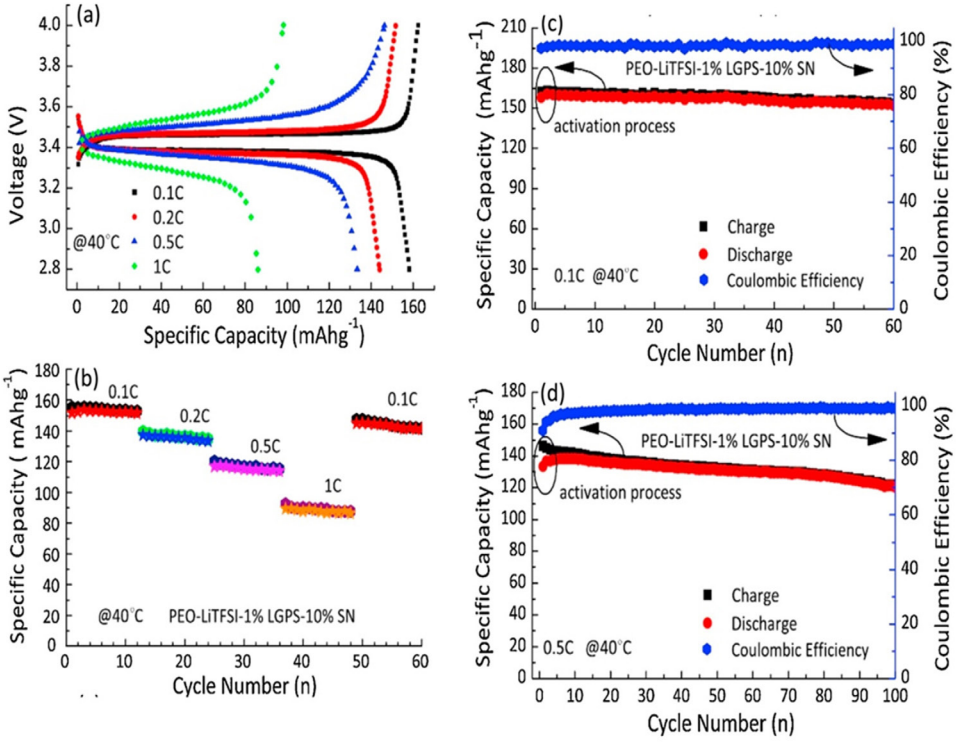

Figure 27. The cycling and rate performance under 40 °C for all-solid-battery Li/PEO_{18}-LiTFSI-1%LGPS-10%SN/$LiFePO_4$; (a) the initial charge and discharge curves under different rates (0.1 C, 0.2 C, 0.5 C, 1 C); (b) the rate cycling performance of the all-solid-battery cell; (c) cycling performance at 0.1 C; (d) cycling performance at 0.5 C. Reprinted from [78], Copyright 2016, with permission from Elsevier.

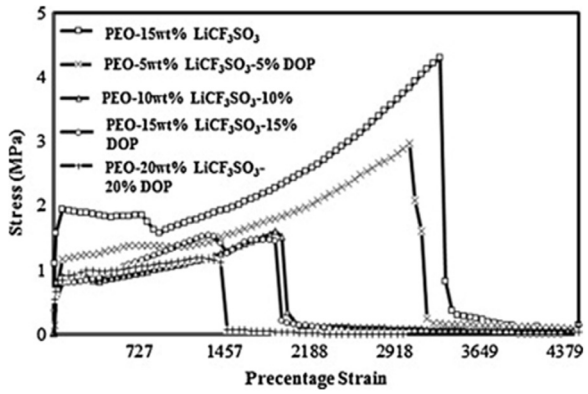

Figure 28. Tensile stress–strain behavior of PEO_{-15} wt% ($LiCF_3SO_3$)-*z* (DOP) solid polymer electrolytes. Reprinted from [76], Copyright 2015, with permission from Elsevier.

interactions, which make the sliding of chains easier by reducing the friction (figure 28). Some important results in terms of ionic conductivity, cation and ion transference numbers, thermal stability, voltage stability window and cyclic stabilities of ionic liquid and gel polymer electrolytes are summarized in table 5.

4.4. Solid polymer electrolyte

As discussed above, a lot of work was done on the addition of ILs and plasticizer in polymer salt sytems. Although they have sufficient ionic conductivity and stability windows, poor mechanical strength and thermal stability led the researchers to make a polymer electrolyte system with improved electrochemical and mechanical properties. The ultimate solution for the above is the preparation of SPEs by the addition of nanofiller and nanoclay. The addition of nanofiller will result in improved properties by the presence of various interactions between the surface group of nanofiller and the polymer salt system [76, 80, 81]. The increase in amorphous content by the addition of nanofiller will lead to enhanced conductivity along with mechanical strength. Incorporation of nanoclay is also an important approach for the enhancement of overall properties. The negative surface charge present in the clay galleries provides space for the intercalation of polymer chains. Also the thermal stability is improved due to presence of polymer chains between the clay galleries. Both these approches and their effect on the PEO properties is discussed in the following section.

4.4.1. Dispersed type polymer electrolyte. We have discussed the polymer salt system and ionic liquid based system. The addition of ionic liquid/plasticizer imrpoves the ionic conductvity but the mechanical properties are disturbed, which affects the performance of the battery system. So, the alternative to this drawback is the use of nanofiller in the polymer salt system, which is one of the best approaches for improving the electrochemical properties as well as mechanical properties. A lot of of work has been done towards enhancement of electrical conductivity, ESW, thermal stability and mechanical stability.

Nanofillers are classified into two types on the basis of support to the transport of ions in the polymer matrix; one is involved in ionic transort and is called active nanofiller

Table 5. Ionic conductivity, cation/ion transference number, thermal stability, voltage stability window and cyclic stability of ionic liquid and gel polymer electrolytes.

Materials used	Electrical conductivity (S cm^{-1})	Transference number (ion/cation)	Electrochemical stability window	Thermal stability	Cyclic stability	Ref.
PEO-LiTFSI-IL	4.2×10^{-5} S cm^{-1}	0.99/0.37	3.34	350 °C	—	[51]
PEO-LiDFOB- EMImTFSI	1.85×10^{-4} S cm^{-1}	—	—	—	Initial specific capacity 155 mAh g^{-1} up to 50 cycles.	[52]
PEO-LiTFSI- EMIMTFSI	2.08×10^{-4} S cm^{-1}	0.99/0.39	4.6	—	The discharge capacity at first cycle is 56 mAh g^{-1} and 120 mAh g^{-1} in the 10^{th} cycle. The discharge efficiency (η) was more than 98% after 100 cycles	[53]
$P(EO)_{20}$LiTFSI-BMPyTFSI	6.9×10^{-4} S cm^{-1} at 40 °C	—	4.8–5.3	—	—	[54]
$P(EO)_{20}$LiTFSI + 1.27PP1.3TFSI	2.06×10^{-4} S cm^{-1}, 8.68×10^{-4} S cm^{-1} at 60 °C	0.339	4.5–4.7	200 °C	Capacity 120 mAh/g with coulomb efficiency greater than 99%.	[56]
PEO-NaMS-BMIM-MS	1.05×10^{-4} S cm^{-1}	0.99/0.46	4–5	300 °C	—	[57]
PEO-LiTFSI-PYR_{13}FSI	3.4×10^{-4} (−20 °C), 2.43×10^{-3} (20 °C) S cm^{-1}, 9.1×10^{-3} S cm^{-1} (60 °C)	—	4.5	200	Capacity 107 mAh g^{-1}	[59]
PEO-LiTFSI-PYR_{13}FSI-EC	1.5×10^{-4} and 1.6×10^{-3} S cm^{-1} at −20 and 20 °C	—	—	—	—	[60]
PEO-LiTFSI-BMITFSI	3.2×10^{-4} S cm^{-1} (25 °C) and 3.2×10^{-3} S cm^{-1} (80 °C)	—	—	—	initial discharge capacity of 90 mAh/g and increases to 140 mAh g^{-1} after 5 cycles.	[61]
PEO-LiTFSI-PYR1ATFSI	$>10^{-4}$ S cm^{-1}	—	—	—	capacity of 125 mAh g^{-1} and 100 mAh g^{-1} at 30 °C and 25 °C	[62]
PEO_{25}·LiTf + 40 wt.%. EMITf	10^{-4} S cm^{-1}	—	4	—	3.1 F g^{-1}, Columbic efficiency (η ~90%	[64]
PEO-$Mg(Tf)_2$-EMITf	—	—	4.8	—	2.4 F g^{-1}, Columbic efficiency (η) ~90%	[64]
$(PEO)_8$LiTFSI- EMImTFSI	10^{-2} S cm^{-1}	—	3.97	—	—	[65]
PEO-LiTf- EMITf	3×10^{-4} S cm^{-1}	0.99	4.9	—	—	[67]
PEO- $LiPF_6$ as liquid electrolyte solution	3.3×10^{-3} S cm^{-1}	0.76	4.9	—	reversible capacity 133 mAh g^{-1} and discharge capacity 103 mAh g^{-1} after 500 cycles. Capacity retention 81%.	[68]
PEO_{20}LiTFSI + EMI-TFSI	2.67×10^{-4} S cm^{-1} at 40 °C	—	5.2	—	specific capacity of 132 mAh g^{-1} at a 0.05 C rate	[69]
PEGMEM/SMA	1.10×10^{-4} S cm^{-1} at 30 °C	—	—	—	initial discharge capacity of 153.5 mAh g^{-1} with capacity retention ratio of 96% after 300 cycles	[75]
PEO-LiTFSI-1% LGPS-SN	1.58×10^{-3} S cm^{-1} at 80 °C and 9.10×10^{-5} S cm^{-1} at 25 °C	—	5.5	255	discharge specific 152.1 mAh g^{-1} after 60 cycles with 99.5% coulombic efficiency	[78]

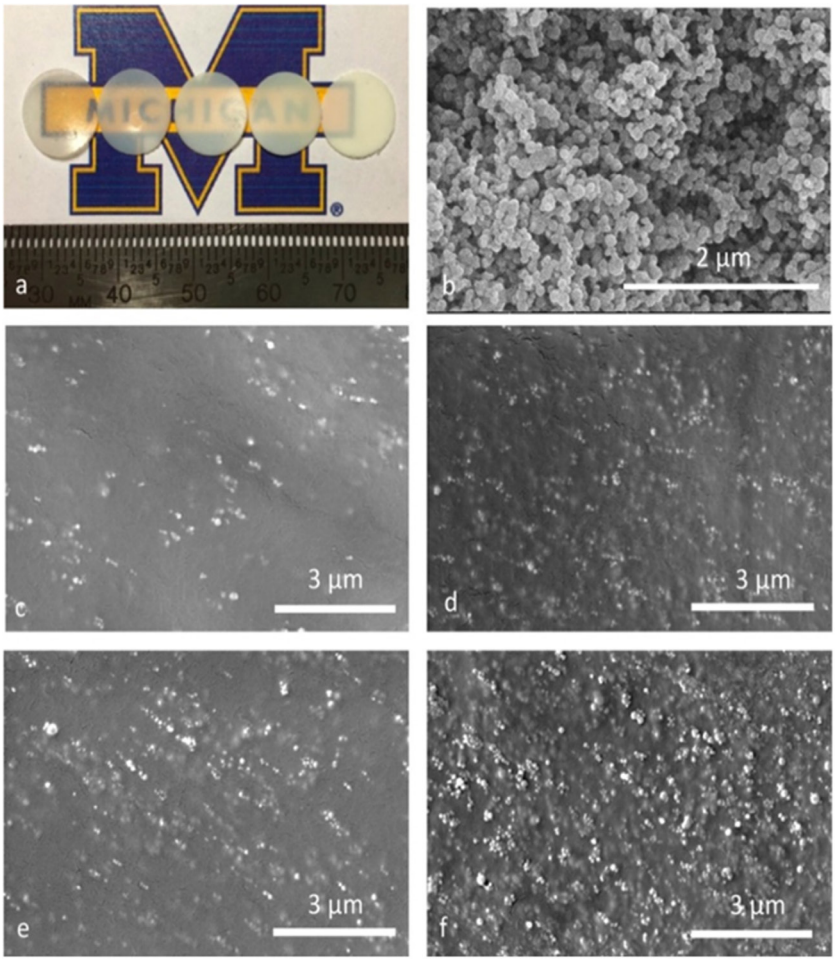

Figure 29. (a) Photograph of composite films; (b) SEM image of LATP particles, as collected from flame spray pyrolysis; SEM images of nanocomposite samples with (c) 5, (d) 10, (e) 15, and (f) 20 wt.% LATP nanoparticles. Reprinted with permission from [85]. Copyright 2017 American Chemical Society.

($Li_{10}GeP_2S_{12}$ (LGPS), $Li_{1.3}Al_{0.z}Ti_{1.7}(PO_4)_3$ (LATP), LiN_2O_3) and the other, which supports the polymer structure only and has no active role in ion transport, is passive filler (Al_2O_3, CeO_2, TiO_2, $BaTiO_3$).

The first report on the addition of nanofiller (α-alumina) in PEO-$LiClO_4$ polymer electrolyte was given by Weston and Steel in 1982 [82]. It concluded that the mechanical stability of film was improved by the addition of 10 wt.% nanofiller. Another report by Wieczorek in 1996 reported the enhancement in conductivity by the Lewis acid base approach with α-Al_2O_3 as nanofiller and PEO as the electrolyte. The presence of various interactions in the polymer matrix between Lewis base centers on ether oxygen and the strong acid Li^+ cation modified the polymer chain structure, which supported fast ionic transport [83]. The effect of nano SiO_2 and TiO_2 fillers on the thermal, mechanical and electrochemical properties of PVA:PVdF:$LiCF_3SO_3$ have been investigated by Hema *et al* [84]. The addition of nanofiller improved the thermal stability, as evidenced by TGA, and was attributed to the bond strength of Si–O, and Ti–O in the nanofiller. The conductivity was enhanced by the addition of nanofiller and was 3.7×10^{-3} S cm^{-1} compared to the filler free system at 303 K. The ESW was 5.2 V and is suitable for the application.

Wang *et al* [85] reported on the preparation of SPE based on PEO-$LiClO_4$ + $Li_{1.3}Al_{0.z}Ti_{1.7}(PO_4)_3$ (LATP), TiO_2, SiO_2. LATP is an active nanofiller while TiO_2 and SiO_2 are passive nanofillers. FTIR spectra of pure PEO and LATP showed no change or shift w.r.t the polymer nanocomposite spectra and it evidenced the mechanical dispersion of LATP in the polymer matrix but was not forming a complex. Complexation of polymer and salt ($LiClO_4$) was confirmed by the FTIR spectra. The prepared films were free-standing and translucent and translucency decreased with increasing LATP loading. SEM micrographs showed the uniform complete distribution for 5 and 10 wt.% of LATP loading, and at high content agglomerates of particles started to appear (figure 29). The XRD spectra of the PEO showed fundamental peaks at 19.3° and 23.4°, which confirmed the crystalline structure, while a broad feature was obtained for LATP at 24° confirming its amorphous nature. The addition of LATP in the polymer salt matrix suppresses the crystallinity. DSC results showed that the addition of LATP nanoparticles gradually reduced the crystallinity from 45% to 37% as nanofiller prevented the polymer chain from regular alignment. The highest ionic conductivity obtained was 1.71×10^{-4} S cm^{-1} at 20 °C, achieved for 10 wt.% LATP nanoparticles and EO/Li = 5, and the activation energy was 2.10 kJ mol^{-1}, which was the lowest among all the samples.

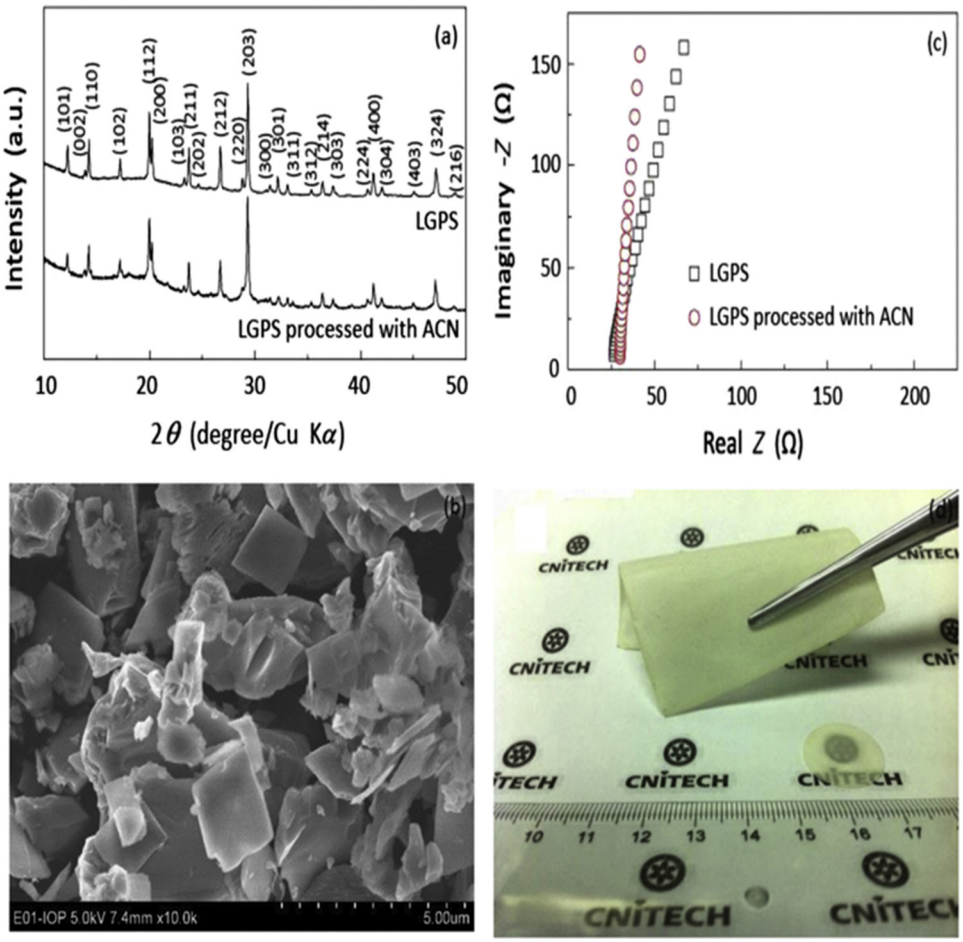

Figure 30. (a) XRD patterns of LGPS before and after processed with ACN; (b) FESEM image of the LGPS particles; (c) AC impedance spectra LGPS before and after processed with ACN and (d) a photo of SPE membrane. Reprinted from [86], Copyright 2016, with permission from Elsevier.

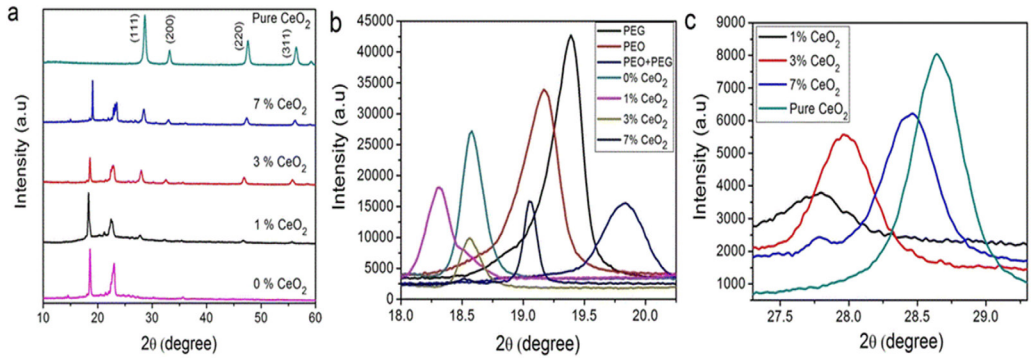

Figure 31. XRD patterns of a pure CeO_2 and PEO–PEG–$LiClO_4$–EC (68:16:11:5) with different weight percentage of CeO_2. (b) PEO/PEG characteristics peaks in pure PEO /PEG, blend polymer, and NCPEs. (c) Maximum intensity peak of CeO_2 in NCPE and its pure form. [88] 2015 © Springer-Verlag Berlin Heidelberg 2014. With permission of Springer.

Zhao *et al* [86] reported the preparation of SPEs using PEO as a host polymer, LiTF as salt and $Li_{10}GeP_2S_{12}$ (LGPS) sulfide electrolyte as nanofiller. DSC results showed that LGPS suppressed the polymer crystallization, which directly suggests an increase in free volume and hence, a more amorphous phase was confirmed which supported fast ionic transport. XRD spectra showed that a cubic single phase (space group 141/acd) of LGPS provided a suitable tunnel for cation migration (figure 30(a)). The SPE film was semi-transparent and flexible, as in figure 30(d). The maximum ionic conductivity was 1.21×10^{-3} S cm^{-1} at 80 °C, which was higher than the ionic conductivity of the PEO-only membrane at only 7.98×10^{-4} S cm^{-1} at 80 °C (figure 30(b)). The enhancement in conductivity was attributed to single ion conductor nature and a transport number of unity for LGPS. Also, the presence of a weaker interaction between lithium and sulfide ions than

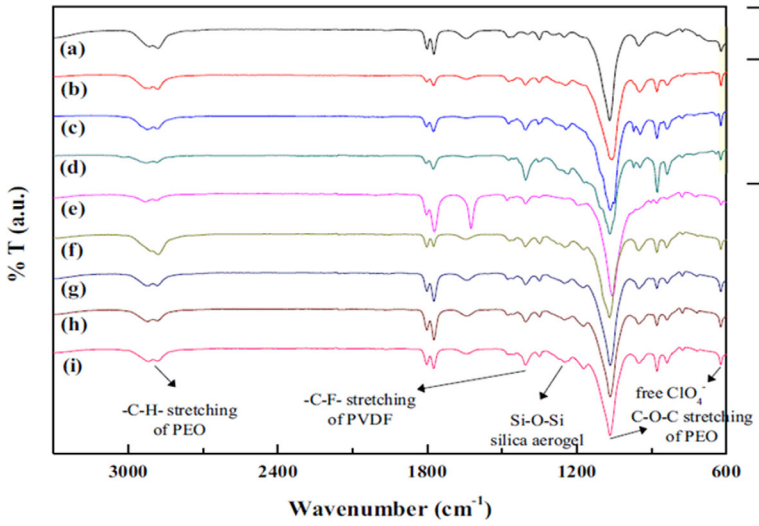

Sample	Peak area (630-610cm^{-1})
SPE-1	0.795
SPE-2	0.818
SPE-3	0.753
SPE-4	0.592

Figure 32. FT-IR spectra of the solid polymer electrolytes (a) SPE-1, (b) SPE-2, (c) SPE-3, (d) SPE-4, (e) SPE-5, (f) SPE-6, (g) SPE-7, (h) SPE-8, (i) SPE-9. Reprinted from [89], Copyright 2013, with permission from Elsevier.

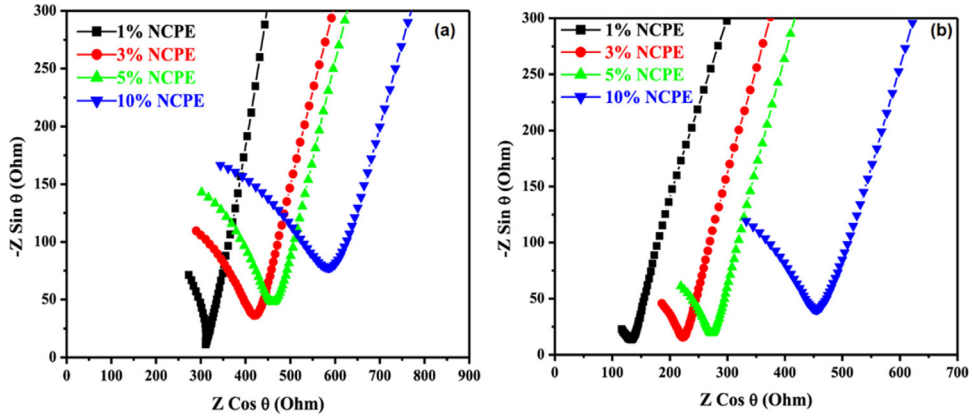

Figure 33. (a) Nyquist plot of the data obtained from AC impedance measurement of NCPE films prepared using chem-SiO_2 nanofillers. (b) Nyquist plot of the data obtained from AC impedance measurement of NCPE films prepared using epoxy-SiO_2 nanofillers. The plot gives the bulk resistance from which the Li^+ ion conductivity is calculated. Reproduced from [91]. © IOP Publishing Ltd. CC BY 3.0.

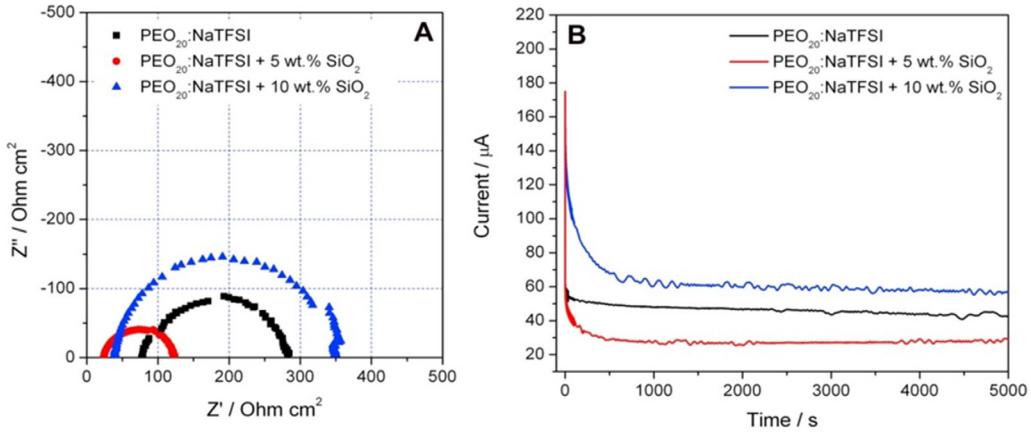

Figure 34. Nyquist plots of the PEO_{20}:NaTFSI polymer membranes with 0/5/10 wt.% of silica added at 75 C before the DC polarization (a) and their corresponding chrono-amperometric curves (b). Reprinted from [93], Copyright 2014, with permission from Elsevier.

that of lithium and oxygen ions concluded that Li ions can easily migrate upon addition of LGPS in the polymer matrix [87]. The ESW was 5.2 V for LGPS-added SPE, which was higher than that of pure PEO 4.2 V, and this may have been due to the wide potential window of LGPS itself. The charge/discharge curve for cell $LiFePO_4/PEO_{18}$-LiTFSI-1% LGPS/Li showed high capacities of 158, 148, 138 and 99 mAh g^{-1} with current rates of 0.1 C, 0.2 C, 0.5 C and 1 C at 60 °C,

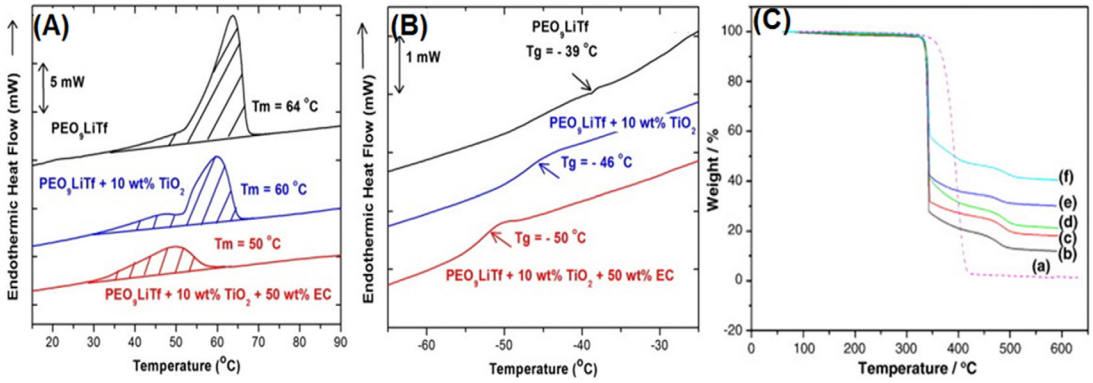

Figure 35. DSC endotherms taken during the heating run for filler-free, 10 wt.% TiO_2 added and 10 wt.% TiO_2 + 50 wt.% EC added solid polymer electrolytes showing the variation of; (A) crystallite melting temperature (T_m). (B) Glass transition temperature (T_g) (Reprinted from [95], Copyright 2014, with permission from Elsevier.) and (C) TGA graphs of the CPEs containing (a) pure PEO, (b) no filler, (c) 5 wt.%, (d) 10 wt.%, (e) 15 wt.%, and (f) 20 wt.% of nano-sized $BaTiO_3$. Reprinted from [96], Copyright 2013, with permission from Elsevier.

respectively, which makes them a promising candidate for application in lithium ion batteries.

Ali *et al* [88] reported on preparation of a polymer electrolyte based on PEO/PEG-$LiClO_4$ and CeO_2 as a nanofiller using a standard SC technique. XRD analysis showed the presence of coordination interactions between the Li^+ ion and ether oxygen atoms of polymer chains which reduced the crystallinity (figure 31). The decrease in crystallinity was due to disorder produced in polymer chains by the addition of nanofiller, which supported amorphous phase formation and hence, faster ion transport. The maximum ionic conductivity was 1.18×10^{-4} S cm^{-1} for 1 wt.% nanofiller dispersion in the polymer matrix and may have been due to interchain and intrachain hopping of ion movements (activation energy = 0.41 eV). Further, at high nanofiller content, conductivity reduction may be attributed to a blockage effect provided by nanofiller particles.

Yoon *et al* [89] reported the effect of silica aerogel on PEO-PVDF-$LiClO_4$ based SPE. XRD analysis concluded that the polymer blend with silica aerogel contained a highly amorphous phase. The complex formation was confirmed by FTIR and various bands corresponding to PEO and PVDF were observed (figure 32). FTIR analysis revealed that at high salt concentrations, ion association occurred, which decreased the number of free charge carriers. The highest ionic conductivity was 1.70×10^{-4} S cm^{-1} at 30 °C for PEO:PVDF ratio 3:1.

Jung *et al* [90] prepared a hybrid polymer electrolyte using LAGP ($Li_{1.5}Al_{0.5}Ge_{1.5}(PO_4)_3$) as nanofiller in a PEO-$LiClO_4$ matrix. FESEM micrographs showed a heterogeneous particle size distribution of LAGP powders in the polymer salt matrix. EDX mapping images suggested complete dissolution of salt and an even distribution of nanofiller. XRD spectra showed disorder in the structure of the SPE, as crystalline peaks corresponding to PEO disappeared upon the addition of LAGP. Also LAGP was in original form as no degradation was observed in the polymer film. The highest ionic conductivity was 1.0×10^{-5} S cm^{-1} for 70 wt.% LAGP, which was higher than the polymer salt system at room temperature and an equivalent circuit in inset represents a solid electrolyte sandwiched between two blocking electrodes. Also, conductivity increased with temperature, to 2.6×10^{-4} S cm^{-1} at 55 °C. The ESW was enhanced from 4.5 V to 4.75 V upon the addition of LAGP in the polymer matrix.

The electrochemical properties were studied by assembling the solid-state Li/$LiFePO_4$ cells with hybrid solid electrolytes (LAGP-60, LAGP-70 and LAGP-80) in the voltage range of 2.6–4.0 V at a constant current rate of 0.2 C and 55 °C. The initial discharge capacities were 137.6 mAh g^{-1} and 142.2 mAh g^{-1} for the 20th cycle. The discharge capacities of the Li/HPE/$LiFePO_4$ cells as a function of the cycle number and discharge capacities of the cells decreased from their initial capacities of 133.0–138.5 mAh g^{-1} to 113.4–121.5 mAh g^{-1} at the 100th cycle, corresponding to 81.9–91.3% of the initial values. Also, the capacity retention was improved by increasing the content of LAGP, which can be ascribed to the high electrochemical stability and good interfacial properties, as LAGP may suppress harmful interfacial side reactions between the electrodes and the electrolyte, which results in good cycling stability.

Mohanta *et al* [91] prepared a PEO-based SPE with lithium trifluromethanesulphonate ($LiCF_3SO_3$) as salt and porous silica as nanofiller. TEM analysis of the electrolyte showed the porous nature of the morphology. FTIR analysis confirmed the epoxy capping on the surface of calcined porous silica nanostructure and successful immobilization of the surface group on the silica surface. The Nyquist plot for the chem-SiO_2 nanofiller and epoxy-SiO_2 nanofiller based electrolytes are shown in figure 33. The highest conductivity was 1.03×10^{-4} S cm^{-1} for 1% epoxy-SiO_2, and that may be due to high amorphous content compared to other samples.

Dam *et al* [92] investigated the conduction mechanism of PNC based on a PEO as polymer host, lithium trifluoromethanesulfonate as salt and nano-crystalline zirconia (ZrO_2) as filler, using broadband dielectric spectroscopy. The maximum value of DC conductivity (σ_{dc}) was 2.04×10^{-5} S cm^{-1} for PEO_{20}-$LiCF_3SO_3$-8 wt.% ZrO_2. The experimental data were fitted using the Jonscher power law (JPL) and showed two mechanisms of conductivity: (i) ion jumps from one site to

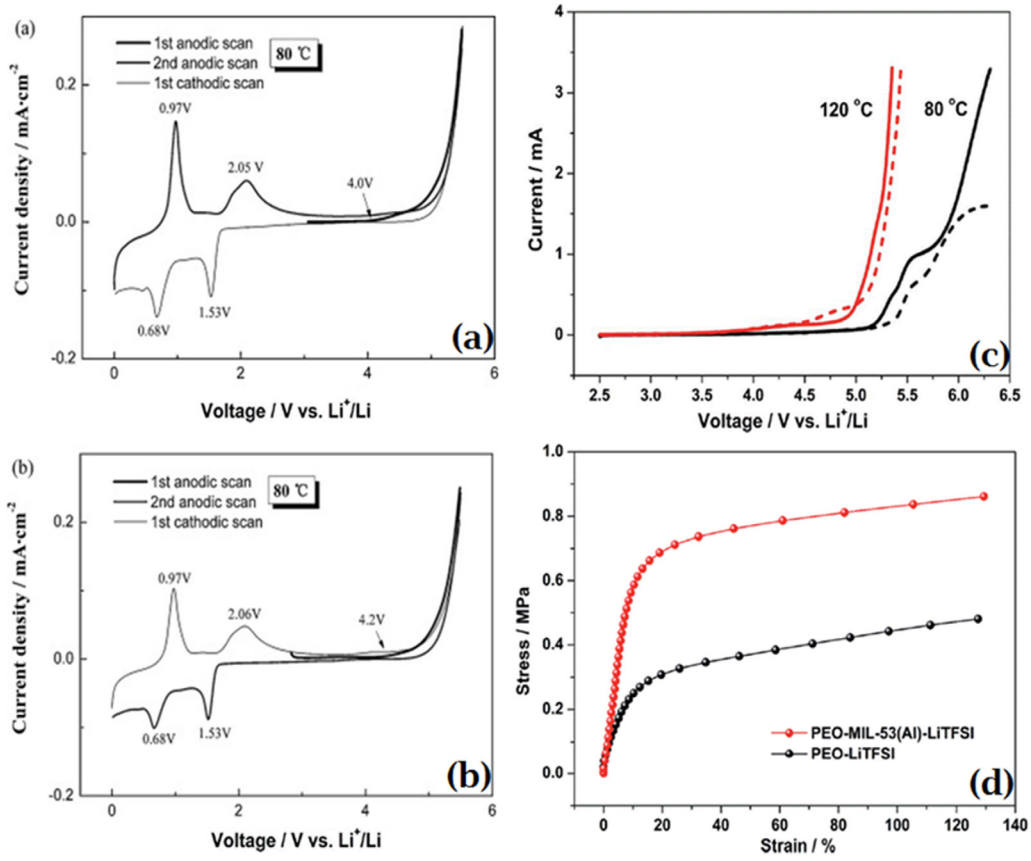

Figure 36. CV curves of PEO_{20}–LiBOB (a) and PEO_{20}–LiBOB–5 wt.% MgO (b) at 80 °C. The first anodic scan, first cathodic scan and second anodic scan are measured in the voltage range of 0–5.5 V (Reprinted from [97], Copyright 2011, with permission from Elsevier.), (c) linear sweep voltammograms of SS/PEO-LiTFSI/Li (solid line) and SS/PEO-MIL-53(Al)-LiTFSI/Li (dotted line) batteries at 80 °C (black) and 120 °C (red). The electrolytes were swept in the potential range from 2.5 V to 6.5 V (versus Li/Li^+) at a rate of 10 mV s^{-1}, and (d) stress–strain curves of the PEO-MIL-53(Al)-LiTFSI and PEOLiTFSI electrolytes. Reproduced from [98] with permission of The Royal Society of Chemisty.

its neighboring favorable vacant site, contributing towards the DC conductivity, and; (ii) in the short time period available the correlated forward and backward hopping of mobile ions gives rise to AC conductivity at high frequencies.

Moremo *et al* [93] reported the preparation of poly (ethylene oxide) (PEO) /sodium bis(trifluoromethanesulfonate) imide (NaTFSI) + SiO_2 based electrolyte using the solvent-free hot-pressing technique with different EO:Na molar ratios. DSC analysis showed T_g at −60.7 °C and a melting peak at 65 °C ($\Delta H_m = 155.7$ J g^{-1}) for pure PEO. The T_g variation showed an irregular trend with varying salt concentration. Initially, the T_g increased as NaTFSI concentration increased by promoting a loss of rigidity of the polymer backbones, and may have been due to stronger interaction and slowing of polymer segmental motion. At the highest concentration (i.e. 6:1), the plasticization effect came into the picture due to the flexibility of the S–N–S bond in TFSI. Two peaks were observed in the melting process in the 12:1–8:1 composition range and were assigned to the onset of small crystallites melting, allowing the growth of larger ones which melted at a higher temperature. At the T_m peak, the crystallinity decreased due to the plasticization action of salt observed for the second endothermic peak. Further addition of SiO_2 in polymer salt complex decreased the melting temperature, which directly enhanced the amorphous content and may have been due to the interaction of nanofiller with the polymer host via Lewis acid base interactions.

The ionic conductivity decreased from 6:1 to 20:1 for PEO:NaTFSI, and the PEO_{20}:NaTFSI and PEO_{12}:NaTFSI system showed values of 1.1 mS cm^{-1} and 1.3 mS cm^{-1} at 80 °C, respectively. A nonlinear effect was observed in conductivity data due to an increase of NaTFSI concentration and may have been due to a compromise between an amorphization effect of the salt and charge carrier number. The addition of nanofiller at 5 wt.% content brought no change to conductivity value and may have been due to a masking of the effect of nanofiller by the plasticizing action of the $TFSI^-$ anion. At 10 wt.% nanofiller a decrease in ionic conductivity may have been due to blockage of ion conducting pathways. The sodium transport number was measured by applying a fixed DC voltage and following the DC current as a function of time. The sodium ion transference number increased up to the addition of 5 wt.% SiO_2 and then slightly decreased for higher filler concentrations, due to the interaction of nanofiller with sodium ion (figure 34).

Ganapatibhotla *et al* [94] reported the influence of nanofiller surface chemistry and ion content on the conductivity of PEO-$LiClO_4$ + Al_2O_3 based SPEs. Alumina nanofiller was

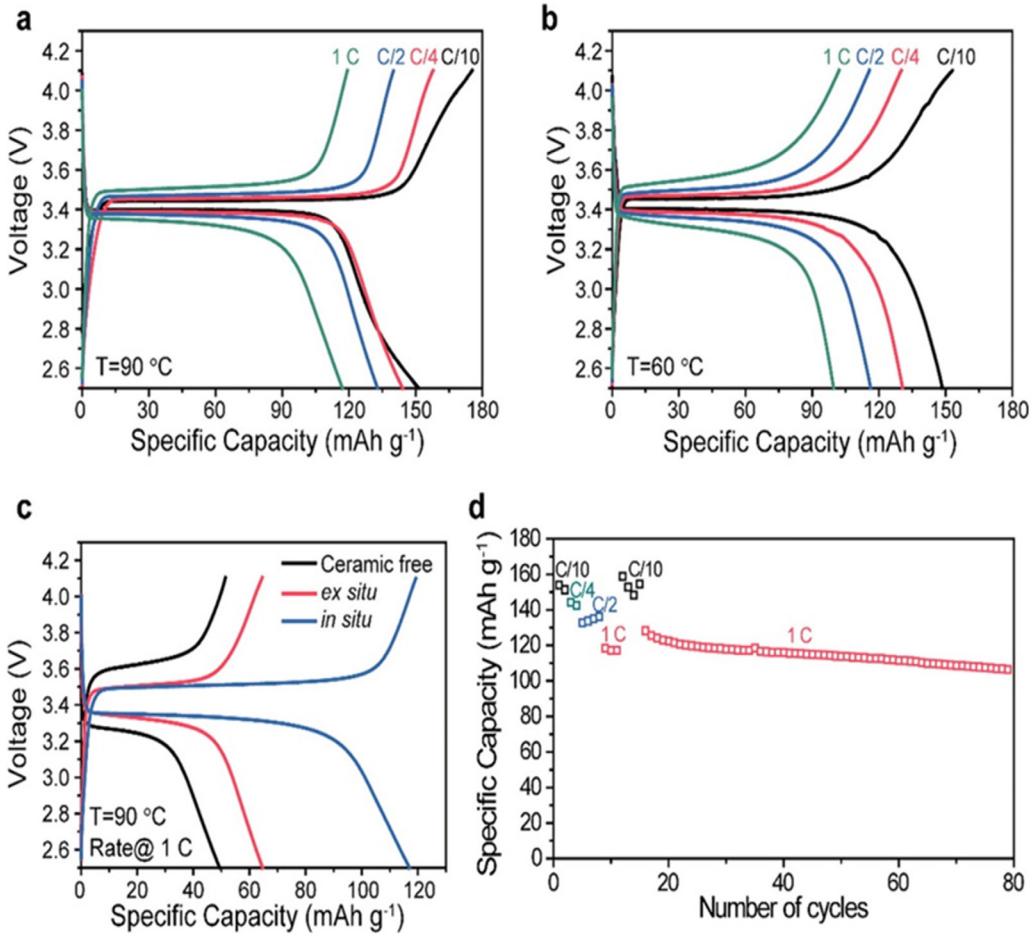

Figure 37. Electrochemical performance of all-solid-state lithium polymer batteries. (a), (b) Rate capability of lithium polymer batteries with configuration of $LiFePO_4$ cathode/*in situ* CPE/lithium foil anode at 90 °C (a) and 60 °C (b). (c) Comparison of capacity retention of batteries with different electrolytes of ceramic-free SPE, *ex situ* CPE, and *in situ* CPE operating at 90 °C and the rate of 1 C. (d) Cycle performance of batteries with *in situ* CPE at 90 °C. Reprinted with permission from [99]. Copyright 2015 American Chemical Society.

chosen due to the existence of polymorphs: the α-form has acidic or electron pair-accepting surface sites, β has basic surface sites or electron withdrawing sites, and γ has a combination of acidic and basic surface sites resulting in neutral surface chemistry.

Here, hydrogen atoms in acidic and neutral particle-filled electrolytes participated in three processes: vibration, segmental relaxation of the PEO, and a rotational process consistent with a liquid analogue of the PEO_6:$LiClO_4$ structure. On the basis of the data, enhancement in conductivity was due to the formation of the hydrogen bonds between $-$OH groups on the acidic particles with the anions. These interaction led to the release of more free charge carriers which contributed in conduction while neutral particles in basic groups formed a hydrogen bond with cations through the ether group of the polymer host, and thus either decreased or had no effect on conductivity. It is proposed in the mechanism that Li ions hop from one coordination site to another, enabled by energy barriers that were accessible at room temperature, while the basic sites in the neutral surface acted as Li traps, interrupting the movement of Li. At eutectic composition, there was no surface chemistry dependence which was due to the stability of multiple layers of PEO_6:$LiClO_4$ and PEO by acidic particles and neutral particles (which have both acidic and basic sites). At a composition of EO/Li = 8:1, acidic fillers enhanced conductivity, the Li transference number, and Li ion diffusivity more than neutral fillers at all temperatures, with the highest enhancement at 30 °C. At a composition of 14:1, fillers enhanced conductivity only above the melting temperature of the PEO, where acidic particles impacted conductivity to a larger extent than neutral fillers. It is notable that the influence of surface chemistry nearly vanished at the eutectic composition (EO/Li = 10:1). Above the eutectic temperature (50 °C), there was no statistically relevant difference, and below the eutectic temperature, the neutral particles were more efficient. These findings indicated that the mechanism of conductivity enhancement at the eutectic composition differed from other compositions.

Vignarooban *et al* [95] reported enhancement in conductivity based on poly (ethylene oxide)–lithium trifluoromethanesulfonate ($LiCF_3SO_3$ or LiTf) based polymer electrolyte with TiO_2 nano-filler. The highest conductivity was of 4.9×10^{-5} S cm^{-1} for 10 wt.% nanofiller and was attributed to the formation of transient conducting pathways due to the Lewis acid base type interactions of the cation with surface groups of the nanofiller. The dual functionality of the nanofiller was pointed out; one function was to promote the ion migration

by reducing the reorganization tendency of the polymer, and the second was a decrease in ionic coupling due to Lewis acid base interactions. DSC spectra showed that the melting point (T_m) decreased from 64 °C to 60 °C and the glass transition temperature (T_g) from −39 °C to −46 °C on the addition of 10 wt.% nanofiller and supported an increase in the ionic conductivity value (figure 35(a)).

Lee *et al* [96] reported the effect of barium titanate nanofiller on the structural modification and electrochemical properties of a PEO-PVdF based system. XRD and DSC analyses indicated that the change in the crystallinity value meant that the crystal growth of the PEO was weakened by the molecular interaction of the polymer matrix by the addition of nanosized $BaTiO_3$. It was concluded that the presence of $BaTiO_3$ improved the ionic conductivity of the CPE, with the highest being at 15 wt.% nanofiller (1.2×10^{-4} S cm^{-1}) by slightly decreasing the CPE crystallinity. At higher nanofiller content, blocking of the effect of nanofiller came into the picture due to nanofiller aggregation which reduced the conductivity. TGA analysis confirmed thermal stability up to 330 °C on the addition of nanofiller, and degradation of polymer matrix occurred at higher temperature. The ESW was enhanced by the addition of nanofiller, from −2.3 to 2.4 V, which is sufficient for energy storage devices (figure 35(b)).

Zhang *et al* [97] prepared a PEO_{20}–LiBOB based SPE with nano-sized MgO as nanofiller. The electrochemical stability was measured by CV and the addition of nano-MgO improved the anodic stability (figures 36(a) and (b)). Two anodic peaks appeared at 0.97 V and 2.05 V, while the two cathodic peaks were at 1.53 V and 0.68 V. The peaks at 0.97 V and 0.68 V were possibly due to reduction and oxidization of ion species formed by dissociation of the lithium salt in PEO segments. The peaks at 1.53 V and 2.05 V were associated with trace water molecules in the SPE. The addition of nanofiller increased the initial oxidative decomposition up to 4.2 V and may have been due to absorption of trace water and unstable compounds present in the polymer salt system. For the polymer salt system, average anodic current density reduced from an initial 0.01 mA cm^{-2} to 0.003 mA cm^{-2} at 4.5 V and remained constant at 3.0 V, that is around 0.003 mA cm^{-2}, during 20 full CV. The compatibility of PEO_{20}–LiBOB and PEO_{20}–LiBOB–5 wt.% MgO toward prepared $LiCoO_2$ and $LiNi_{1/3}Co_{1/3}Mn_{1/3}O_2$ was studied. The polymer salt system showed a charge capacity and discharge capacity of 168.8 and 156.8 mAh g^{-1}, respectively, and discharge capacity degraded to 142.5 mAh g^{-1} after 20 cycles. The addition of 5 wt.% nanofiller gave a discharge capacity value of 157 mAh g^{-1}. The application of LiBOB and nano-sized metal oxides is a convenient and economical way to develop PEO-based polymer electrolytes for 4 V class cathodes.

Zhu *et al* [98] reported on the preparation of a PEO-LiTFSI based electrolyte with aluminum 1,4-benzenedicarboxylate (MIL-53(Al)) as nanofiller. The ionic conductivity of the electrolyte was 3.39×10^{-3} S cm^{-1} at 120 °C and an EO: Li ratio of 15:1. The addition of filler disrupted the polymer host crystallization nature and dissociated the salt to release a number of charge carriers. A decrease of the phase transition temperature was seen with the addition of nanofiller, and suggested that the amorphous phase formed supported the ionic transport to achieve high ionic conductivity. The cation transport number obtained by AC impedance spectroscopy was 0.343, higher than the 0.252 for the polymer salt system. This increase in cation transport was attributed to the formation of the metal organic framework. Also, the ESW was improved from 5.13 V (4.99 at 120 °C) to 5.31 V (5.10 V at 120 °C) on the addition of filler in the polymer salt system at 80 °C (figure 36(c)). All electrolyte systems were thermally stable up to 200 °C. The dynamical properties studied by stress–strain curve showed an increase of stress after the addition of filler (figure 36(d)). The cycling performance of the battery showed an initial discharge capacity of 127.1 mA h g^{-1} (at 5 C) at 80 °C and 136.4 mA h g^{-1} at 120 °C. After 300 cycles, the discharge capacity was 116.0 mA h g^{-1} at 80 °C and 129.2 mA h g^{-1} at 120 °C.

Lin *et al* [99] reported on the preparation of a poly (ethylene oxide) (PEO)-$LiClO_4$ + monodispersed ultrafine SiO_2 ($MUSiO_2$) composite polymer electrolyte via an *in situ* synthesis. The *in situ* hydrolysis was used as it offers the opportunity to form a much stronger interaction between polymer chains of PEO and SiO_2 nanospheres, which is crucial for decreasing polymer crystallinity. Two interaction mechanisms were discussed here which affect the polymer chain density and reduce the crystallinity. In the former, under hydrolysis conditions the hydroxyl groups at the ends of PEO chains can chemically bind with those on the SiO_2 surface, and the other deals with the mechanical wrapping of polymer chains when the SiO_2 spheres grow. The addition of salt in the PEO caused a decrease of intensity in the XRD spectra which is direct evidence of a decline of crystallinity. The DSC analysis confirmed a higher fraction of the amorphous phase for the *in situ* PEO-$MUSiO_2$ composite, which may have been due to the presence of strong interactions between $MUSiO_2$ spheres and polymer chains; also, the uniform distribution of $MUSiO_2$ spheres from *in situ* hydrolysis improved the effective surface area of SiO_2. The dissociation or separation of Li^+ and ClO_4^- was studied by FTIR using a Gaussian–Lorentz fit, and for the *in situ* CPE, a 98.1% dissociation ratio was observed, which was higher than for ceramic-free SPE (85.0%), PEO-fumed SiO_2 CPE (87.4%), and *ex situ* CPE (92.8%) counterparts. So, the *in situ* hydrolysis technique resulted in more dissociation of salt and may be attributed to the maximum surface area of SiO_2 with the small size and interactions of ClO_4^- with the SiO_2 surface. The decrease of crystallinity from XRD revealed the improved segmental motion of polymer chains and enhanced the coordinating interaction of Li^+ with ether groups of PEO chains. The ionic conductivity obtained from *in situ* hydrolysis was in the range of $10^{-4} - 10^{-5}$ S cm^{-1} and is a value ten times higher than for the *ex situ* PEO-$MUSiO_2$ CPE counterparts. At 60 °C the ionic conductivity value was 1.2×10^{-3} S cm^{-1} and was comparable to the liquid electrolyte. The ESW was 4.7 V for *ex situ* CPE and 5.5 V for *in situ* CPE and was attributed to a strong adsorption effect on the anion for *in situ* CPE, which suppressed its anodic decomposition at high potential.

The electrochemical properties were tested between 2.5 and 4.1 V, with similar charge and discharge rates. Figure 37(a) shows the voltage profiles of all-solid-state batteries with

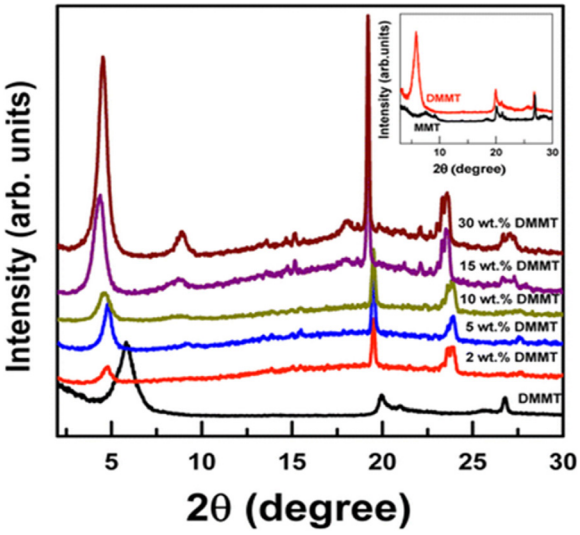

Figure 38. XRD patterns of DMMT and PEO_{20}-$LiAsF_6$ + *x*wt.% DMMT $x = 0$, 2, 5, 10, 15, and 30. Inset shows comparison of XRD patterns of MMT and DMMT. [108] 2015 © Springer-Verlag Berlin Heidelberg 2015. With permission of Springer.

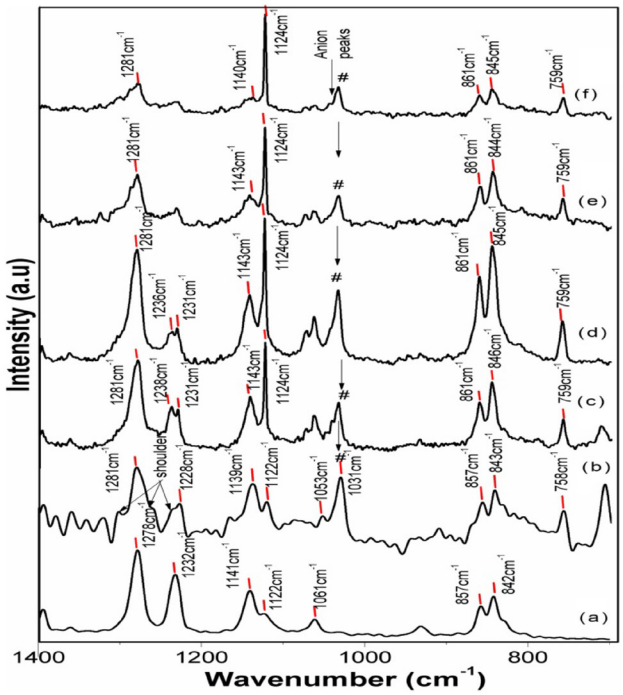

Figure 39. Raman spectrum of clay based PNC (a) PEO, (b) polymer blend salt, (c) 1 wt.% clay, (d) 3 wt.% clay, (e) 5 wt.% clay, and (f) 7 wt.% clay. Arrow indicates significant changes in the Raman profile. Reprinted from [109], Copyright 2017, with permission from Elsevier.

in situ CPE under different rates at an elevated temperature (90 °C), and for a rate below 1 C (170 mAh g^{-1}, based on the weight of $LiFePO_4$), the cell showed a high capacity retention of 120 mAh g^{-1} while the flat plateau with low over potential indicates the fast kinetics of Li^+ transport in CPE. Figure 37(b) shows excellent rate capability with >100 mAh g^{-1} specific capacity retention at a lower operating temperature (60 °C). The higher value of over potential at 60 °C than at 90 °C, may have been due to the decreased ionic conductivity and slower Li^+ transport kinetics at 60 °C. Figure 37(c) shows the comparison of rate capabilities of ceramic-free SPE, *ex situ* CPE, and *in situ* CPE at a 1 C rate and at 90 °C. Capacity was improved and an almost doubled capacity retention (~ 120 mAh g^{-1}) was observed for *in situ* CPE compared to *ex situ* CPE (~ 65 mAh g^{-1}). The ceramic-free CPE showed a much lower capacity retention (~ 50 mAh g^{-1}) and much higher over potential, indicating slow Li^+ transport. For *in situ* CPE, cycle stability was higher, and after 80 cycles over 105 mAh g^{-1} of specific capacity can still be retained (figure 37(d)), and the absence of any growth of dendrites supports the excellent electrochemical stability of our CPE within the voltage window.

Nancy *et al* [100] reported the effect of Al_2O_3 nanofiller on a blend of PEO and polypropylene glycol (PPG) with zinc trifluoromethanesulfonate [$Zn(CF_3SO_3)_2$] as salt. XRD analysis showed a decrease of intensity upon the addition of salt and nanofiller, which indicated the altering of the structure of the polymer chain due to the feasibility of coordination interactions occurring between zinc ions and the ether group of the PEO. Crystallinity also decreases with the addition of nanofiller only up to 3 wt. % nanofiller, but for Al_2O_3 content (>3 wt.%) an increase in crystallinity was observed due to the possible reorientation of PEO polymer chains. It may be attributed to the reduction of dipole–dipole interaction or hydrogen bonding of the polar groups near the surface of nano-Al_2O_3 and the free volume of the polymer matrix decreases. SEM analysis shows a remarkably rough structure for pyre PEO, indicating its crystalline nature and how the addition of salt changes the surface homogeneity. Further addition of nanofiller shows a relatively smooth surface through the whole polymer electrolyte with irregularly sized small pores due to a decrease of the spherulite structure. No phase separation occurrence was seen in the polymer nanocomposite film. DSC analysis shows a decrease of area and a shift in the melting peak upon the addition of nanofiller and is attributed to an enhanced amorphous phase and polymer flexibility. The increase of ionic conductivity on the addition of nanofiller indicates the presence of a strong Lewis acid base interaction between polymer/salt and nanofiller. Also, the activation energy decreases up to 3 wt.% nanofiller content and its lowest value is 0.44 eV. The ESW was 3.6 V.

Pandey *et al* [101] made a comparative study of preparations of nanocomposite polymer electrolytes based on PEO: NH_4HSO_4 + SiO_2 by hot press technique (HP) and SC technique. The HP technique was preferred over the SC technique as it is rapid, the least expensive, and a dry procedure to prepare solvent-free polymer electrolyte films. The SEM micrograph of polymer salt complex film prepared by SC technique showed distinct spherulites separated by dark boundaries, while samples prepared by HP showed the absence of spherulitic texture. The presence of spherulites indicates the lamellar structure of the crystalline phase, and dark boundaries are associated with polymer amorphous nature. The addition of nanofiller in a polymer salt matrix disturbs the spherulitic texture. The XRD patterns of pure PEO were affected by preparation techniques and were observed in terms of peak broadening, while the Scherrer length '*l*' (a measure of crystallite size of the PEO) was shortened for samples prepared by the

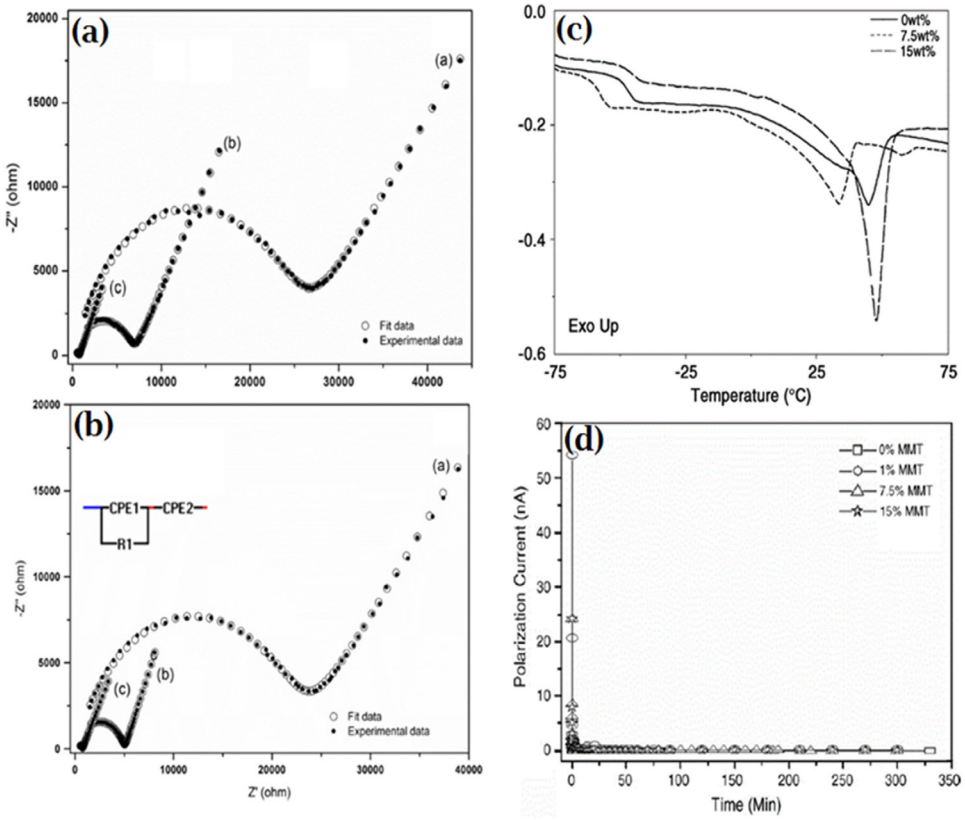

Figure 40. (A) Impedance spectra of nanocomposite electrolyte films (a) $(PEO)_{16}LiCBSM$, (b) $(PEO)_8LiCBSM$ and (c) $(PEO)_4LiCBSM$ at 298 K and (B) impedance spectra of nanocomposite electrolyte films (a) $(PEO)_{16}LiCBSM$, (b) $(PEO)_8LiCBSM$ and (c) $(PEO)_4LiCBSM$ at 323 K. ([110] 2016 © Springer-Verlag Berlin Heidelberg 2016. With permission of Springer.) (C) DSC thermograms of PEO/clay/Li^+ nanocomposite electrolytes ([112] John Wiley & Sons. Copyright © 2007 Society of Chemical Industry.) and (D) variation of polarization current as function of time under constant applied voltage ($V = 50$ mV) for different concentration ($x = 0$, 1, 7.5, 15) of DMMT clay. Reprinted from [111], Copyright 2009, with permission from Elsevier.

HP technique. The formation of a lamellar structure observed in SEM for samples prepared by the SC technique was confirmed by XRD. The presence of a broad region in the 2θ range ~15°–30° for SiO_2 dispersed NCPE films is evidence of the increase of amorphous content. DSC analysis confirmed the presence of a dominant endothermic peak at ~ 58–62 °C associated with semi crystalline-amorphous phase transition and/or melting temperature (T_m) of PEO, as well as to two-step changes owing to glass transition temperature. Both T_g and T_m decrease with the addition of nanofiller when compared to the pure polymer, and an additional endothermic broad peak observed at ~85 °C was attributed to the amorphous nature of polymer nanocomposites. FTIR confirmed the formation of composites on the addition of nanofiller in the polymer salt system. The conduction was dominated by ions in the polymer nanocomposites as a high ion transference number was observed, which is t_{ion} ~ 0.97–0.98. The ionic conductivity was highest for samples prepared by the HP technique over the SC technique and is also evidenced by the low value of activation energy.

Klongkan prepared an SPE using PEO-$LiCF_3SO_3$ as host matrix, Al_2O_3 as nanofiller and dioxyphthalate (DOP) and polyethylene glycol (PEG) as plasticizers by a ball milling method followed by a hot pressing process [76]. The highest ionic conductivity was 1.00×10^{-6} S cm^{-1} for 15 wt.% $LiCF_3SO_3$ and was due to an increase in the number of free cations. A decrease at high concentration was due to ion–ion interaction which trapped the cation and reduced the conducting pathway [81]. DSC spectra showed a reduction in T_m, T_g and X_c values to 54.34 °C, 64.37 °C and 37.31%, respectively, for 15 wt.% $LiCF_3SO_3$, and suggested an increase in the segmental motion of the polymer chain. Capiglia *et al* [102] prepared an SPE comprising a PEO as polymer host, $LiClO_4$ and $LiN(CF_3SO_2)_2$ as the doping salts, with SiO_2 as nanofiller. The highest ionic conductivity was 1.4×10^{-4} S cm^{-1} for PEO–$LiN(CF_3SO_2)_2$–5 wt.% SiO_2 and the activation energy was 0.54 V. It was concluded that calcination of nanofiller also affected the ionic conductivity.

Sun *et al* [103] reported the effect of ferroelectric filler ($BaTiO_3$) on the PEO-$LiClO_4$ based polymer matrix. The highest ionic conductivity achieved was 1×10^{-5} S cm^{-1} for 1.4 wt.% of filler at 25 °C and 1.2×10^{-3} S cm^{-1} at 70 °C. The cation transference number was 0.37, which is much higher than that of polymer electrolyte without filler. The ESW was more than 4 V for all samples. Appetecchi *et al* [104] prepared a solvent-free polymer electrolyte by a hot-press technique using PEO as polymer host, $LiCF_3SO_3$ as salt and SiO_2 as nanofiller. The cell Li/PEO:$LiCF_3SO_3$:SiO_2/$LiFePO_4$ showed 100% efficiency up to 400 cycles.

Choudhary *et al* [105] synthesized the (PEO-PMMA)-$LiClO_4$ based polymer nanocomposite electrolyte with various nanofillers of different particle sizes and dielectric

permittivities (Al_2O_3, SiO_2, SnO_2 or ZnO) using the SC method followed by a melt-press technique. XRD concluded that the salt becomes completely dissociated via the formation of ion-dipolar coordination in the polymer matrix, and the blend polymer is less crystalline than the pure PEO. From an impedance study it was found that the conductivity variation followed the order of: no filler (NF) > ZnO > SnO_2 > S iO_2 > Al_2O_3 and all PNCs showed conductivity of the order of 10^{-5} S cm^{-1}. The decrease of the ionic conductivity was attributed to the slowdown of the cooperative polymers chain segmental motion on the dispersion of nanofiller.

Keller *et al* [106] synthesized hybrid ceramic-polymer electrolytes, with $Li_7La_3Zr_2O_{12}$ (LLZO) as the ceramic and $P(EO)_{15}$LiTFSI as the polymer salt matrix, using the hot-press technique. The salt (LiTFSI) was chosen due to superior charge delocalization of the anion resulting in less coordinated Li^+ cations. The crystallinity was decreased upon the addition of salt while the addition of ceramic had no effect on the onset of the melting point or the glass transition temperature, although the change in the shape of the glass transition curve suggests a disruption of the crystallization which evidenced the increase in the amorphous content. Thermal stability of all the films was up to 370 °C.

Scroasti *et al* [107] reported the impedance spectroscopy study of two different types of nanocomposite polymer electrolyte membranes with the addition of TiO_2 and SiO_2 nanofiller in the PEO-$LiClO_4$ salt matrix. The electrical conductivity, transport number and mechanical properties were improved. The increase in conductivity may have been due to the presence of cross-linking centers for the PEO segments provided by a surface group of nanofiller which decreased the polymer chain reorganization tendency. The modification in the polymer chain led to the formation of conducting paths via interaction by surface groups on nanofiller.

4.4.2. Intercalated type SPE. Dam *et al* [108] reported on the structural and electric properties of polymer nanocomposite electrolytes consisting of PEO as polymer host, lithium hexafluoroarsenate ($LiAsF_6$) as salt, and dodecylamine modified montmorillonite (DMMT) clay with a surfactant (organic dodecyl amine). XRD spectra of prepared PNCs shows (0 0 1) reflection at an angle $2\theta = 7.51°$ for MMT ($d_{001} = 11.77$ Å) and modification of clay peak shifts toward a lower angle $2\theta = 5.82°$ ($d_{001} = 15.78$ Å). The increase of interlayer spacing may be due to cation exchange between the clay layers and the surfactant. Figure 38 shows that the addition of DMMT in the polymer salt complex shifts the DMMT (0 0 1) plane towards the lower angle side up to 15 wt.% of DMMT concentrations. The increase in basal interlayer spacing evidences the successful intercalation of polymer chains in the clay layers. At a high clay content (>30 wt.%) the basal interlayer spacing decreases as now, intercalation of the polymer chain is restricted in DMMT clay layers due to the increased clay content. The absence of an XRD peak corresponding to $LiAsF_6$ in PNC indicates the complete dissolution of salt in the polymer matrix. An almost negligible effect was observed on the characteristic peaks of PEO upon the addition of clay.

The conductivity variation with temperature follows VTF behavior which suggests that polymer segmental motion affects the DC conductivity. The increase of temperature increased the diffusion rate and segmental motion of polymer chains. The highest conductivity was 4.0×10^{-5} S cm^{-1} at 273 K for 2 wt.% DMMT. The increase in conductivity may have been due to the Lewis base nature of silicate layers of the DMMT clay and interaction with lithium cations resulting in an increase of the fraction of free ions (number density of charge carriers n_i). The optimum concentration of clay was better for the conductivity than the lower or higher content.

Das *et al* [109] prepared PNC using PEO-PDMS + $LiCF_3SO_3$ and Hectorite clay. The presence of an ion polymer and ion–clay interaction was confirmed by Raman spectroscopy. The polymer clay interaction was confirmed and observed in terms of the shift in the peak positions of 842 cm^{-1} and 857 cm^{-1}, and peak profiles of 1061 cm^{-1} and 1232 cm^{-1} (figure 39). And, an increase in COC stretching at 1122 cm^{-1} corresponding to the PEO is evidence of ion polymer interaction due to clay intercalation inside the polymer matrix. Further analysis was done to study the ion dissociation effect by deconvolution of the anion peak, and for PNC with 1% clay content a higher free area suggests the number of free charge carriers for conduction. The highest conductivity was 5.2×10^{-5} S cm^{-1} for 1 wt. % PNC.

As layered silicates disrupt the crystallization of polymer, Sunitha *et al* [110] reported the effect of MMT on a $(PEO)_4$LiCBSM based polymer electrolyte. DSC and XRD analysis showed an increase of the amorphous phase, and the highest ionic conductivity was 2.15×10^{-4} S cm^{-1} at 323 K (figures 40(a) and (b)).

Mohapatra *et al* [111] reported the preparation of a PEO-$LiClO_4$ based SPE with Na-montmorillonite (MMT) as clay. XRD analysis evidenced the decrease of PEO crystallinity, as observed in terms of decreased peak intensity and increased FWHM. The decrease of crystallinity was attributed to the interaction of clay with the polymer salt complex. Also, the basal spacing increased on the modification of clay and strong intercalation of the polymer salt complex was observed in clay galleries due to dipolar interaction. TEM analysis further evidenced the intercalation/exfoliation in the clay galleries. DSC analysis showed a decrease in the glass transition temperature with the addition of clay and was an indication of an enhancement in polymer flexibility. The thermal stability of prepared PNCs was up to 300 °C and may be due to a barrier effect in which clay layers prevented decomposing of the polymer salt complex. But at high content clay layers may accumulate heat on the surface and decrease the degradation temperature. The highest conductivity obtained was ~ 9.43×10^{-4} S cm^{-1} for a 1 wt.% clay loading. The voltage stability was increased for 7.5% clay loading and was 3 V. The ionic transference number achieved was 0.99 while the cation transference number was 0.50, which was much higher than the polymer salt system, at 0.25–0.30 (figure 40(d)).

Ratna *et al* [112] prepared the poly (ethylene oxide) (PEO)/clay (Nanocore I30E)) nanocomposites with $LiBF_4$ as salt. The increase of basal spacing indicates the formation of intercalated nanocomposites. Crystallinity was reduced after

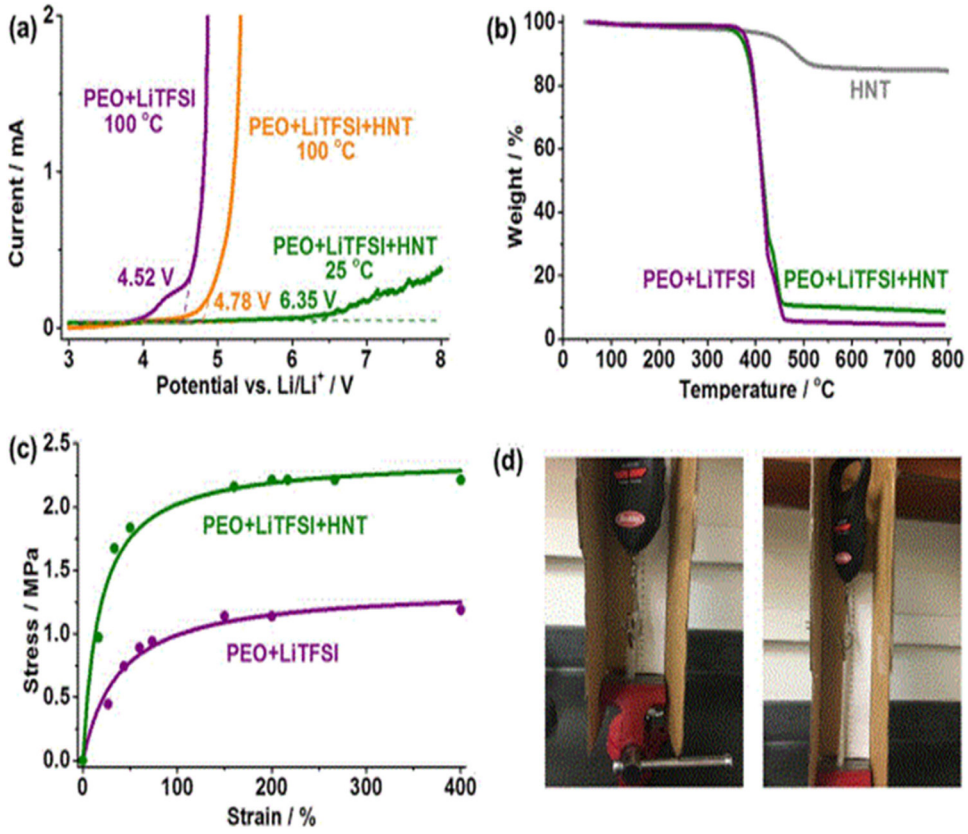

Figure 41. Electrochemical, thermal and mechanical stability of the HNT nanocomposite electrolyte. (a) Linear sweep voltammetry Li/PEO + LiTFSI + HNT/SS cells at 25 °C and 100 °C, and Li/PEO + LiTFSI/SS cells at 100 °C at a rate of 10 mV s^{-1}. (b) Thermogravimetric analysis of PEO + LiTFSI + HNT, PEO + LiTFSI, and HNT. (c) Stress–strain curves of the PEO + LiTFSI + HNT and PEO + LiTFSI electrolytes. (d) Photos of the PEO + LiTFSI + HNT film at initial and final tension state. Reprinted from [113], Copyright 2017, with permission from Elsevier.

the addition of salt in the pure polymer and was due to the interaction of cations with the polymer ether group, as concluded by DSC (figure 40(c)). The PEO/Li^+/clay composites and PEO/clay composts showed different behavior due to the interaction of negatively charged clay layers with the cation. It was concluded that two effects are present in PEO/Li^+/clay composite electrolytes: one reduces the crystallinity and the other favors the crystallinity. The former dominates at low clay loadings due to steric hindrance produced by the huge surface area of randomly oriented clay in the polymer matrix. At high clay loadings, the latter dominates due to the expansion of the silicate layers and clay content, which reduces the PEO–Li^+ interaction, and crystallinity increases. The highest conductivity was obtained for a 7.5% clay loading due to the interaction of lithium cations with silicate layers, which disrupts the strong intra-association between Li^+–BF_4^- and supports the fast migration of lithium ions.

Recently, Lin *et al* [113] reported the preparation of an SPE comprising PEO-LiTFSI and natural halloysite nano-clay (HNT). The highest ionic conductivities values for PEO + LiTFSI (EO:Li = 15:1) + HNT(10%) are 1.11×10^{-4}, 1.34×10^{-3} and 2.14×10^{-3} S cm^{-1} at 25 °C, 60 °C, and 100 °C, respectively. Also the optical microscope study evidenced the increase in conductivity as a reduction of phase transition temperature and the crystal size was observed. The cation transport number (t^+) was 0.40 and is much higher than that of pure PEO ($t^+ = 0.10$). Also, the ESW was much higher as measured by LSV and confirmed the stability up to 6.35 and 4.78 V respectively at 25 °C and 100 °C. TGA analysis confirmed thermal stability up to 430 °C (figure 41(b)). The addition of HNT also improved the mechanical strength of SPE, and for 400% strain the stress for HNT-based SPE is 2.25 MPa, which is large compared to 1.25 MPa for PEO-LiTFSI electrolyte (figure 41(c)).

The enhancement in conductivity was due to the presence of two face surfaces; the outer surface contains a –Si–O–Si– silica tetrahedral sheet, while the inner surface consists of –Al–OH groups from the octahedral sheet. HNT supports salt dissociation and the cation is coordinated with an outer layer having a negative surface charge layer, while the anion is adsorbed on the inner surface of HNT. The Lewis acid base interactions between the PEO–LiTFSI–HNT shorten the path for Li^+ via formation of 3D channels and a high speed pathway enhances ionic conductivity. Also the battery was fabricated using SPE as the electrolyte and stable discharge capacities were observed, with an averaged value of 745 ± 21 mAh g^{-1} over 100 discharge/charge cycles. The 87% retention was observed compared to the second discharge capacity, and is close to 100% efficiency for each cycle.

Zhang *et al* [114] prepared an SPE comprising of PEO, lithium bis (trifluromethanesulfonyl)imide (LiTFSI), and montmorillonite (MMT). XRD spectra showed a strong (0 0 1)

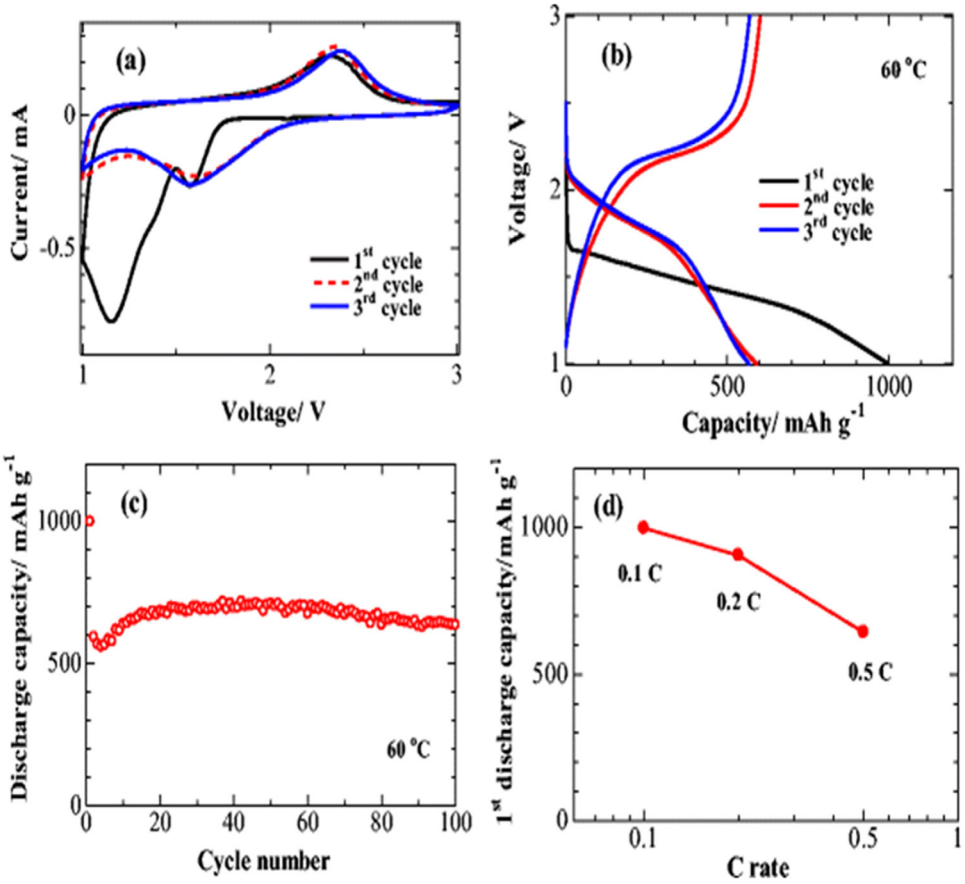

Figure 42. (a) Initial CV profiles of all solid-state Li/S cell at 60 °C; the measurement is conducted at a scan rate of 0.1 mV s^{-1} in the voltage range of 1.0–3.0 V versus Li^+/Li; (b) charge/discharge profiles (at 0.1 C) of all solid-state Li/S cell at 60 °C; (c) cycle performance (at 0.1 C) of all solid-state Li/S cell at 60 °C; (d) rate capability of all solid-state Li/S cell at 60 °C. [114] 2015 © Springer-Verlag Berlin Heidelberg 2014. With permission of Springer.

reflection at $2\theta = 5.0°$ corresponding to MMT with interlayer spacing of 1.76 nm. The addition of MMT in polymer salt composites indicated an increase in interlayer spacing to 1.96 nm and was due to polymer chain intercalation in nanoclay galleries. Also, the decrease in peak intensity with the addition of nanoclay indicated an increase of amorphous content. The maximum conductivity was 2.75×10^{-5} S cm^{-1} at 25 °C for the composite containing 10 wt.% MMT, and 3.22×10^{-4} S cm^{-1} at 60 °C. Further, at higher clay content, the insulating nature of clay dominated, which reduced the ionic conductivity. The Li^+ transference number was increased from 0.17 to 0.45 for the PEO/LiTFSI/10% MMT-based polymer electrolyte and this was attributed to the interaction of Lewis acid sites on the anionic surface of MMT with the ether group of the PEO. The ESW is 4 V and is useful for the application purpose. The electrochemical performance of Li/S cells was investigated using galvanostatic charge/discharge at 60 °C. The specific capacity of 998 mAh g^{-1} was obtained in the first discharge at 0.1 C, and a reversible capacity of 591 mAh g^{-1} was achieved in the second cycle (figure 44(b)). Figure 42(c) shows the cycling performance of the cells with PEO/MMT SPE, and initially a capacity increase is seen for the first 20 cycles at 0.1 C. After 100 cycles, the reversible specific discharge capacity of 634 mAh g^{-1} was obtained, and is equivalent to a 63.5% capacity retention of the initial discharge capacity. Figure 44(d) shows the rate capabilities of cells for different C rates, namely 0.1, 0.2, and 0.5 C. It shows a general trend of decrease of capacity with an increase of discharge rate.

Thakur *et al* [115] reported the preparation of (PEO_{25}–$NaClO_4$) and an organically modified sodium montmorillonite (NaMMT) based polymer nanocomposite by a tape casting technique. The XRD patterns confirmed the intercalation of clay in the polymer salt complex and an increase in basal interlayer spacing was observed due to an ion exchange on clay modification, which confirmed the strong interaction between polymer chain and clay. The clay peak d_{001} reflection shifts towards the lower angle side and evidence of the successful intercalation of polymer into the clay nanometric channels, which increased its width and were observed only at low clay contents. At high clay content, width decreased due to a decrease of intercalation of polymer in clay channels. The FTIR spectrum evidenced the presence of strong interactions on the intercalation of clay in the polymer salt system. Also, the stretching band of the ClO_4^- ion evidences change in peak intensity and width, which suggests the strong ion–clay interaction. AFM study confirms the formation of new nanostructures on the addition of clay. The presence of humps in the AFM image suggests atomic corrugation at the nanoscale and the multiphase composite behavior of the intercalated

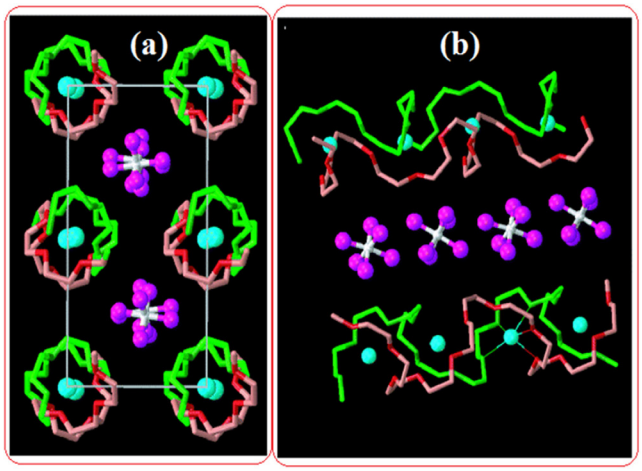

Figure 43. (a) View of the PEO_6:$LiAsF_6$ structure along a, showing rows of Li^+ ions perpendicular to the page. Blue spheres, lithium; white spheres, arsenic; magenta, fluorine; light green, carbon in chain 1; dark green, oxygen in chain 1; pink, carbon in chain 2; red, oxygen in chain 2. (b) View of the structure showing the relative positions of the chains and their conformations. Thin lines indicate coordination around the Li^+ cation. The lithium–ether oxygen distances (Å) for chain 1 are 2.07(5), 2.26(4), 2.28(4); for chain 2 they are 2.05(5), 2.14(6). Reprinted by permission from Macmillan Publishers Ltd: Nature [119], Copyright 1999.

polymer matrix is confirmed by the color pattern. Also, the conductivity increased with the addition of clay, with a maximum at a 5% clay concentration at room temperature with a value of ~2.20×10^{-7} S cm^{-1}. The increase in conductivity may have been due to the interaction of negative changes in the nanoclay surface and sodium cations, as confirmed by XRD dominating at low clay content. At high clay content the inverse effect was seen, which showed a decrease of mobility due to the formation of ion pairs and is in good agreement with FTIR results.

Chaudhary *et al* [116] prepared the SPE based on poly (ethylene oxide) (PEO), lithium perchlorate ($LiClO_4$) with montmorillonite (MMT) nanoplatelets by direct melt compounded HP technique. The DC conductivity variation followed the Jonscher power law with an exponent value of 0.87–0.91. The highest conductivity was 4.69×10^{-7} S cm^{-1} for the 2 wt.% clay content. The synthesis methods used in this study affected the arrangements of intercalated/exfoliated MMT nanoplatelets and aligned them parallel to the film surface, which affected the ion conduction paths, and may have favored the enhancement in ionic conductivity. Table 6 shows some significant results of ionic conductivity, cation and ion transference numbers, thermal stability, voltage stability windows and cyclic stability in dispersed and intercalated type SPEs.

5. Proposed ion transport mechanisms

For the complete understanding of improvements in the properties of polymer electrolyte systems it becomes crucial to know how the transport of ions occurs in the polymer matrix. For ion transport, one important property of the polymer host is that it must have an electron-rich donor group, such as ether group (—Ö—) as in the case of PEO and a high dielectric

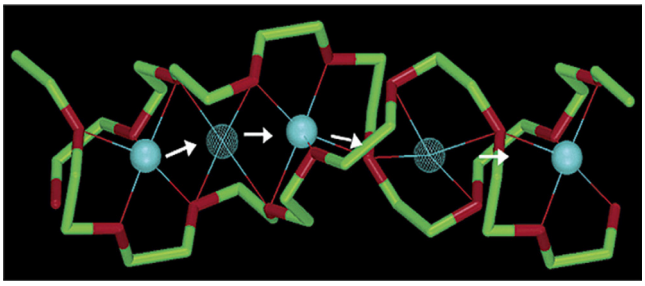

Figure 44. Schematic diffusion pathway of the Li^+ cations in PEO_6:$LiPF_6$. Thin lines indicate coordination around the Li^+ cation; solid blue spheres, lithium in the crystallographic five-coordinate site (note that the fifth thin line is very short in this view); meshed blue spheres, lithium in the intermediate four-coordinate site; green, carbon; red, oxygen. Reprinted with permission from [120]. Copyright 2003 American Chemical Society.

constant (~4–5). This ether group will support the dissociation of salt via coordinating interaction to the cation and making the anion immobile, which is supposed to attach with the polymer chain backbone. Further, for complete dissociation of salt in a polymer matrix, it must have low lattice energy, which will release a number of free charge carriers for transport. The conductivity is proportional to the number of free charge carriers, electric charge and charge carrier mobility ($\sigma = ne\mu$). So, the number of free charge carriers is directly linked to the dissociation of salt and is further affected by the lattice energy of the salt and the dielectric constant of the host polymer [117, 118].

The second factor which is important is 'ion mobility and polymer flexibility'. In the polymer electrolyte, polymer flexibility plays an important role in ion transport. Polymer flexibility is observed by the glass transition temperature of the polymer host (T_g), and at this temperature a rigid phase changes into the rubbery or viscous phase. A lower T_g will provide a more flexible phase easily, and this will increase the polymer chain flexibility which plays a crucial role in ion transport. Above the glass transition temperature more free volume is created due to the fast segmental motion of polymer chains, and provides enough sites for conduction. The increased polymer flexibility will increase the disorder in the polymer chain and will enhance the ion mobility by providing suitable coordinating sites for transport via interaction with electron-rich sites.

5.1. Polymer salt system

The addition of salt in the polymer host provides free ions for transport. MacGlashan *et al* [119] reported a structure of the PEO:$LiAsF_6$ complex with a 6:1 composition and proposed a conduction mechanism in which the Li^+ cations were arranged in rows, with each row located inside a cylindrical surface formed by two PEO chains (figures 43(a) and (b)). Each polymer chain adopts a non-helical conformation that defines a half-cylinder; the two half-cylinders, which are related by a center of inversion, interlock on both sides.

Six ethylene oxide units, starting from a C–O bond, represent chain conformation and each cation is coordinated simultaneously by both chains, involving three ether oxygens

Table 6. Ionic conductivity, cation/ion transference number, thermal stability, voltage stability window and cyclic stability of dispersed and intercalated type solid polymer electrolytes.

Materials used	Electrical conductivity (S cm^{-1})	Transference number (ion/cation)	Electrochemical stability Window (V)	Thermal stability (°C)	Cyclic stability	Ref.
PEO-$LiClO_4$ + LATP	1.71×10^{-4} S cm^{-1} at 20 °C	—	—	—		[85]
PEO-LiTF-LGPS	1.21×10^{-3} S cm^{-1} at 80 °C	—	5.2	—	Capacities of 158, 148, 138 and 99 mAh g^{-1} with current rate 0.1 C, 0.2 C, 0.5 C and 1 C at 60 °C	[86]
PEO-$LiClO_4$-LAGP	1.0×10^{-5} S cm^{-1}	—	4.75	—	Initial discharge capacity was 137.6 mAh g^{-1} and 142.2 mAh g^{-1} For the 20th cycle, initial capacities of 133.0–138.5 mAh g^{-1} to 113.4–121.5 mAh g^{-1} at the 100th cycle	[90]
PEO-PVdF-$BaTiO_3$	1.2×10^{-4} S cm^{-1}	—	4.7	330	—	[96]
PEO_{20}–LiBOB-MgO	—	—	4.2	—	Charge capacity and discharge capacity 168.8 and 156.8 mAh g^{-1}, respectively, and discharge capacity degrades to 142.5 mAh g^{-1} after 20 cycles	[97]
PEO-LiTFSI-MIL-53(Al)	3.39×10^{-3} S cm^{-1} at 120 °C	0.343	5.13	—	Initial discharge capacity 127.1 mA h g^{-1} (at 5 C) at 80 °C and 136.4 mA h g^{-1} at 120 °C. After 300 cycles 116.0 mA h g^{-1} at 80 °C and 129.2 mA h g^{-1} at 120 °C.	[98]
(PEO)-$LiClO_4$ + MU-SiO_2	1.2×10^{-3} at 60 °C	—	4.7 V for *ex situ* CPE and is 5.5 V for *in situ* CPE	—	Capacity retention 120 mAh g^{-1} was observed for *in situ* CPE and 65 mAh g^{-1} *ex situ* CPE	[99]
PEO-$LiClO_4$-$BaTiO_3$	1×10^{-5} S cm^{-1} at 25 °C and 1.2×10^{-3} S cm^{-1} at 70 °C	0.37	4	—	—	[103]
PEO-$LiClO_4$-MMT	9.43×10^{-4} S cm^{-1}	0.99/0.50	3	—	—	[111]
PEO-LiTFSI-HNT	1.11×10^{-4} at 25 °C, 1.34×10^{-3} at 25 °C, and 2.14×10^{-3} S cm^{-1} at 100 °C	0.40	6.35, 4.78	430 °C	Discharge capacities 745 ± 21 mAh g^{-1} in the 100 discharge/charge cycles with 87% capacity retention	[113]
PEO-LiTFSI-MMT	2.75×10^{-5} S cm^{-1} at 25 °C and 3.22×10^{-4} S cm^{-1} at 60 °C	0.45	4	—	The specific capacity of 998 mAh g^{-1} in the first discharge and a reversible capacity of 591 mAh g^{-1} is achieved in the second cycle. After 100 cycles, the reversible specific discharge capacity of 634 mAh g^{-1}	[114]

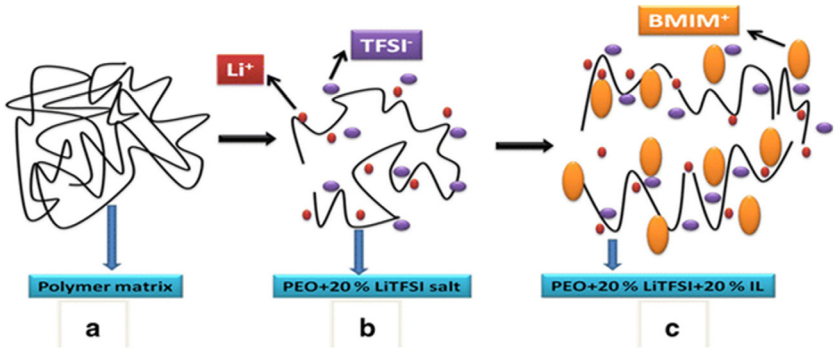

Figure 45. Schematic representation to understand the ionic transport behavior of pristine PEO and SPEs PEO + 20 wt.% LiTFSI and PEO + 20 wt.% LiTFSI + 20 wt.% BMIMTFSI at room temperature (30 °C). [121] 2017 © Springer-Verlag Berlin Heidelberg 2017. With permission of Springer.

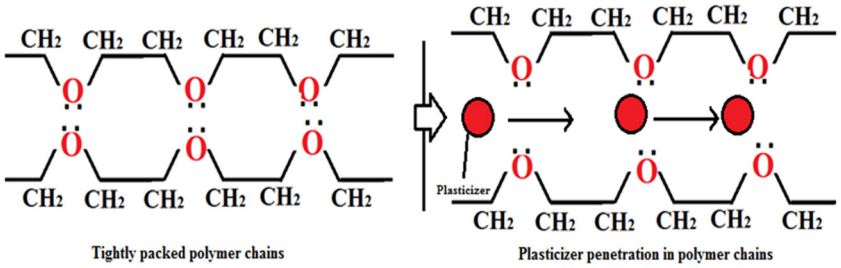

Figure 46. Effect of plasticizer in polymer matrix.

from one and two from the other, giving a total coordination around Li^+ of 5 and forming a somewhat distorted square pyramid (figure 43(b)). The cation is coordinated with the ether group while anions are located outside the dimensions of the cylinder in the interchain space. The crystal structure possesses highly aligned cylindrical tunnels, and the tunnels promote easy Li^+ ion transport along the chains, involving the sixth ether oxygen, which is not part of the static coordination environment around Li^+. The highly aligned tunnels provide a path for cation transport from one tunnel to the next, which results in high ionic conductivity (figure 44) and the anions are unable to penetrate the tunnels due to there being less separation between PEO cylinders, which prevents anion passage in between [120].

5.2. Ionic liquid polymer electrolyte

The addition of ILs in the polymer salt matrix reduces the intermolecular interaction between the polymer chains and hence increases the mobility and flexibility of the polymer chain segment which results in increased amorphous content. The enhancement in the number density of charge carriers (n) on the incorporation of IL content evidences the enhancement in ionic conductivity. The ionic liquid may become incorporated in the PEO matrix and two possibilities are: (i) liquid drop retaining its separate identity (they may be as 'coalesced drops' giving a continuous pathway or 'uncoalasced drops'), and; (ii) the IL cation ($EMIM^+$) complexed with ether oxygen C–O–C group of PEO is spread uniformly throughout the membrane [46]. The pure polymer is of crystalline nature (figure 45(a)) and the addition of salt makes the polymer chain flexible (figure 45(b)). Further, the addition of ionic liquid in the polymer salt system increases the polymer segmental motion or flexibility, which results in faster ionic transport or ionic conductivity (figure 47(c)) [121].

5.3. Gel polymer electrolyte

A plasticizer is a low molecular weight organic solvent that may be added to increase polymer segmental motion and flexibility and thereby improve the ionic conductivity of salts dissolved in the system (figure 46). Plasticizer penetrates into the polymer matrix and the presence of an interaction between polymer and plasticizer disrupts the arrangement of the polymer chain. The addition of plasticizer enhances the flexibility of the polymer electrolytes, as reported by many researchers [122, 123]. Plasticizer reduces the cohesive force between polymer chains and the disordered arrangement of polymer chains provides more coordinating sites to the ion for transport. This disruption in the crystallization of the polymer host also reduces the glass transition temperature and the increased segmental motion of the polymer chain leads to high ionic conductivity due to the availability of more free volume.

5.4. Solid polymer electrolyte

5.4.1. Dispersed type SPE. The ability of nanofiller to promote fast ion transport is due to the use of its structure for ion conduction via surface interaction. More importantly, nanofiller also enhances a mechanical property which is important in preventing dendrite growth formation and is related to the modulus of the polymer electrolyte. As ceramic nanofiller supports fast ion transport in polymer electrolytes, so it becomes essential to know the role played by nanofiller in conduction.

A report by Croce *et al* [124] reported the above with support for a model. The significant interaction between surface groups of the ceramic nanofiller, host polymer and anion of salt was remarkable regarding this enhancement in conductivity. It was concluded that competition occurs between a surface group of nanofiller and cation for the making of a complex with a polymer chain and the anion of salt. Structural modification of polymer chains occurs due to these types of interactions: (i) nanofiller surface group interacts with polymer and hinders the polymer reorganization tendency, which directly supports the fast migration of cations via ceramic surface, and (ii) salt dissociation is improved due to a decrease in ionic coupling by surface interactions of nanofiller.

Another model was reported by Sun Ji *et al* [125] based on the dielectric properties of nanofiller and the dipole orientation of polymer by their ability to align dipole moments. In a polymer salt system, two dipole moments are arranged in opposite directions to minimize its energy and form a stable state, and the addition of nanofiller changes the dipole moment of the system, which directly increases the dielectric constant value. Another possibility is that the nanofiller can penetrate the space between the polymer chains and the large surface area of nanofiller prevents or retards crystallization of the polymer host. It was concluded that the observed change in dipole moment creates a vibration which provides activation energy to the polymer matrix and facilitates the ion transport, which increases the conductivity.

Croce *et al* proposed a model addressing the role of the different surface groups of filler in enhancing the transport properties and specific interaction of PEO + $LiCF_3SO_3$–Al_2O_3 (basic, acidic and neutral) based composite polymer electrolytes. The addition of nanofiller helps in controlling the PEO chain crystallization kinetics, as well as leading to specific surface interactions with the electrolyte components. The Lewis acid groups of the added ceramics (e.g. the OH groups on the Al_2O_3 surface) may compete with the Lewis–acid lithium cations for the formation of complexes with the PEO chains, as well as with the anions of the added LiX salt [124, 126].

The structural modifications occurring at the ceramic surfaces, due to the specific actions of the polar surface groups of the inorganic filler, may act as cross-linking centers for the PEO segments and for the X^- anions and Lewis acid base interaction centers with the electrolyte ionic species, which together increases the number of free ions. The former promotes the structure modifications, and the latter enhances the salt dissociation by lowering the ionic coupling. The acidic surface group of filler favors the hydrogen bonding with anion and polymer chains segments. This results in an enhancement in salt dissociation and amorphous phase formation, as observed in ionic conductivity measurement (figure 47(a)), while in the filler with the neutral surface the weak interactions with both the polymer and anion of salt affect the ionic conductivity a little (figure 47(b)). In the case of a filler with a basic surface group, (figure 47(c)) confirms that, although no obvious changes occur, structural modifications can be in the order: Al_2O_3 acidic > Al_2O_3 neutral > Al_2O_3 basic.

Jayathilaka *et al* [127] proposed a model based on a Lewis acid base type interactions between the filler with different surface groups (basic, neutral, weakly acidic and acidic)

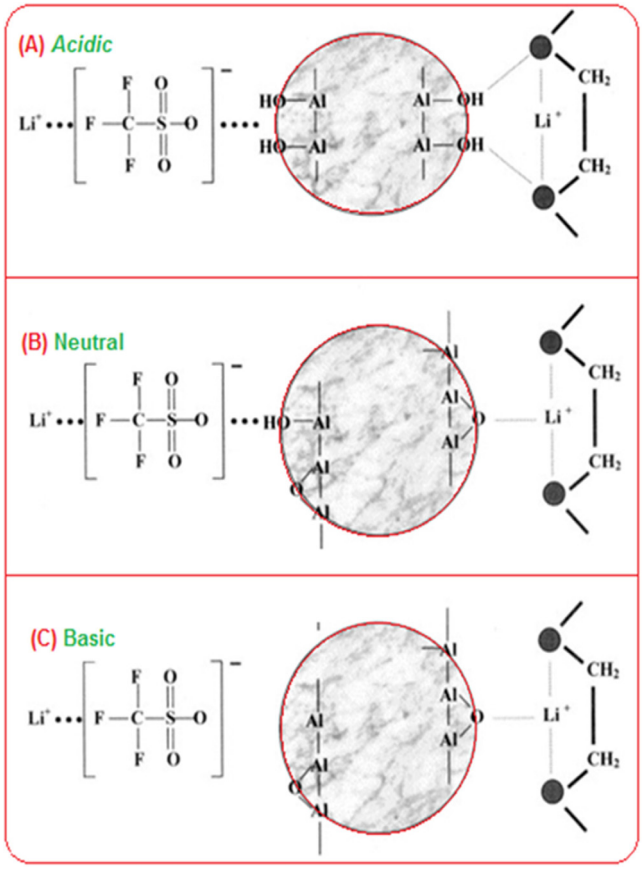

Figure 47. Pictorial model of the surface interactions between three forms of dispersed nanosized Al_2O_3 ceramic and the PEO–$LiSO_3CF_3$ electrolyte complex. (A) Al_2O_3 acidic; (B) Al_2O_3 neutral; (C) Al_2O_3 basic. Reprinted from [124], Copyright 2001, with permission from Elsevier.

and the ionic species comprising of $(PEO)_9$LiTFSI/10 wt.% Al_2O_3. As in a PEO-based polymer electrolyte, a Li^+ ion is coordinated to about four ether oxygen atoms of the same or different PEO chains, and ion movement occurs by the continuous breaking of old coordinating sites and the formation of new sites supports the fast segmental motion of polymer chain. Now the dispersion of nanofiller Al_2O_3 (particle size 104 μm and pore size 5.8 nm) is with a different surface group (a) filler free; (b) acidic; (c) basic; (d) neutral; and (e) weakly acidic. The different surface group provides a path for ionic transport by interactions with polymer and salt.

For the polymer electrolyte system without nanofiller, the anion is attached weakly with polymer segmental motion and provides no direct support for ion transport. For the Al_2O_3 filler with the acidic surface, the $TFSI^-$ anion is attracted strongly with the filler surface having OH polar groups via hydrogen bonding and is separated from the salt, while the free lithium ion now coordinates with the polymer ether group and migrates [128]. In a PEG–$LiClO_4$–Al_2O_3 system with basic surface groups, a strong interaction between Li cations and oxygen at a surface group of the filler is confirmed by FTIR spectra [129]. A weak bond formation occurs between lithium cations and oxygen surface groups of filler which provides additional sites for lithium ion migration along with coordinating sites of the polymer host. This dual path formation for

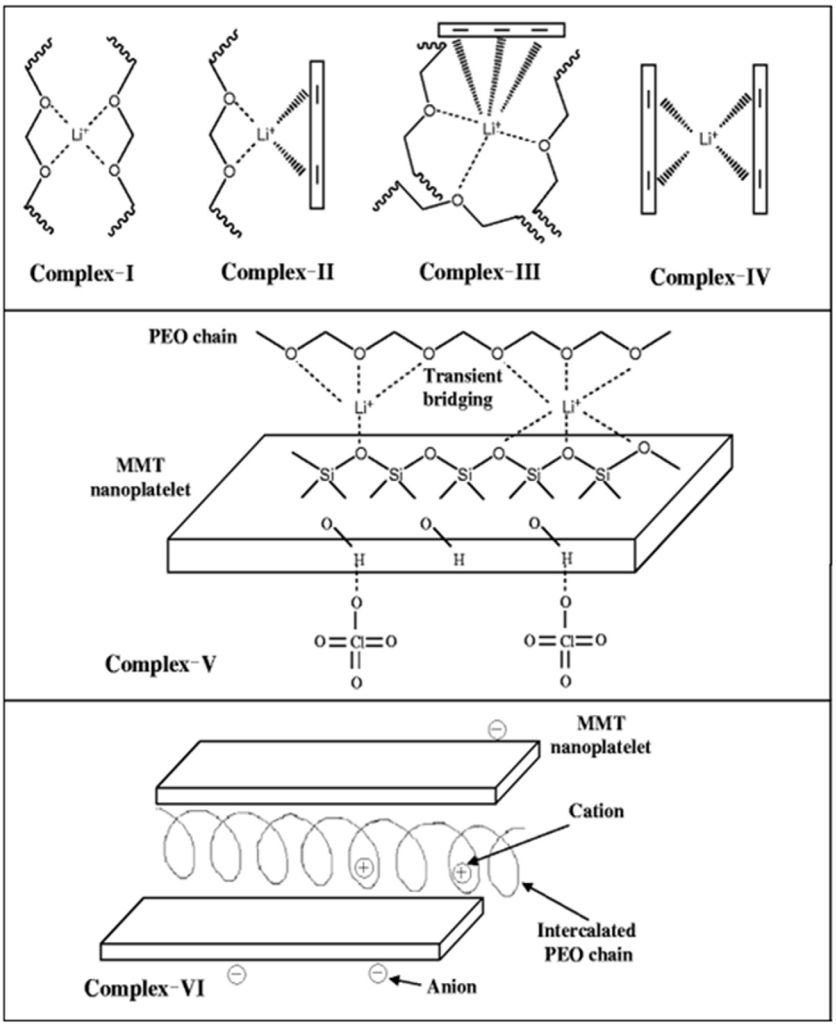

Figure 48. Schematic illustration of PEO–Li^+–MMT interactions: PEO complex with Li^+ (complex I), PEO and MMT complexes with Li^+ (complex II and III), MMT complex with Li^+ (complex IV), transient cross-linking of PEO and exfoliated MMT nano-platelet through Li^+ (complex V), Li^+ coordinated PEO intercalation in MMT gallery (complex VI). [116] 2011 © Springer-Verlag 2011. With permission of Springer.

ion transport enhances the overall mobility or the conductivity. It was concluded from the above that the degree of conductivity enhancement is higher for acidic alumina grains than basic alumina grains, as the acidic alumina increases the anionic contribution to the conductivity.

Now, in the case of a filler with neutral surface, acidic and basic sites are supposed to be the same and the former are meant to promote the anion migration and the latter the cation migration. Now the anions may interact with both acidic and basic sites due to the random distribution of sites on filler surface, and cation–anion interactions reduce the mobility compared to the pure acidic and basic surface group. For the weakly acidic surface groups, the alumina grain is expected to be of a more acidic nature than the basic groups, which reduces the number of additional sites for the cation, and a decrease in conductivity is seen for weakly acidic alumina. The above model concludes that the enhancement in ionic mobility is due to a Lewis acid base surface group's interaction with cations and anions which support the creation of additional sites, resulting in favorable conduction pathways for the migration of ions.

Thakur *et al* [130] reported substantial improvement in the mechanical stability, thermal stability, and conductivity of four series of ion-conducting dispersed phase composite polymer electrolytes (PEO + $NaClO_4$–Na_2SiO_3, SnO_2) and proposed a mechanism based on polymer–filler interaction among the composite components. FTIR spectroscopy concluded that the addition of filler is effective in the loosening and stiffening of the polymeric segments. Cations coordinate with four ether oxygens in PEO–salt complexes and an ion–polymer interaction results in two types of transient cross-links (inter- or intra-molecular) of polyether chains [131, 132]. The filler Na_2SiO_3 is an inert oxide with a net dipolar shift in the dielectric medium, and SnO_2 is an oxide of acidic nature. In the former the electropositive end of the dipoles may interact with the ether group of the polymer host or ClO_4^- ions, while the later has a natural tendency to interact with the aforementioned electronegative species. The cross-link formation between polymer chains may occur, which increase the viscosity and reduce the polymer chain flexibility. Two types of transient cross-linking between two nearby polymers are possible:

(i) directly through the cation;
(ii) through cation–anion interaction or a combination of both.

At low filler concentration, two possibilities arise. One is that the filler may interact with the polymer directly, and the second is that the filler may compete with cations (Na^+) coordinated with ether oxygen or with anions (ClO_4^-). Both types of interactions reduce the chances of transient cross-linking of polymeric chains and increase the flexibility of the polymer matrixes, as also evidenced by FTIR spectra (downshifting of C–O–C stretching band). At high filler content, polymer–filler interaction leads to a bridging effect between two polymeric chains via acidic or polar filler particles and enhances polymer stiffening, as observed in FTIR spectra (upward shifting of the maximum of the C–O–C stretching band). So a polymer backbone with improved mechanical strength is obtained, which can be improved with a high filler concentration.

5.4.2. Intercalated/exfoliated type SPE. Polymer-layered silicate nanocomposite has aroused much interest since Toyota's first successful formulation of Nylon 6-clay nanocomposite. The controlled parametres like conductvity and mobility can be achieved by incorporation of clay in the polymer, which also prevents the migration of the anion in the matrix. This also results in the large intefacial area which hinders the polymer chain arrangement and increases amorphous content while maintaining the mechanical properties. The incorporation of clays is a promising approach for enhancing ionic conductivity due to three properties: (i) high cationic exchange capacity, (ii) ability for participating in intercalation and swelling processes, (iii) provides single ion conduction. The single ion conduction obtained in PNC with clay is due to the layered structure of clay. The main advantage of the addition of clay is that the cation is easily intercalated in the clay galleries. One common approach to enhance the conduction is a modification of clay from a hydrophilic to a hydrophobic nature, which increases the interlayer spacing. The growth of the interlayer spacing is a major factor that provides the soft intercalation of the polymer–salt complex into the clay layers. The addition of clay in polymer electrolytes favors the cationic movement, as cations will be allowed to move freely through the clay layers, whereas the bulky and heavy anions are not authorized to pass through the clay layers. Another significant role played by clay is restricting the movement of anions through clay layers, but also by increasing the viscosity, and the cationic contribution dominates in the polymer matrix [131].

The exfoliated nanoplatelets of MMT in the PNCE films minimize the ion pairing effect, while intercalation impedes the polymer crystallization and enhances the nanometric channels for cation mobility [132–136]. Modification of clay is necessary for better dispersion in a solvent via intercalation with a polymer [137]. On the basis of the presence of a type of interaction between the polymer matrix and organically modified layered silicate (OMLS), three types of polymer nanocomposites are achieved: intercalated and exfoliated [138].

- *Intercalated nanocomposites*: this is the result of the penetration of the polymer matrix in the galleries between silicate layers and forms an alternate arrangement of polymer chains and silicate layer in a regular fashion. The above arrangement is independent of the polymer to clay ratio and the distance between them is in the range of few nanometers (1–4 nm). XRD is used to identify intercalated structures due to the presence of the alternate arrangement of polymer chains and clay.
- *Flocculated nanocomposites*: they are the same as intercalated nanocomposites, except for the fact that some silicate layers are, sometimes, flocculated due to edge–edge interactions between hydroxyl groups of the silicate.
- *Exfoliated nanocomposites*: it is the result of the complete separation of individual layers of silicate layers and radnom dispersion with the average distance (>6 nm) in the polymer matrix depanding on clay charge. Generally, the clay content in an exfoliated nanocomposite is much lower than in an intercalated nanocomposite and is preferred over intercalated as they provide the best property improvements. Also it depends on clay loading, unlike the intercalated case. XRD patterns show no peak for this due to the absence of ordered arrangement and large spacing.

Jing *et al* [139] investigated the free volume, structural transition and ionic conduction for PEO/$LiClO_4$/clay (OREC) nanocomposite electrolytes. It was concluded that OREC content increases the ionic conductivity of PNC and is highest for 3 wt.% clay content. At this clay content, the increase in free volume was maximum. XRD analysis showed an increase in the *d*-spacing by organic modification of the clay and this evidences polymer intercalation in clay. Also, the polymer chain is disturbed, and the interaction of nano-rectorite with the polymer matrix enhances the free volume. The conductivity mechanism is reported and explained on the basis of free volume theory. The addition of the PEO hinders the interaction between cation and polymer and leads to the release of more free ions. Also, the addition of OREC can create a higher interfacial area between the polymer matrix and the clay which provides a path for cation migration and enhances the conductivity of the nanocomposite. But once OREC exceeds 3% then ion movement is restricted due to the formation of two types of complexes, and free volume decreases.

Another model was proposed by Choudhary *et al* [116] on the basis of dielectric parameters to explain the effect of various interactions on the PEO local chain dynamics and the mechanism of PEO coordinated lithium cation motion. It is generally agreed that the Li^+ ion has four to six sites of coordination with PEO and MMT nanoplatelets [2, 10]. In figure 48 (complex I), the Li^+ coordination with four neighbor etheric oxygens of the PEO segments in the PEO–Li^+ domain is depicted, and after the incorporation of clay in the polymer salt matrix, complex formation of the exfoliated MMT and ether group of PEO with Li^+ is observed, as depicted in complex II and complex III. Another complex formation is observed between MMT siloxane groups and lithium cation, as shown in complex IV of figure 48. Complex V depicts the presence of a supramolecular transient cross-linked structure between the PEO and exfoliated MMT nanoplatelet, while

polymer chain intercalation with the cation in the MMT gallery is sketched in complex VI. Complex VI also evidences that anions (ClO_4^-) are immobile due to their bulky size, and for an MMT loaded system the anions stay outside the clay galleries. This supports the fast ionic conduction for cations via polymer chain segmental motion [140]. But the interaction of exfoliated MMT structures prevents cation migration due to the lesser number of conduction paths. It was concluded that cation mobility is enhanced by two ways: (i) faster segmental motion of polymer chains, and; (ii) number of available ion conduction paths, as well as the height of potential barrier, for the successful jump from one site to another.

6. Summary and prospects

The electrolyte is a critical component of any ESCD. The electrolyte plays the dual role of providing physical separation of the electrodes and a medium for the to and fro swimming of ions, enabling the transport. An ideal separator must possess some characteristic properties such as minimum thickness, low internal resistance, shape flexibility, broad thermal/ESW, mechanical stability and structural stability. However it is difficult to uphold all properties together, but PEO separators provide balanced properties amongst all polymers due to the presence of the ether group and low glass transition temperatures, which enable us to build a high performance system.

In this review, we have introduced the recent progress in prospective PEO-based polymer electrolytes with a sharp focus on the dispersed and intercalated type, and ionic liquid/plasticizer incorporated polymer electrolyte for energy storage devices. The desirable properties of the polymer host, salt, solvent, nanofiller, ionic liquid, plasticizer and nanoclay required for synthesization and good performance of electrolyte in the battery are summarized. In addition to this, the preparation methods for the polymer electrolytes by various researchers are described, and it also includes the required characterization for studying the surface properties, electrochemical properties, thermal properties, and stability properties done in the area of polymer electrolytes. The key roles of the ionic liquid, nanofiller, plasticizer and clay in the enhancement of electrochemical properties of polymer electrolyte in energy storage devices are reported. The reliable transport mechanisms proposed by various researchers to explain the increase in transport properties are concluded with a sharp eye on the presence of various types of interaction, such as polymer–salt, polymer–nanofiller, salt–nanofiller, polymer–ionic liquid, and polymer–clay.

The property of solvent, salt, nanofiller and plasticizer also affects the performance of polymer electrolyte. Salts with bulky anion size, high room temperature stability and low lattice energy are beneficial candidates for achieving high ionic conductivity. Salts with broader ESW and environmentally friendly nature will fulfill the need for ideal salts for the polymer electrolyte. Also the role of solvent cannot be neglected in the preparation of polymer electrolyte. The solvent must be of nonflammable nature, of low viscosity, and must be capable of complete dissolution of polymer chains inside, which results in increased interaction of polymer chains with cations by swelling properly. A plasticizer with a high dielectric constant and low viscosity is an alternative candidate for enhancing the properties of polymer electrolytes. Passive filler only indirectly supports the ion migration by providing additional conducting pathways via Lewis acid base interactions, and also dissociates more salt. Instead of passive fillers, active fillers can be an alternative for the promotion of ions due to their supportive nature in ion transport and increased number of charge carriers.

At present, ionic liquid based polymer electrolytes are interesting candidates for separators in energy storage device. They provide improved conductivity and electrochemical properties due to the release of more free charge carriers and a decrease of crystallinity. Although ionic conductivity is higher for gel polymer electrolytes, poor mechanical properties limit them for practical applications in high performance energy storage devices.

Low molecular weight plasticizer incorporated polymer electrolytes have also been used over the last decade as separators. They provide hindrance in the polymer chain arrangement by penetrating the chain, which increases polymer chain flexibility and supports fast migration of ions, which is a characteristic of a high performance device. Also, the free volume by plasticizer provides an easy path to the cation for migration. The addition of plasticizer also reduces the interaction of cation with polymer ether group, which is evidence of enhanced conductivity. But disturbance of mechanical properties affects the performance of the device and is one of the drawbacks of these types of systems.

So, the best alternative for balanced ionic conductivity and mechanical properties is the SPE, which can be classified into two types based on the addition of nanofiller and nanoclay, known as dispersed and intercalated type polymer electrolytes. Further, nanofillers are of two types on the basis of support to transport of ions in a polymer matrix; the one that is involved in ionic transport is called an active nanofiller, and the other, which supports the polymer structure only and has no active role in ion transport, is a passive filler. The high dielectric constant of nanofiller dissociates more salt and releases more free charge carriers. Nanofiller mainly plays a dual role here; it promotes ion migration by reducing the reorganization tendency of polymer, and it decreases ionic coupling due to Lewis acid base interactions. Improved conductivity values are obtained for the dispersed type polymer electrolyte along with suitable thermal and mechanical properties which make them an alternative to the energy storage device.

Clay intercalated polymer electrolyte is promising for a high energy storage system. The intercalation of clay in the polymer chain increases the basal spacing which supports fast ion transport. Another advantage of the intercalated type polymer electrolyte is that a single ion conductor can be obtained, which is desirable in the case of polymer electrolytes, as the anion is supposed to become trapped within the polymer chains. Clay blocks the anion outside the clay galleries and only the cation is transported inside.

So, for the successful development of an advanced polymer electrolyte with overall balancing properties, SPEs are

attractive, and further optimizing the properties of SPEs can fulfill the ambition of an ideal energy storage device using polymer electrolytes. In context to the above, one important thing we have to keep in mind is that cost and properties as well as safety must be appropriate for human beings. In the future, polymer electrolyte/separators with shape flexibility are needed due to people's lack of time and space. Even an interesting one is the development of a device which can be folded easily and can sustain for long periods in remote areas during a journey. There is also need to search for new methods of battery fabrication, including layer by layer deposition, and some different physical structure which can provide an advanced energy storage system.

Acknowledgment

One of the authors acknowledges with thanks the financial support from CUPB and partial funding from UGC Startup Grant (GP-41).

References

[1] Zhang H, Li C, Piszcz M, Coya E, Rojo T, Rodriguez-Martinez L M, Armand M and Zhou Z 2017 Single lithium-ion conducting solid polymer electrolytes: advances and perspectives *Chem. Soc. Rev.* **46** 797–815
[2] Goodenough J B and Park K S 2013 The Li-ion rechargeable battery: a perspective *J. Am. Chem. Soc.* **135** 1167–76
[3] Bhatt M D and O'Dwyer C 2015 Recent progress in theoretical and computational investigations of Li-ion battery materials and electrolytes *Phys. Chem. Chem. Phys.* **17** 4799–844
[4] Lee H, Yanilmaz M, Toprakci O, Fu K and Zhang X 2014 A review of recent developments in membrane separators for rechargeable lithium-ion batteries *Energy Environ. Sci.* **7** 3857–86
[5] Bruce P G, Scrosati B and Tarascon J M 2008 Nanomaterials for rechargeable lithium batteries *Angew. Chem., Int. Ed. Engl.* **47** 2930–46
[6] http://batteryuniversity.com/learn/article/global_battery_markets
[7] http://indianexpress.com/article/technology/tech-news-technology/googles-chairman-eric-schmidt-calls-lithium-ion-successor-batteries-to-be-promising-4568874
[8] Scrosati B and Vincent C A 2000 Polymer electrolytes: the key to lithium polymer batteries *MRS Bull.* **25** 28–30
[9] Shin J H, Henderson W A and Passerini S 2005 An elegant fix for polymer electrolytes *Electrochem. Solid-State Lett.* **8** A125–7
[10] Arya A and Sharma A L 2017 Polymer electrolytes for lithium ion batteries: a critical study *Ionics* **23** 497–540
[11] Sharma A L and Thakur A K 2015 Relaxation behavior in clay-reinforced polymer nanocomposites *Ionics* **21** 1561–75
[12] Bhatt C, Swaroop R, Arya A and Sharma A L 2015 Effect of nano-filler on the properties of polymer nanocomposite films of PEO/PAN complexed with $NaPF_6$ *J. Mater. Sci. Eng.* B **5** 418–34
[13] Linford R G 1995 EXAFS studies of polymer electrolytes *Chem. Soc. Rev.* **24** 267–77
[14] Arya A, Sharma A L, Sharma S and Sadiq M 2016 Role of low salt concentration on electrical conductivity in blend polymeric films *J. Integr. Sci. Technol.* **4** 17–20
[15] MacCallum J R and Vincent C A 1989 *Polymer Electrolyte Reviews* vol 2 (Berlin: Springer)
[16] MacCallum J R and Vincent C A 1987 *Polymer Electrolyte Reviews* vol 1 (New York: Elsevier)
[17] www4.ncsu.edu/~hubbe/PEO.htm
[18] Dahal U R and Dormidontova E E 2017 The dynamics of solvation dictates the conformation of polyethylene oxide in aqueous, isobutyric acid and binary solutions *Phys. Chem. Chem. Phys.* **19** 9823–32
[19] Arya A and Sharma A L 2016 Conductivity and stability properties of solid polymer electrolyte based on PEO-PAN + $LiPF_6$ for energy storage *Appl. Sci. Lett.* **2** 72–5
[20] Xue Z, He D and Xie X 2015 Poly(ethylene oxide)-based electrolytes for lithium-ion batteries *J. Mater. Chem.* A **3** 19218–53
[21] Liang B, Tang S, Jiang Q, Chen C, Chen X, Li S and Yan X 2015 Preparation and characterization of PEO-PMMA polymer composite electrolytes doped with nano-Al_2O_3 *Electrochim. Acta* **169** 334–41
[22] Armand M, Endres F, MacFarlane D R, Ohno H and Scrosati B 2009 Ionic-liquid materials for the electrochemical challenges of the future *Nat. Mater.* **8** 621–9
[23] Lu J, Yan F and Texter J 2009 Advanced applications of ionic liquids in polymer science *Prog. Polym. Sci.* **34** 431–48
[24] Leones R, Sabadini R C, Esperança J M, Pawlicka A and Silva M M 2017 Playing with ionic liquids to uncover novel polymer electrolytes *Solid State Ion.* **300** 46–52
[25] Pradhan D K, Choudhary R N P, Samantaray B K, Karan N K and Katiyar R S 2007 Effect of plasticizer on structural and electrical properties of polymer nanocomposite electrolytes *Int. J. Electrochem. Sci.* **2** 861–71
[26] Sharma A L and Thakur A K 2010 Improvement in voltage, thermal, mechanical stability and ion transport properties in polymer-clay nanocomposites *J. Appl. Polym. Sci.* **118** 2743–53
[27] Ueki T and Watanabe M 2008 Macromolecules in ionic liquids: progress, challenges, and opportunities *Macromolecules* **41** 3739–49
[28] Feuillade G and Perche P 1975 Ion-conductive macromolecular gels and membranes for solid lithium cells *J. Appl. Electrochem.* **5** 63–9
[29] Stephan A M 2006 Review on gel polymer electrolytes for lithium batteries *Eur. Polym. J.* **42** 21–42
[30] Sharma A L and Thakur A K 2010 Polymer–ion–clay interaction based model for ion conduction in intercalation-type polymer nanocomposite *Ionics* **16** 339–50
[31] Sharma A L and Thakur A K 2011 AC conductivity and relaxation behavior in ion conducting polymer nanocomposite *Ionics* **17** 135–43
[32] Jinisha B, Anilkumar K M, Manoj M, Pradeep V S and Jayalekshmi S 2017 Development of a novel type of solid polymer electrolyte for solid state lithium battery applications based on lithium enriched poly (ethylene oxide)(PEO)/poly (vinyl pyrrolidone)(PVP) blend polymer *Electrochim. Acta* **235** 210–22
[33] Agrawal R C, Chandra A, Bhatt A and Mahipal Y K 2008 Investigations on ion transport properties of and battery discharge characteristic studies on hot-pressed Ag^+-ion-conducting nano-composite polymer electrolytes:$(1-x)$ $[90PEO:10AgNO_3]:xSiO_2$ *New J. Phys.* **10** 043023
[34] Appetecchi G B, Croce F, Persi L, Ronci F and Scrosati B 2000 Transport and interfacial properties of composite polymer electrolytes *Electrochim. Acta* **45** 1481–90
[35] Harun F, Chan C H and Winie T 2017 Influence of molar mass on thermal properties, conductivity and intermolecular interaction of poly (ethylene oxide) solid polymer electrolytes *Polym. Int.* **66** 830–8

[36] Boschin A and Johansson P 2015 Characterization of NaX (X: TFSI, FSI)–PEO based solid polymer electrolytes for sodium batteries *Electrochim. Acta* **175** 124–33

[37] Polu A R, Kim D K and Rhee H W 2015 Poly (ethylene oxide)-lithium difluoro (oxalato) borate new solid polymer electrolytes: ion–polymer interaction, structural, thermal, and ionic conductivity studies *Ionics* **21** 2771–80

[38] Karuppasamy K, Kim D, Kang Y H, Prasanna K and Rhee H W 2017 Improved electrochemical, mechanical and transport properties of novel lithium bisnonafluoro-1-butanesulfonimidate (LiBNFSI) based solid polymer electrolytes for rechargeable lithium ion batteries *J. Ind. Eng. Chem.* **52** 224–34

[39] Anilkumar K M, Jinisha B, Manoj M and Jayalekshmi S 2017 Poly (ethylene oxide)(PEO)–Poly (vinyl pyrrolidone) (PVP) blend polymer based solid electrolyte membranes for developing solid state magnesium ion cells *Eur. Polym. J.* **89** 249–62

[40] Chapi S, Raghu S and Devendrappa H 2016 Enhanced electrochemical, structural, optical, thermal stability and ionic conductivity of (PEO/PVP) polymer blend electrolyte for electrochemical applications *Ionics* **22** 803–14

[41] Luo H, Liang X, Wang L, Zheng A, Liu C and Feng J 2014 Highly mobile segments in crystalline poly (ethylene oxide)$_8$:$NaPF_6$ electrolytes studied by solid-state NMR spectroscopy *J. Chem. Phys.* **140** 074901

[42] Zhang H, Liu C, Zheng L, Xu F, Feng W, Li H, Huang X, Armand M, Nie J and Zhou Z 2014 Lithium bis (fluorosulfonyl) imide/poly (ethylene oxide) polymer electrolyte *Electrochim. Acta* **133** 529–38

[43] Bitner-Michalska A *et al* 2017 Fluorine-free electrolytes for all-solid sodium-ion batteries based on percyano-substituted organic salts *Sci. Rep.* **7** 40036

[44] Ma Q *et al* 2016 Novel Li [(CF_3SO_2)(n-$C_4F_9SO_2$)N]-based polymer electrolytes for solid-state lithium batteries with superior electrochemical performance *ACS Appl. Mater. Interfaces* **8** 29705–12

[45] Judez X, Zhang H, Li C, González-Marcos J A, Zhou Z B and Armand M and Rodriguez-Martinez L M 2017 Lithium Bis (fluorosulfonyl) imide/poly (ethylene oxide) polymer electrolyte for all solid-state Li–S Cell *J. Phys. Chem. Lett.* **8** 1956–60

[46] Ibrahim S, Yassin M M, Ahmad R and Johan M R 2011 Effects of various $LiPF_6$ salt concentrations on PEO-based solid polymer electrolytes *Ionics* **17** 399–405

[47] Thiam A, Antonelli C, Iojoiu C, Alloin F and Sanchez J Y 2017 Optimizing ionic conduction of poly (oxyethylene) electrolytes through controlling the cross-link density *Electrochim. Acta* **240** 307–15

[48] Osada I, De Vries H, Scrosati B and Passerini S 2016 Ionic-liquid-based polymer electrolytes for battery applications *Angew. Chem., Int. Ed. Engl.* **55** 500–13

[49] Das S and Ghosh A 2016 Structure, ion transport, and relaxation dynamics of polyethylene oxide/poly (vinylidene fluoride co-hexafluoropropylene)—lithium bis (trifluoromethane sulfonyl) imide blend polymer electrolyte embedded with ionic liquid *J. Appl. Phys.* **119** 095101

[50] Chaurasia S K, Gupta A K, Verma Y L, Singh V K, Tripathi A K, Saroj A L and Singh R K 2015 Role of ionic liquid [$BMIMPF_6$] in modifying the crystallization kinetics behavior of the polymer electrolyte PEO-$LiClO_4$ *RSC Adv.* **5** 8263–77

[51] Gupta H, Balo L, Singh V K, Chaurasia S K and Singh R K 2016 Effect of phosphonium based ionic liquid on structural, electrochemical and thermal behaviour of polymer poly (ethylene oxide) containing salt lithium bis (trifluoromethylsulfonyl) imide *RSC Adv.* **6** 87878–87

[52] Polu A R and Rhee H W 2017 Ionic liquid doped PEO-based solid polymer electrolytes for lithium-ion polymer batteries *Int. J. Hydrog. Energy* **42** 7212–9

[53] Balo L, Gupta H, Singh V K and Singh R K 2017 Flexible gel polymer electrolyte based on ionic liquid EMIMTFSI for rechargeable battery application *Electrochim. Acta* **230** 123–31

[54] Cheng H, Zhu C, Huang B, Lu M and Yang Y 2007 Synthesis and electrochemical characterization of PEO-based polymer electrolytes with room temperature ionic liquids *Electrochim. Acta* **52** 5789–94

[55] Chaurasia S K, Singh R K and Chandra S 2011 Structural and transport studies on polymeric membranes of PEO containing ionic liquid, EMIM-TY: evidence of complexation *Solid State Ion.* **183** 32–9

[56] Yongxin A, Xinqun C, Pengjian Z, Lixia L and Geping Y 2012 Improved properties of polymer electrolyte by ionic liquid $PP_{1.3}$TFSI for secondary lithium ion battery *J. Solid State Electrochem.* **16** 383–9

[57] Singh V K, Chaurasia S K and Singh R K 2016 Development of ionic liquid mediated novel polymer electrolyte membranes for application in Na-ion batteries *RSC Adv.* **6** 40199–210

[58] DeVries H, Jeong S and Passerini S 2015 Ternary polymer electrolytes incorporating pyrrolidinium-imide ionic liquids *RSC Adv.* **5** 13598–606

[59] Simonetti E, Carewska M, Di Carli M, Moreno M, De Francesco M and Appetecchi G B 2017 Towards improvement of the electrochemical properties of ionic liquid-containing polyethylene oxide-based electrolytes *Electrochim. Acta* **235** 323–31

[60] Simonetti E, Carewska M, Maresca G, De Francesco M and Appetecchi G B 2017 Highly conductive, ionic liquid-based polymer electrolytes *J. Electrochem. Soc.* **164** A6213–9

[61] Choi J W *et al* 2007 Poly (ethylene oxide)-based polymer electrolyte incorporating room-temperature ionic liquid for lithium batteries *Solid State Ion.* **178** 1235–41

[62] Kim G T, Appetecchi G B, Alessandrini F and Passerini S 2007 Solvent-free, PYR 1A TFSI ionic liquid-based ternary polymer electrolyte systems: I. Electrochemical characterization *J. Power Sources* **171** 861–9

[63] Joost M, Kim G T, Winter M and Passerini S 2015 Phase stability of Li-ion conductive, ternary solid polymer electrolytes *Electrochim. Acta* **113** 181–5

[64] Pandey G P, Kumar Y and Hashmi S A 2011 Ionic liquid incorporated PEO based polymer electrolyte for electrical double layer capacitors: a comparative study with lithium and magnesium systems *Solid State Ion.* **190** 93–8

[65] Karuppasamy K, Rhee H W, Reddy P A, Gupta D, Mitu L, Polu A R and Shajan X S 2016 Ionic liquid incorporated nanocomposite polymer electrolytes for rechargeable lithium ion battery: a way to achieve improved electrochemical and interfacial properties *J. Ind. Eng. Chem.* **40** 168–76

[66] Das S and Ghosh A 2015 Effect of plasticizers on ionic conductivity and dielectric relaxation of PEO-$LiClO_4$ polymer electrolyte *Electrochim. Acta* **171** 59–65

[67] Kumar Y, Hashmi S A and Pandey G P 2011 Lithium ion transport and ion–polymer interaction in PEO based polymer electrolyte plasticized with ionic liquid *Solid State Ion.* **201** 73–80

[68] Li W, Pang Y, Liu J, Liu G, Wang Y and Xia Y 2017 A PEO-based gel polymer electrolyte for lithium ion batteries *RSC Adv.* **7** 23494–501

[69] Zhu C, Cheng H and Yang Y 2008 Electrochemical characterization of two types of PEO-based polymer electrolytes with room-temperature ionic liquids *J. Electrochem. Soc.* **155** A569–75

[70] Egashira M, Todo H, Yoshimoto N and Morita M 2008 Lithium ion conduction in ionic liquid-based gel polymer electrolyte *J. Power Sources* **178** 729–35

[71] Natarajan A, Stephan A M, Chan C H, Kalarikkal N and Thomas S 2017 Electrochemical studies on composite gel polymer electrolytes for lithium sulfur-batteries *J. Appl. Polym. Sci.* **134** 44594

[72] Jayasekara I and Teeters D 2017 Investigation of a nanoconfined, ceramic composite, solid polymer electrolyte *Electrochim. Acta* **247** 1147–54
[73] Kim Y T and Smotkin E S 2002 The effect of plasticizers on transport and electrochemical properties of PEO-based electrolytes for lithium rechargeable batteries *Solid State Ion.* **149** 29–37
[74] Kriz J, Abbrent S, Dybal J, Kurkova D, Lindgren J, Tegenfeldt J and Wendsjo A 1999 Nature and dynamics of lithium ion coordination in oligo (ethylene glycol) dimethacrylate-solvent systems: NMR, Raman, and quantum mechanical study *J. Phys. Chem.* A **103** 8505–15
[75] Ma C, Zhang J, Xu M, Xia Q, Liu J, Zhao S, Chen L, Pan A, Ivey D G and Wei W 2016 Cross-linked branching nanohybrid polymer electrolyte with monodispersed TiO_2 nanoparticles for high performance lithium-ion batteries *J. Power Sources* **317** 103–11
[76] Klongkan S and Pumchusak J 2015 Effects of nano alumina and plasticizers on morphology, ionic conductivity, thermal and mechanical properties of PEO-$LiCF_3SO_3$ solid polymer electrolyte *Electrochim. Acta* **161** 171–6
[77] Bandara T M W J, Karunathilaka D G N, Ratnasekera J L, De Silva L A, Herath A C and Mellander B E 2017 Electrical and complex dielectric behaviour of composite polymer electrolyte based on PEO, alumina and tetrapropylammonium iodide *Ionics* **23** 1711–9
[78] Chen B, Huang Z, Chen X, Zhao Y, Xu Q, Long P, Chen S and Xu X 2016 A new composite solid electrolyte PEO/$Li_{10}GeP_2S_{12}$/SN for all-solid-state lithium battery *Electrochim. Acta* **210** 905–14
[79] Pitawala H M, Dissanayake M A and Seneviratne V A 2007 Combined effect of Al_2O_3 nano-fillers and EC plasticizer on ionic conductivity enhancement in the solid polymer electrolyte $(PEO)_9LiTf$ *Solid State Ion.* **178** 885–8
[80] Wieczorek W, Raducha D, Zalewska A and Stevens J R 1998 Effect of salt concentration on the conductivity of PEO-based composite polymeric electrolytes *J. Phys. Chem.* B **102** 8725–31
[81] Shanmukaraj D and Murugan R 2005 Characterization of PEG: $LiClO_4^+$ $SrBi_4Ti_4O_{15}$ nanocomposite polymer electrolytes for lithium secondary batteries *J. Power Sources* **149** 90–5
[82] Weston J E and Steele B C 1982 Effects of inert fillers on the mechanical and electrochemical properties of lithium salt-poly (ethylene oxide) polymer electrolytes *Solid State Ion.* **7** 75–9
[83] Wieczorek W, Stevens J R and Florjańczyk Z 1996 Composite polyether based solid electrolytes. The Lewis acid-base approach *Solid State Ion.* **85** 67–72
[84] Hema M and Tamilselvi P 2016 Lithium ion conducting PVA: PVdF polymer electrolytes doped with nano SiO_2 and TiO_2 filler *J. Phys. Chem. Solids* **96** 42–8
[85] Wang W, Yi E, Fici A J, Laine R M and Kieffer J 2017 Lithium ion conducting polyethylene oxide-based solid electrolytes containing active or passive ceramic nanoparticles *J. Phys. Chem.* C **121** 2563–73
[86] Zhao Y, Wu C, Peng G, Chen X, Yao X, Bai Y, Wu F, Chen S and Xu X 2016 A new solid polymer electrolyte incorporating $Li_{10}GeP_2S_{12}$ into a polyethylene oxide matrix for all-solid-state lithium batteries *J. Power Sources* **301** 47–53
[87] Takada K 2013 Interfacial nanoarchitectonics for solid-state lithium batteries *Langmuir* **29** 7538–41
[88] Ali T M, Padmanathan N and Selladurai S 2015 Effect of nanofiller CeO_2 on structural, conductivity, and dielectric behaviors of plasticized blend nanocomposite polymer electrolyte *Ionics* **21** 829–40
[89] Yoon M Y, Hong S K and Hwang H J 2013 Fabrication of Li-polymer/silica aerogel nanocomposite electrolyte for an all-solid-state lithium battery *Ceram. Int.* **39** 9659–563
[90] Jung Y C, Lee S M, Choi J H, Jang S S and Kim D W 2015 All solid-state lithium batteries assembled with hybrid solid electrolytes *J. Electrochem. Soc.* **162** A704–10
[91] Mohanta J, Singh U P, Panda S K and Si S 2016 Enhancement of Li^+ ion conductivity in solid polymer electrolytes using surface tailored porous silica nanofillers *Adv. Nat. Sci.* **7** 035011
[92] Dam T, Tripathy S N, Paluch M, Jena S S and Pradhan D K 2016 Investigations of relaxation dynamics and observation of nearly constant loss phenomena in PEO_{20}-$LiCF_3SO_3$-ZrO_2 based polymer nano-composite electrolyte *Electrochim. Acta* **202** 147–56
[93] Moreno J S, Armand M, Berman M B, Greenbaum S G, Scrosati B and Panero S 2014 Composite PEO_n: NaTFSI polymer electrolyte: preparation, thermal and electrochemical characterization *J. Power Sources* **248** 695–702
[94] Ganapatibhotla L V and Maranas J K 2014 Interplay of surface chemistry and ion content in nanoparticle-filled solid polymer electrolytes *Macromolecules* **47** 3625–34
[95] Vignarooban K, Dissanayake M A, Albinsson I and Mellander B E 2014 Effect of TiO_2 nano-filler and EC plasticizer on electrical and thermal properties of poly (ethylene oxide)(PEO) based solid polymer electrolytes *Solid State Ion.* **266** 25–8
[96] Lee L, Park S J and Kim S 2013 Effect of nano-sized barium titanate addition on PEO/PVDF blend-based composite polymer electrolytes *Solid State Ion.* **234** 19–24
[97] Zhang D, Yan H, Zhu Z, Zhang H and Wang J 2011 Electrochemical stability of lithium bis (oxatlato) borate containing solid polymer electrolyte for lithium ion batteries *J. Power Sources* **196** 10120–5
[98] Zhu K, Liu Y and Liu J 2014 A fast charging/discharging all-solid-state lithium ion battery based on PEO-MIL-53(Al)-LiTFSI thin film electrolyte *RSC Adv.* **4** 42278–84
[99] Lin D, Liu W, Liu Y, Lee H R, Hsu P C, Liu K and Cui Y 2015 High ionic conductivity of composite solid polymer electrolyte via *in situ* synthesis of monodispersed SiO_2 nanospheres in poly (ethylene oxide) *Nano Lett.* **16** 459–65
[100] Nancy A C and Suthanthiraraj S A 2017 Effect of Al_2O_3 nanofiller on the electrical, thermal and structural properties of PEO: PPG based nanocomposite polymer electrolyte *Ionics* **23** 1439–49
[101] Pandey G P, Hashmi S A and Agrawal R C 2008 Hot-press synthesized polyethylene oxide based proton conducting nanocomposite polymer electrolyte dispersed with SiO_2 nanoparticles *Solid State Ion.* **179** 543–9
[102] Capiglia C, Mustarelli P, Quartarone E, Tomasi C and Magistris A 1999 Effects of nanoscale SiO_2 on the thermal and transport properties of solvent-free, poly (ethylene oxide)(PEO)-based polymer electrolytes *Solid State Ion.* **118** 73–9
[103] Sun H Y, Sohn H J, Yamamoto O, Takeda Y and Imanishi N 1999 Enhanced lithium-ion transport in PEO-based composite polymer electrolytes with ferroelectric $BaTiO_3$ *J. Electrochem. Soc.* **146** 1672–6
[104] Appetecchi G B, Hassoun J, Scrosati B, Croce F, Cassel F and Salomon M 2003 Hot-pressed, solvent-free, nanocomposite, PEO-based electrolyte membranes: II. All solid-state Li/$LiFePO_4$ polymer batteries *J. Power Sources* **124** 246–53
[105] Choudhary S and Sengwa R J 2017 Effects of different inorganic nanoparticles on the structural, dielectric and ion transportation properties of polymers blend based nanocomposite solid polymer electrolytes *Electrochim. Acta* **247** 924–41
[106] Keller M, Appetecchi G B, Kim G T, Sharova V, Schneider M, Schuhmacher J, Roters A and Passerini S 2017 Electrochemical performance of a solvent-free

hybrid ceramic-polymer electrolyte based on $Li_7La_3Zr_2O_{12}$ in $P(EO)_{15}$LiTFSI *J. Power Sources* **353** 287–97
[107] Scrosati B, Croce F and Persi L 2000 Impedance spectroscopy study of PEO-based nanocomposite polymer electrolytes *J. Electrochem. Soc.* **147** 1718–21
[108] Dam T, Karan N K, Thomas R, Pradhan D K and Katiyar R S 2015 Observation of ionic transport and ion-coordinated segmental motions in composite (polymer-salt-clay) solid polymer electrolyte *Ionics* **21** 401–10
[109] Das A, Thakur A K and Kumar K 2017 Raman spectroscopic study of ion dissociation effect in clay intercalated polymer blend nano composite electrolyte *Vibr. Spectrosc.* **92** 14–9
[110] Sunitha V R and Radhakrishnan S 2016 Impedance and dielectric studies of nanocomposite polymer electrolyte systems using MMT and ferroelectric fillers *Ionics* **22** 2437–46
[111] Mohapatra S R, Thakur A K and Choudhary R N 2009 Effect of nanoscopic confinement on improvement in ion conduction and stability properties of an intercalated polymer nanocomposite electrolyte for energy storage applications *J. Power Sources* **191** 601–13
[112] Ratna D, Divekar S, Patchaiappan S, Samui A B and Chakraborty B C 2007 Poly (ethylene oxide)/clay nanocomposites for solid polymer electrolyte applications *Polym. Int.* **56** 900–4
[113] Lin Y, Wang X, Liu J and Miller J D 2017 Natural halloysite nano-clay electrolyte for advanced all-solid-state lithium-sulfur batteries *Nano Energy* **31** 478–85
[114] Zhang Y, Zhao Y, Gosselink D and Chen P 2015 Synthesis of poly (ethylene-oxide)/nanoclay solid polymer electrolyte for all solid-state lithium/sulfur battery *Ionics* **21** 381–5
[115] Thakur A K, Pradhan D K, Samantaray B K and Choudhary R N 2006 Studies on an ionically conducting polymer nanocomposite *J. Power Sources* **159** 272–6
[116] Choudhary S and Sengwa R J 2011 Dielectric spectroscopy and confirmation of ion conduction mechanism in direct melt compounded hot-press polymer nanocomposite electrolytes *Ionics* **17** 811–9
[117] Sharma A L and Thakur A K 2013 Plastic separators with improved properties for portable power device applications *Ionics* **19** 795–809
[118] Berthier C, Gorecki W, Minier M, Armand M B, Chabagno J M and Rigaud P 1983 Microscopic investigation of ionic conductivity in alkali metal salts-poly (ethylene oxide) adducts *Solid State Ion.* **11** 91–5
[119] MacGlashan G S, Andreev Y G and Bruce P G 1999 Structure of the polymer electrolyte poly (ethylene oxide)$_6$: $LiAsF_6$ *Nature* **398** 792–4
[120] Stoeva Z, Martin-Litas I, Staunton E, Andreev Y G and Bruce P G 2003 Ionic conductivity in the crystalline polymer electrolytes PEO_6: $LiXF_6$, X = P, As, Sb *J. Am. Chem. Soc.* **125** 4619–26
[121] Singh V K, Balo L, Gupta H, Singh S K and Singh R K 2017 Solid polymer electrolytes based on Li^+/ionic liquid for lithium secondary batteries *J. Solid State Electrochem.* **21** 1713–23
[122] Kelly I E, Owen J R and Steele B C 1985 Poly (ethylene oxide) electrolytes for operation at near room temperature *J. Power Sources* **14** 13–21
[123] Huq R, Farrington G C, Koksbang R and Tonder P E 1992 Influence of plasticizers on the electrochemical and chemical stability of a Li^+ polymer electrolyte *Solid State Ion.* **57** 277–83
[124] Croce F, Persi L, Scrosati B, Serraino-Fiory F, Plichta E and Hendrickson M A 2001 Role of the ceramic fillers in enhancing the transport properties of composite polymer electrolytes *Electrochim. Acta* **46** 2457–61
[125] Ji K S, Moon H S, Kim J W and Park J W 2003 Role of functional nano-sized inorganic fillers in poly (ethylene) oxide-based polymer electrolytes *J. Power Sources* **117** 124–30
[126] Croce F, Curini R, Martinelli A, Persi L, Ronci F, Scrosati B and Caminiti R 1999 Physical and chemical properties of nanocomposite polymer electrolytes *J. Phys. Chem.* B **103** 10632–8
[127] Jayathilaka P A, Dissanayake M A, Albinsson I and Mellander B E 2002 Effect of nano-porous Al_2O_3 on thermal, dielectric and transport properties of the $(PEO)_9$LiTFSI polymer electrolyte system *Electrochim. Acta* **47** 3257–68
[128] Kumar B and Scanlon L G 1999 Polymer–ceramic composite electrolytes: conductivity and thermal history effects *Solid State Ion.* **124** 239–54
[129] Marcinek M, Bac A, Lipka P, Zalewska A, Zukowska G, Borkowska R and Wieczorek W 2000 Effect of filler surface group on ionic interactions in PEG − $LiClO_4$ − Al_2O_3 composite polyether electrolytes *J. Phys. Chem.* B **104** 11088–93
[130] Thakur A K 2011 Mechanism for improvement in mechanical and thermal stability in dispersed phase polymer composites *Ionics* **17** 109–20
[131] Sharma A L, Shukla N and Thakur A K 2008 Studies on structure property relationship in a polymer–clay nanocomposite film based on $(PAN)_8LiClO_4$ *J. Polym. Sci.* B **46** 2577–92
[132] Petersen G, Torell L M, Panero S, Scrosati B, Da Silva C J and Smith M 1993 Ionic interactions in MCF_3SO_3-polyether complexes containing mono-, di-and trivalent cations *Solid State Ion.* **60** 55–60
[133] Chen B and Evans J R 2004 Preferential intercalation in polymer-clay nanocomposites *J. Phys. Chem.* B **108** 14986–990
[134] Sengwa R J, Sankhla S and Choudhary S 2010 Effect of melt compounding temperature on dielectric relaxation and ionic conduction in PEO–$NaClO_4$–MMT nanocomposite electrolytes *Ionics* **16** 697–707
[135] Anadao P 2011 *Clay-Containing Polysulfone Nanocomposites* (Rijeka: INTECH Open Access Publisher)
[136] Sharma A L and Thakur A K 2011 Polymer matrix–clay interaction mediated mechanism of electrical transport in exfoliated and intercalated polymer nanocomposites *J. Mater. Sci.* **46** 1916–31
[137] Kotal M and Bhowmick A K 2015 Polymer nanocomposites from modified clays: recent advances and challenges *Prog. Polym. Sci.* **51** 127–87
[138] Sinha Ray S, Okamoto K and Okamoto M 2003 Structure − property relationship in biodegradable poly (butylene succinate)/layered silicate nanocomposites *Macromolecules* **36** 2355–67
[139] Jing G, Zhen-Li G, Xiao-Li Y, Shu G, Zhong-Liang Z and Bo W 2012 Investigation of the free volume and ionic conducting mechanism of poly (ethylene oxide)-$LiClO_4$ polymeric electrolyte by positron annihilating lifetime spectroscopy *Chin. Phys.* B **21** 107803
[140] Dyre J C and Schrøder T B 2000 Universality of ac conduction in disordered solids *Rev. Mod. Phys.* **72** 873